Daylighting, Artificial Lighting and Non-Visual Effects Study for a Residential Building

†Prof. John Mardaljevic, ‡Prof. Marilyne Andersen,
*Nicolas Roy and **Dr. Jens Christoffersen

†School of Civil and Building Engineering, Loughborough University,
Loughborough, Leicestershire, LE11 3TU, UK
e-mail: j.mardaljevic@lboro.ac.uk
Tel: +44 1509 222630

‡Interdisciplinary Laboratory of Performance-Integrated Design (LIPID),
School of Architecture, Civil and Environmental Engineering (ENAC),
Ecole Polytechnique Fédérale de Lausanne (EPFL),
Lausanne, CH - 1015, Switzerland
e-mail: marilyne.andersen@epfl.ch
Tel: +41 21 693 08 82

*VELUX A/S, Ådalsvej 99, DK-2970
Hørsholm, Denmark
e-mai:l nicolas.roy@velux.com
Tel: +45 45 16 47 60

**VELUX A/S, Ådalsvej 99, DK-2970
Hørsholm, Denmark
e-mail: jens.christoffersen@velux.com
Tel: +45 45 16 78 99

Contents

List of Tables

List of Figures

Main Findings

The study uses a domestic dwelling as the setting to investigate and explore the applicability of daylighting metrics for residential buildings. The metrics address daylight provision for task and electric lighting usage. In addition to these it also investigates the formulation of preliminary metrics to evaluating the potential for non-visual effects. The setting, a residential building with and without skylights, was evaluated for all 32 combinations of eight European climates and four building orientations covering the cities of Hamburg, London, Madrid, Moscow, Ostersund, Paris, Rome and Warsaw. The evaluation is based on a real life renovation case in which new skylights have been added to the kitchen, living room, large and small bathrooms and staircase.

This section summarises the findings based on 64 unique sets of climate-based daylight simulation (32 combinations x 2 design variants) in which three different aspects of daylight are evaluated: daylighting performance, energy savings for lighting and non-visual effects.

Daylighting performance

The daylighting performance is evaluated using the Useful Daylight Illuminance (UDI) metric, which permits to predict the occurence of illuminance levels throughout the year in specific range, i.e. 300 – 3,000 lux range. The results below present the change in UDI that result from addition of skylights.

- The results for the living room (wg01) show decreases in the occurrence of illuminances in the 100 – 300 lux range, and corresponding increases in the desired 300 – 3,000 lux range, Figure 19. The results also show decreases around 10% in the occurrence of illuminances less than 100 lux, and increases up to 20% in the 3,000 lux and above range.

- There is a pronounced improvement in the daylighting performance of the kitchen (wg02), Figure 20. The occurrence of illuminances in the desired 300 – 3,000 lux range increases by up to 40% or more, and for all but Madrid and Rome, there is a decrease around 20% for illuminances less than 100 lux. There is a slight increase in the occurrence of illuminances greater than 3,000 lux, especially for orientations where the kitchen glazing is facing south or west.

- The hall (wg03) does not have a dedicated skylight, but receives light from adjacent spaces in which skylights were added. For this space, we see increases of 10% in the occurrence of illuminances in the desired 300 – 3,000 lux range and corresponding decreases of 10% in the 100 – 300 lux range, Figure 21.

- The small bathroom (wg04) does not have a pre-existing window. With the addition of a skylight we see illuminances in the 100-3,000 lux range occurring for between 65% to nearly 80% of the year, Figure 22.

- The large bathroom (wg05) daylighting is also greatly improved by the addition of the skylight: the occurrence of illuminances in the desired 300 – 3,000 lux range increases from 25% to 50%, Figure 23.

- The staircase (wg06) only received light spillage from the poorly lit entrance hall. The addition of the skylight greatly improves the daylight provision for this space, we see increases in the occurrence of illuminances in the 100 – 3,000 lux range of between 30% to 40%, Figure 24.

Energy savings for lighting

The energy savings for lighting are evaluated following the RT 2005 model in which an occupancy schedule, a default lighting power density, as well as coefficients for the use of electrical lighting are specified.

- For any one location, there is generally low sensitivity in the predicted saving with respect to building orientation for the living room space. Sensitivity to orientation is generally higher for the other spaces, but rarely very large.
- The generally low sensitivity to orientation is most probably the result of the low illuminances which largely govern the light switching regime.
- The predicted energy savings for the living room are typically around 20% for the six less sunny climates and around 13% for the two sunny climates (i.e. Madrid and Rome) (Table 43).
- The predicted energy savings for the kitchen (wg02) vary between 15% and 29% (Table 47).
- Even though the hall space (wg03) did not have a skylight option, the light spillage resulting from skylights in adjacent spaces resulted in savings of up to 6% (Table 48).
- The small bathroom (wg04) did not have any pre-existing windows, so the addition of a skylight resulted in savings of up to 46% (Table 49).
- The large bathroom (wg05) had two small windows positioned high on the (internal) wall. The positioning combined with the reveal depth resulted in very uneven illumination (see UDI plot for case without skylights in Figure 46). Here the addition of a skylight also resulted in major savings: up to 45% (Table 50).
- The space with the stairs to the basement (wg06) showed savings in the range of 22% to 36% (Table 51).

Non-visual effects

A preliminary framework for evaluating non-visual effects of daylight is proposed, described more extensively in Andersen, Mardaljevic & Lockley [1]. Based on vertical illuminance received at the eye level, three periods of the day are distinguished for their differentiated effects on circadian entrainment and alertness (see details in paper): 06:00-10:00 (hereafter 'morning' period), 10:00-18:00 (hereafter 'afternoon' period) and 18:00-06:00 (hereafter 'night' period).

- The addition of skylights results in a marked increase in predicted potential for non-visual effects for the 'morning' and 'afternoon' periods in all cases, but there is a lot of variation resulting from climate and orientation.
- There is often a factor two difference in predicted potential for non-visual effects for the 'morning' period across the four orientations of each location, Figure 34.

- The preferential orientation with the highest potential for non-visual effects in the 'morning' for any one locale is when the glazing faces east.
- To maximize the potential for non-visual effects for the 'afternoon' period the preferred orientation is usually that with the glazing facing south.
- The predicted potential for non-visual effects in the living room (wg01) saw increases in the range of 10% to 25% for the 'morning' period, and 25% to 55% for the 'afternoon' period.
- The predicted potential for non-visual effects in the kitchen (wg02) saw increases in the range of 5% to 25% for the 'morning' period, and 20% to 50% for the 'afternoon' period.
- The patterns in predicted potential for non-visual effects in the large bathroom (wg05) are similar to those obtained for the kitchen, with typical increases in the range of 5% to 20% for the 'morning' period, and 20% to 50% for the 'afternoon' period.

Abstract

It is now widely accepted that the standard method for daylighting evaluation - the daylight factor - is due for replacement with metrics founded on absolute values for luminous quantities predicted over the course of a full year using sun and sky conditions derived from standardised climate files. The move to more realistic measures of daylighting introduces significant levels of additional complexity in both the simulation of the luminous quantities and the reduction of the simulation data to readily intelligible metrics. The simulation component, at least for buildings with standard glazing materials, is reasonably well understood. There is no consensus however on the composition of the metrics, and their formulation is an ongoing area of active research. Additionally, non-domestic and residential buildings present very different evaluation scenarios and it is not yet clear if a single metric would be applicable to both. This study uses a domestic dwelling as the setting to investigate and explore the applicability of daylighting metrics for residential buildings. In addition to daylighting provision for task and disclosing the potential for reducing electric lighting usage, we also investigate the formulation of measures for non-visual effects such as entrainment of the circadian system and alertness.

1 Introduction

The primary concern in the daylighting of buildings has generally been to provide illumination for task, e.g. 500 lux on the horizontal work plane. In the last few decades however there has been a gradual increase in awareness of the non-visual effects of daylight/light received by the eye [2]. It is well-known that building occupants almost without exception will prefer a workstation with a view of the outdoor environment to a windowless office [3]. A view to the outside indicates of course the presence of daylight, although the relation between view and daylight provision is not straightforward being dependent on many factors. In addition to subjective preferences for daylit spaces, it is now firmly established that the light has measurable biochemical effects on the human body, in particular with respect to maintaining a healthy sleep - wake cycle. Could the quality and nature of the internal daylit environment have a significant effect on the health of the human body which can proven through the measurement of, say, hormone levels? Evidence is indeed suggestive of links between daylight exposure and both health and productivity [4]. Insomnia is believed to affect about a third of the general population, and about 12% of those that report difficulty in sleeping have delayed sleep phase disorder, i.e. a circadian related disorder [5]. It is now understood that daylight exposure plays a key role in establishing and maintaining a healthy circadian cycle, and so is likely to be a factor in a significant number of clinical insomnia cases.

This study uses a domestic dwelling as the setting to investigate and explore the applicability of daylighting metrics for residential buildings. The metrics address daylight provision for task and electric lighting usage. In addition to these we also investigate the formulation of metrics for non-visual effects. The setting, a residential building with and without skylights, was evaluated for all 32 combinations of eight European climates and four building orientations. Daylight for task was assessed using the useful daylight illuminance schema [6]. Electrical lighting usage was predicted on the basis of typical schedules and daylight availability using the RT 2005 switching model and occupancy scenarios [7]. Although there are uncertainties regarding the precise calibration, there is now sufficient empirical data to parameterise models that simulate the non-visual aspects of daylight, e.g. for circadian entrainment and a general sense of 'alertness'. For these non-visual aspects, vertical illuminance at the eye was predicted using a modified climate-based daylight modelling approach.

2 Methodology

A residential dwelling was used a 'virtual laboratory' for the investigations described below. The dwelling is based on a real house which has a design commonly found throughout Europe. The following sections describe the 3D model of the building, the configuration of calculation planes and the climate data. Then follows an outline of simulation approach.

2.1 Outline

The 3D model for the residential building is shown in Figure 1. The sensitivity of metrics to daylight design interventions was investigated by predicting for cases with and without skylights - the 3D graphics in Figure 1 show the building with skylights. The coloured areas in the plan view show the horizontal calculation planes where illuminance was predicted. The spaces evaluated were: the living room (wg01); the kitchen (wg02); the entrance hall (wg03); small bathroom (wg04); large bathroom (wg05); and the stairs to the basement (wg06). The calculation planes are at table and work-top height for the living room and kitchen respectively. For the other spaces the calculation planes are at floor level, which for the stairs was the individual steps. General daylighting provision and the requirement for electric lighting were based on daylight illuminance predicted at these planes. Additionally, there are smaller square planes in three of the spaces: sixteen in the living room (wg01); four in the kitchen (wg02); and, one in the larger bathroom (wg05). These represent locations at head-height where vertical illuminance at the eye was predicted for the determination of non-visual effects. At each of these locations, the vertical illuminance was determined for four view directions, i.e. at 90° increments.

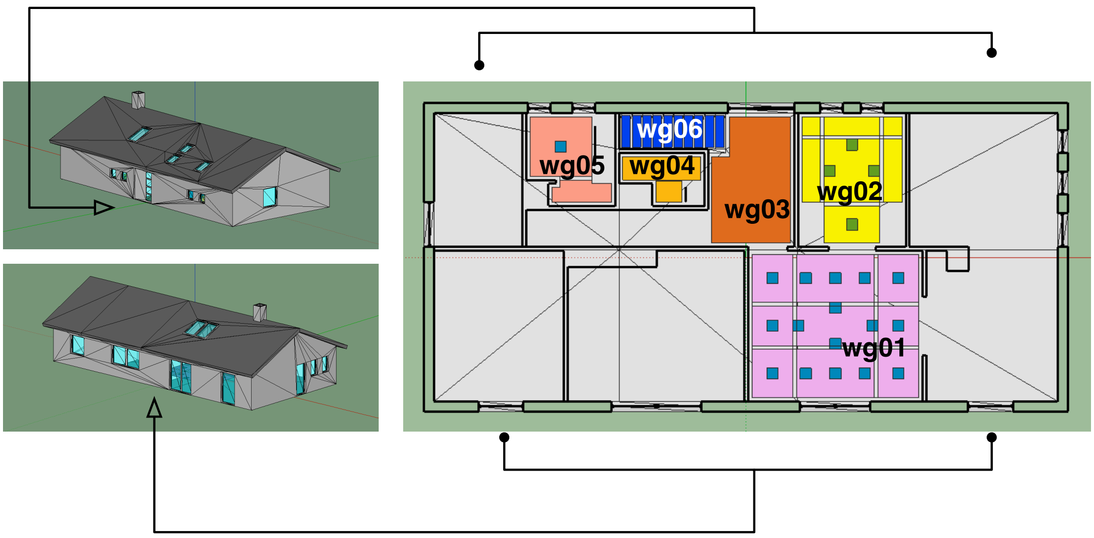

Figure 1: Images of the two main building facades (variant with skylights) together with a plan view showing the calculation planes for the spaces and the smaller, square planes for the N-VE model.

A cylindrical "wall" of radius 50m and centred on building was used to represent the obstruction to the horizon that would be expected in any typical housing development. Wall heights of 5m and 10m were used, Figure 2. Internal surfaces were assigned diffuse reflectance values typical of ceiling, walls and floor, i.e. 0.70, 0.55 and 0.25 respectively. All windows were modelled as clear double-pane 6mm low-emissivity with a transmittance of 0.74.

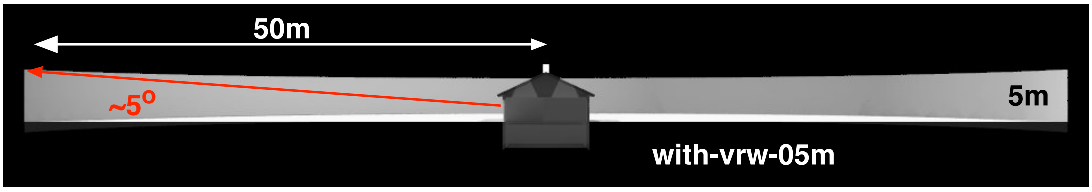

Figure 2: Section view showing cylindrical 'horizon' obstruction of heights 5m and 10m

The calculation planes - i.e. those areas containing the points where daylight illuminances were predicted - are shown in Figure 3. The calculation planes are shown by coloured areas against a grey backdrop of the floor plan. The small square areas in three of the rooms indicate additional calculation planes where illuminances were predicted for the purpose of determining the circadian potential of the various spaces. The lower graphic in Figure 3 has the skylights superposed.

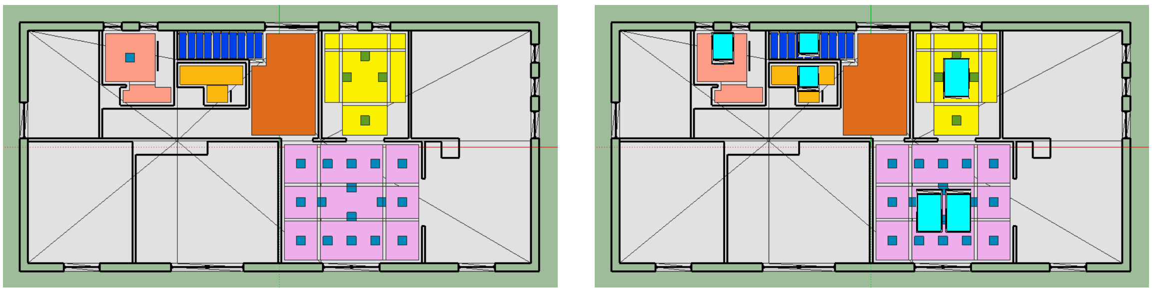

Figure 3: Plan view showing the calculation planes in relation to the vertical glazing and, in the right-hand plot, with the skylights superposed.

2.2 The climate data

The principal sources of basic data for climate-based daylight modelling are the standard climate files which were originally created for use by dynamic thermal modelling programs [8]. These datasets contain averaged hourly values for a full year, i.e. 8,760 values for each parameter. For lighting simulation, the required parameters may be either of the following pairs:

- Global horizontal irradiance and either diffuse horizontal irradiance or direct normal irradiance.
- Global horizontal illuminance and either diffuse horizontal illuminance or direct normal illuminance.

Standard climate data for a large number of locales across the world are freely available for download from several websites. One of the most comprehensive repositories is that compiled for use with the EnergyPlus thermal simulation program [9].

The eight locales were Hamburg (Germany), Madrid (Spain), Paris (France), London (UK), Rome (Italy), Warsaw (Poland), Moscow (Russia) and Ostersund (Sweden). The lat/lon coordinates of each city/station and the short name ID given for this study are listed in Table 1. The climate file data used for the simulations was diffuse horizontal illuminance and direct normal illuminance. The pattern of hourly values in a climate dataset is unique and, because of the random nature of weather, they will never be repeated in precisely that way. Climate datasets are however representative of the prevailing conditions measured at the site, and they do exhibit much of the full range in variation that typically occurs. Furthermore, these standard datasets provide definitive yardstick quantities for modelling purposes. The last column in Table 1 gives the number of "sunny" days for each of the climate files. There is no widely accepted definitive definition for the occurrence of a sunny day in a climate file. Here, a sunny day was taken to be one where more than half of the daily total of global horizontal illuminance was due to direct solar radiation. This quantity varied from 49 days (Moscow) to 194 (Madrid) and appears to serve as a sensitive discriminator to summarise the overall degree of "sunnyness" for the climates.

ID	City/ Station	Country	Latitude	Longitude	"Sunny" days
DEU-Hamburg	Hamburg	Germany	53.63	-10.00	50
ESP-Madrid	Madrid	Spain	40.41	3.68	194
FRA-Paris	Paris	France	48.73	-2.4	64
GBR-London	London	UK	51.15	0.18	71
ITA-Roma	Rome	Italy	41.80	-12.50	107
POL-Warsaw	Warsaw	Poland	52.17	-20.97	53
RUS-Moscow	Moscow	Russia	55.75	-37.63	49
SWE-Ostersund	Ostersund	Sweden	63.18	-14.50	59

Table 1: The eight climate files used in the study

The climate file illuminance data for two locations are shown in Figure 4. The original hourly data were interpolated to a 15 minute time-step. The shading in Figure 4 represents the magnitude of the illuminance with zero values shaded light-grey. In the plot for diffuse illuminance the grey area indicates the hours of darkness. Presented in this way it is easy to appreciate both the prevailing patterns in either quantity and their short-term variability. Most obvious is the daily/seasonal pattern for both illuminances: short periods of daylight in the winter months, longer in summer. The hour-by-hour variation in the direct normal illuminance (smoothed by interpolation to a 15 minute step) is clearly visible, though it is also present to a lesser degree in the diffuse horizontal illuminance (i.e. from the sky). The horizontal green lines delineate the different periods in the day for the simulation of non-visual effects, which will be described later.

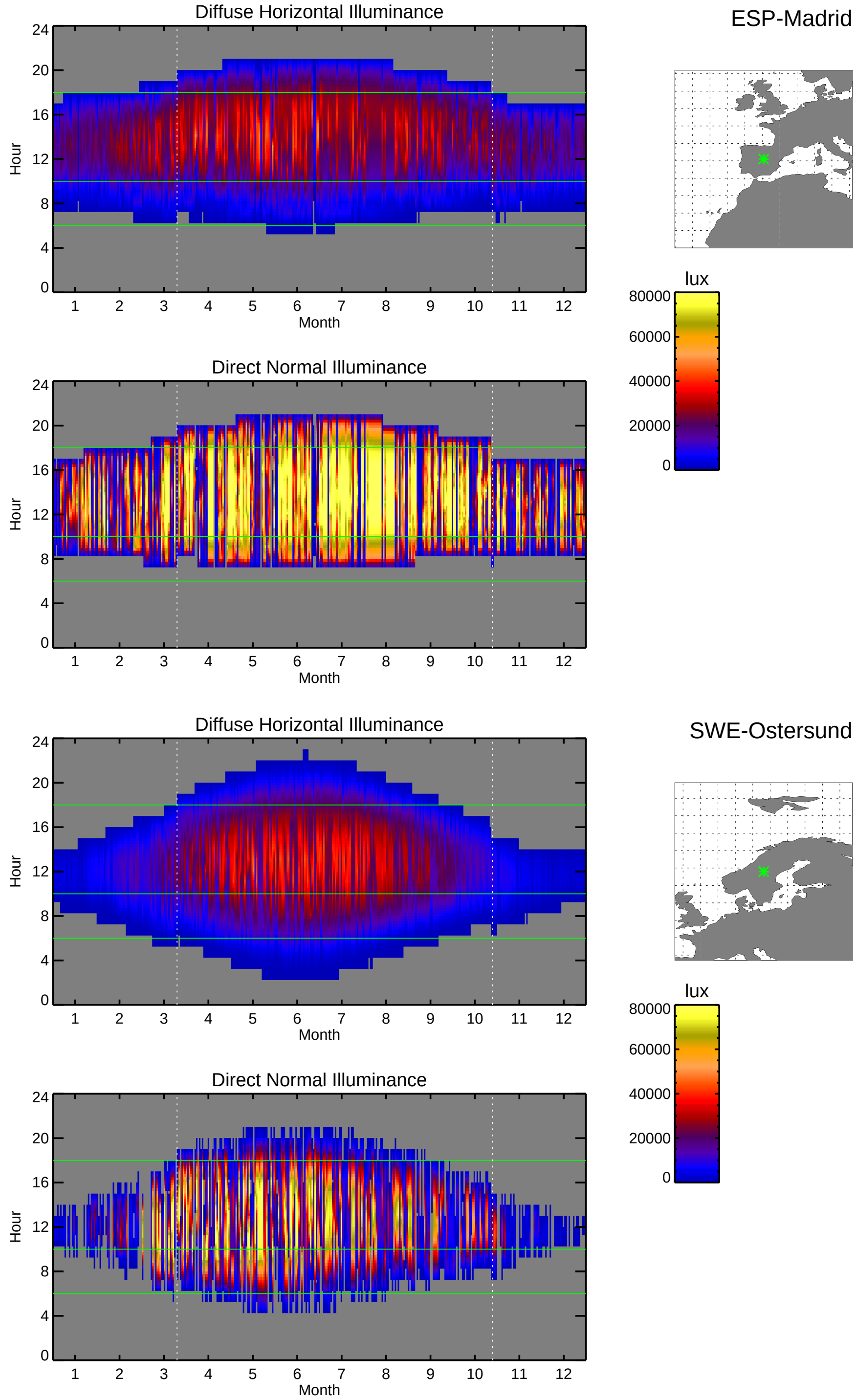

Figure 4: Two of the eight climates: Madrid and Ostersund.

2.3 Climate-based daylight modelling

The term climate-based daylight modelling does not yet have a formally accepted definition - it was first coined in the title of a paper given at the 2006 CIBSE National Conference [10]. However it is generally taken to mean any evaluation that is founded on the totality (i.e. sun and sky components) of contiguous daylight data appropriate to the locale for a period of a full year. In practice, this means sun and sky parameters found in, or derived from, the standard meteorological data files which contain hourly values for a full year. Given the self-evident nature of the seasonal pattern in daylight availability, an evaluation period of a full year is needed to fully capture all of the naturally occurring variation in conditions that is represented in the climate dataset.

A climate-based analysis is intended to represent the prevailing conditions over a period of time rather than be simply a "snapshot" of specific conditions at a particular instant. Because of the seasonal variation of daylight, the evaluation period is normally taken to be an entire year, although sometimes seasonal or monthly analyses may be required. Analyses may be restricted to include just those hours in the year that cover, for example, the working period. There are a number of possible ways to use climate-based daylight modelling [11, 12, 13]. A cumulative analysis is the prediction of some cumulative measure of daylight (e.g. total annual illuminance) founded on the aggregated luminance effect of (hourly) sky and the sun conditions derived from the climate datset. A time-series analysis involves predicting instantaneous measures (e.g. illuminance) based on all the hourly (or sub-hourly) values in the annual climate dataset. The evaluation described here is founded on an analysis of a time-series of predicted daylight illuminance values across calculation planes in various rooms. The calculation planes were horizontal areas to represent either physical surfaces for specific tasks (e.g. kitchen work-tops) or more generally to characterise the overall daylighting provision of the various spaces. Time-varying daylight illuminance values were predicted at hundreds of points evenly distributed across the horizontal calculation planes. Another set of calculation planes were used for the prediction of daylight illuminance for the non-visual effects (N-VE) model, discussed in section 5. The N-VE model requires as input vertical illuminance at the eye. The horizontal planes used in the N-VE model were 30cm squares located at approximate head height for a seated person. At the points that comprise these planes, the vertical illuminance was predicted, in turn, for four orientations in 90° steps. These squares represent possible locations in the various spaces for an occupant's head.

2.4 Simulation 'engine'

In principle, climate-based daylight modelling (CBDM) could be carried out using either computer simulation techniques or scale models in a sky simulator (i.e. physical modelling). To date however CBDM has been demonstrated using only computer simulation techniques.[1] Computer simulation techniques were used for this study. The basic steps in the evaluation were as follows - for every combination of building orientation and locale:

1. Obtain basic climate data from the designated standard meteorological file for that locale.

[1] Sky simulator domes are subject to both fundamental limiting factors such as parallax error [14] and several practical/operational constraints such as lamp stability, incomplete sky coverage and the demonstrated inaccuracy of scale model construction [15, 16].

2. Generate a sky luminance distribution using a sky model based on the value for diffuse horizontal illuminance in the climate data.

3. Create a description of the sun (position and luminance) from the value of direct normal illuminance in the climate data.

4. Compute the internal daylight illuminance distribution (repeat steps 2 to 4 for each time-step).

5. Process the illuminance predictions to determine various daylight metrics and generate plots etc.

A so called "brute-force" approach would require a full lighting simulation for each of the four thousand or so unique sky and sun configurations that can be derived from all the daylight hours in the climate dataset. Although a brute-force approach is tractable, the simulation times may prove excessively long. In 1983, Tregenza and Waters described an accelerated approach to predict internal illuminance based on what they called daylight coefficients [17]. The daylight coefficient approach requires that the sky be broken into many patches. The internal illuminance at a point that results from a patch of unit-luminance sky is computed and cached. This is done for each patch of sky. It is then possible, in principle, to determine the internal illuminance for an arbitrary sky luminance distribution (and sun luminance/position) using relatively simple (i.e. quick) arithmetic operations on matrices. The computational expense of a daylight coefficient calculation for a sky with N patches is comparable to that for N standard simulations. Provided therefore that the number of patches is less than the number of skies that need to be modelled, the technique has the potential to be computationally more efficient than treating each sky individually.

The computational "engine" that was used to predict the daylight daylight coefficients was the freely available *Radiance* lighting simulation system [18]. The *Radiance* system is the most rigourously validated lighting simulation program currently available. *Radiance* has been proven to be capable of high accuracy predictions and it has become a *de facto* standard for researchers and practitioners world-wide.

The basic daylight coefficient (DC) scheme described by Tregenza and Waters was implemented into the *Radiance* lighting simulation system and illuminance tested against the BRE-IDMP validation dataset [19]. That scheme divided the sky into 145 patches and used these to determine the contribution from both the sun and the sky. The basic DC scheme produced large errors whenever there was a significant divergence between the actually occurring sun position and the nearest pre-computed DC patch value. The basic DC scheme was improved and a refined formulation was devised which gave accuracies comparable the best that could achieved using the standard *Radiance* calculation method, i.e. typically within ±10% of measurements from the BRE-IDMP validation dataset [11][20].

The refined DC method computes separate coefficients for the direct and diffuse components from the 145 patches on the hemisphere. The 145 patch scheme is used to compute direct sky illuminance $\mathbf{E}^{d}$, indirect sky illuminance $\mathbf{E}^{i}$ and indirect sun illuminance $\mathbf{E}^{si}$. The direct sun component $\mathbf{E}^{sd}$ however is determined from a finely discretised set of 5000 patches on the hemisphere. This ensures that the spatio-temporal dynamics of direct sun exposure are precisely determined. This also allows a time-step shorter than one hour to be used without loss of precision. The total illuminance $\mathbf{E}$ is the sum of the individual components:

$$\mathbf{E} = \mathbf{E}^d + \mathbf{E}^i + \mathbf{E}^{sd} + \mathbf{E}^{si} \quad (1)$$

The refined DC method was not originally conceived with a view to predicting for non-visual effects. However, it turned out to be fortuitous for this study since it allowed for the separation of the sun and sky components of illumination which was required for the modelling of non-visual effects (Section 5).

Preparatory tests showed that the hourly time-step of the climate data needs to be reduced using suitable interpolation methods to minimise alias-like sampling errors in the prediction of the degree (magnitude and occurrence) and spatial distribution of direct solar illumination. The prediction of this component needs to be both reliable and consistent so as not to confound the metrics since they are particularly sensitive to the degree and occurrence of direct solar illumination. Interpolation of the climate data to a 15 minute time-step was found to be sufficient to finely resolve the progression of the sun thereby reducing sampling errors to a minimum. Internal daylight lluminances therefore were predicted at 15 minute intervals. The sky model mixing function described by Mardaljevic in 2005 [21] was used to determine the varying sky luminance patterns at each time-step. Four building orientations were evaluated covering the 360° compass range in steps of 90°.

3 Daylight metrics

3.1 Useful daylight illuminance: A human factors-based metric

The metric used to evaluate the daylighting provision was the "useful daylight illuminance" (UDI) scheme [6, 10, 22]. Put simply, achieved UDI is defined as the annual occurrence of illuminances across the work plane that are within a range considered "useful" by occupants. The range considered "useful" is based on a survey of reports of occupant preferences and behaviour in daylit offices with user operated shading devices. Daylight illuminances in the range 100 to 300 lux are considered effective either as the sole source of illumination or in conjunction with artificial lighting. Daylight illuminances in the range 300 to around 3,000 lux are often perceived either as desirable or at least tolerable. Note that these values are based on surveys carried out in non-residential, largely office buildings where daylight-originated glare on visual display devices is a common problem. Many of these surveys were carried out before LCD display panels - which are much less prone to glare than CRT screens - became commonplace. In contrast to office buildings, tasks in the domestic setting are not, of course, largely desk and display screen orientated. Accordingly, the upper limit for preferred/tolerated daylight illuminance used for this study was 3,000 lux. However it should be noted that there is considerable uncertainty regarding preferred/tolerated upper limits for both non-domestic and residential buildings, and that the UDI ranges for this application should be seen as illustrative.

UDI achieved is therefore defined as the annual occurrence of daylight illuminances that are between 100 and 3,000 lux. The UDI range is further subdivided into two ranges called UDI-supplementary and UDI-autonomous. UDI-supplementary gives the occurrence of daylight illuminances in the range 100 to 300 lux. For these levels of illuminance, additional artificial lighting *may* be needed to supplement the daylight for common tasks such as reading. UDI-autonomous gives the occurrence of daylight illuminances in the range 300 to 3000 lux where additional artificial lighting will most likely not be needed.

The UDI scheme is applied by determining at each calculation point the occurrence of daylight levels where:

- The illuminance is less than 100 lux, i.e. UDI 'fell-short' (or UDI-f).
- The illuminance is greater than 100 lux and less than 300 lux, i.e. UDI supplementary (or UDI-s).
- The illuminance is greater than 300 lux and less than 3,000 lux, i.e. UDI autonomous (or UDI-a).
- The illuminance is greater than 100 lux and less than 3,000 lux, i.e. UDI combined (or UDI-c).
- The illuminance is greater than 3,000 lux, i.e. UDI exceeded (or UDI-e).

As noted, the UDI ranges were based on a distillation of values from surveys carried out in office spaces, and many of them before LCD screens became commonplace. Also, the recent findings regarding the role of illumination in maintaining the circadian rhythm suggest that regular exposure to high illuminances during daytime could have long-term beneficial health effects [2]. Webb notes a Japanese study by Noguchi [23] who found that:

> *. . . bright lighting in the office (2500 lux compared to 750 lux, provided for 2 hours in the morning and one hour after lunch for several weeks) boosted alertness and mood, especially in the afternoon. It also seemed to promote melatonin secretion and fall in body temperature at night, changes that should improve the quality of sleep. Although this work was based on a small number of people and further work is needed, it shows promise for alterations in office lighting in terms of productivity and health of the workers.*

Thus it is suggested here that the occurrence of illuminances greater than 3,000 lux (i.e. UDI-e) should not, by design, be eliminated altogether, and that moderate occurrence may in fact be beneficial. What exactly the "optimum" levels of exposure might be is not yet known. For those cases where solar gain in summer must be controlled to minimise cooling requirements, careful attention should be paid to the degree of occurrence of the UDI-e metric. The findings here will be re-evaluated at a later date to include actions resulting from over-heating predicted by dynamic thermal modelling using the same climate data files.

3.2 UDI and "good" daylighting

Whilst there are no official guidelines or recommendations yet for illuminance levels predicted using climate-based modelling, there is sufficient evidence in the published literature to propose the following:

> Good daylighting for task is deemed to be that which offers high levels of useful daylight (i.e. 100 to 3,000 lux), and where a significant part of the occurrence of useful daylight is due to illuminances that fall within the autonomous range (i.e. 300 to 3,000 lux). Furthermore, recent findings regarding the beneficial health effects of occasional high illuminances (i.e. greater than 3,000 lux) suggest that moderate occurrences of UDI exceeded should de considered desirable and not excluded altogether.

Provision of adequate levels daylight illuminance is known to affect the use of electric lighting. For non-domestic buildings a number of studies have found that the switch-on probability is small for desktop illuminances above 250 lux [24, 25]. At present, it is uncertain how these findings for users in office buildings might relate to user behaviour in a domestic setting - this is clearly an area where information is lacking at present. Nonetheless, it is reasonable to suppose that similar behaviour might ensue, and so good levels of daylight illuminances are likely to be associated with lower levels of electric lighting usage. Consequently, the following can be reasonably assumed or stated:

- The switch-on probability will be high for illuminance less than 100 lux (i.e. UDI-e).
- The switch-on probability will reduce from high to low as the illuminances increase from 100 to 300 lux, i.e. that covered by the UDI-s range. Note that this range is broader than the 100 to 200 lux interval used in the RT 2005 model where the switch-on probability changes from 1 to 0.05 (Section 4.1).
- There is significant variability and associated uncertainty in user switching behaviour over the illuminance range where the probability of switching on reduces from high to low.

Thus, there is reasonable certainty that an illuminance in the UDI-a range (i.e. 300 to 3,000 lux) will *not* result in a switch-on, whereas there is considerable uncertainty regarding the probability of a switch-on event when the illuminance is in the UDI-s range (i.e. 100 to 300 lux). Accordingly, maximisation of the occurrence of the UDI-a metric should be taken as the most reliable indicator that the overall level of electric lighting usage (for that space) will be low.

3.3 Example UDI results

Useful daylight illuminance plots are shown for the case without and with skylights for just one climate/orientation combination (Ostersund/180), Figure 5. The time period considered for the UDI plots is 08h00 to 20h00. And so for the Ostersund example this period includes hours of darkness in winter (Figure 4).

The false-colour shading shows the annual occurrence in hours for illuminances in the various UDI ranges that were achieved across the nine calculation planes for this room. The annotation on each calculation plane gives the mean value of the achieved hours across the plane, and at the base of each plot is an area-weighted average for all of the planes. The addition of skylights significantly increases the occurrence of illuminances in the 300 to 3,000 lux range, which now extend across the planes into the corners of the room. Illuminances greater than 3,000 lux are also predicted to occur more frequently, particularly in the centre of the room.

A complete set of twelve UDI plots for one climate and orientation are given in the Appendix (Section 8.1). Note that a complete set of UDI figures for all climates and orientations would comprise 384 such plots (i.e. 12×8×4). The results for all combinations of climate and orientation are summarised more compactly in Section 6.1.

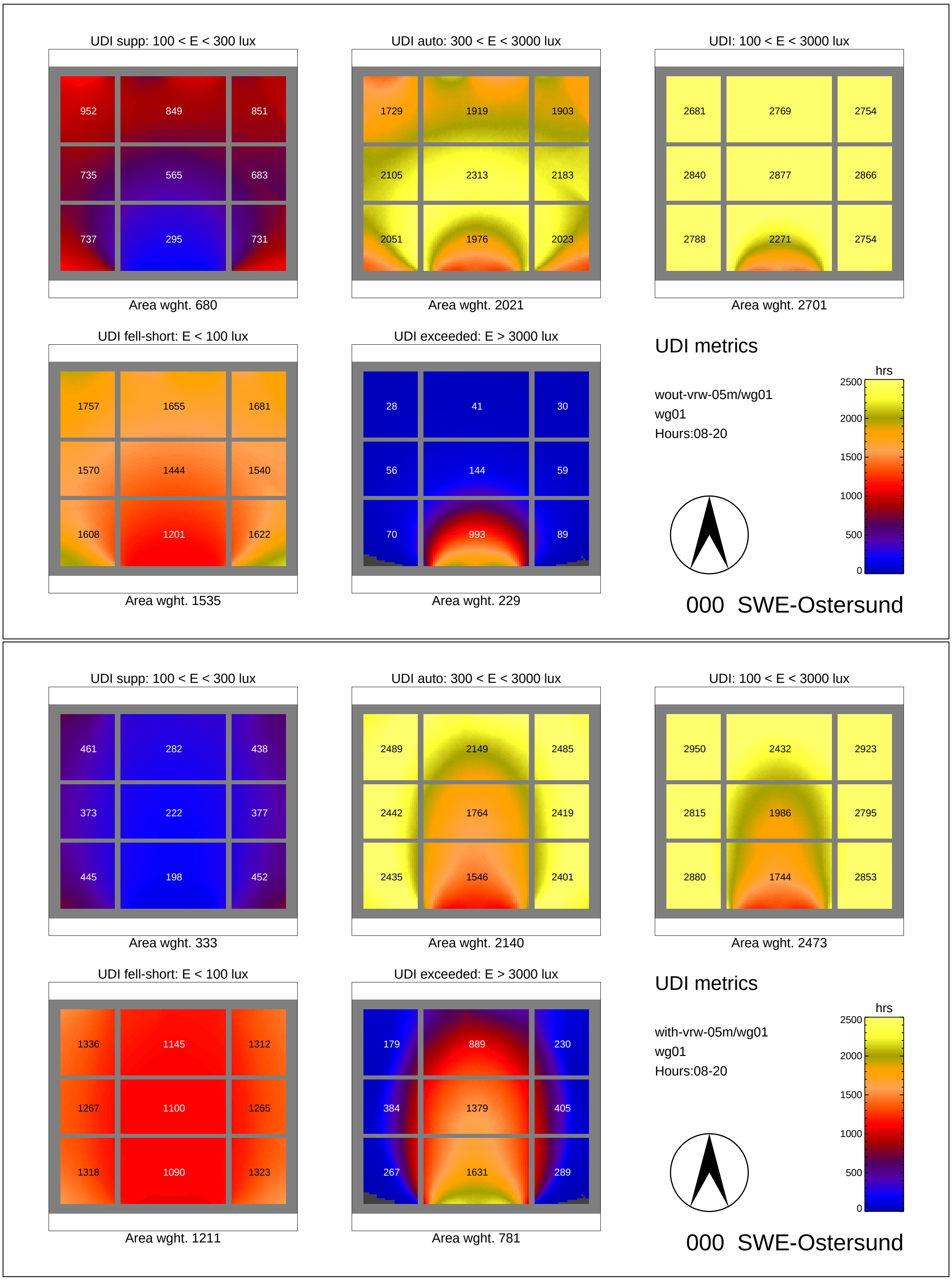

Figure 5: UDI plots for the living room without (top) and with (bottom) skylights (Ostersund climate).

4 Electric lighting model

Building users entering a space where there is little daylight will of course switch on the electric lights. The probability that users switch-on electric lights was found to be correlated with the minimum daylight illuminance on the working plane [26]. The correlation presented by Hunt in 1980 was based on just a handful of samples and there was considerable scatter in the switch-on probability when the daylight illuminance was in the range 50 to 500 lux, which is typical of the range experienced in many buildings. A later study provided support for the Hunt model, but as with the original study there was large scatter in the measured daylight illuminances that triggered the switching on of lights [25]. In addition to the switch-on probability, there will also be switch-off probabilities. Relatively little field study data has been published regarding switch-off behaviour, and determining a correlation with daylight is more confounding than for switch-on since other factors come into play. For example, switch-off probabilities could be significantly determined by the overall appearance of the space and the particular design of the lights, since it is sometimes not obvious to the occupant that lights have been left on when daylight provision is high. Furthermore, the studies that have been carried out are mostly for non-domestic buildings, commonly office spaces. One of the few domestic models is known as RT 2005 which originated in France.

4.1 The RT 2005 residential model

In the RT 2005 residential model the calculation of consumption in each zone Q_z is determined from:

$$Q_z = \frac{P_z C_1 C_2}{1000} \tag{2}$$

The installed lighting power for the zone is P_z. No artificial lighting control other than hand switch is used, which indicates that the coefficient $C_1 = 0.9$. The coefficient C_1 corresponds to an average percentage of use of artificial lighting. It is further weighted by a coefficient C_2 which gives the probability of activation of artificial lighting depending on the level natural lighting. It is determined by linear interpolation between the four points given in Table 2. These points are plotted in Figure 6. The steep fall-off in switch-on

Daylight illuminance [lux]	Coefficient C_2
0	1
100	1
200	0.05
2,800	0

Table 2: Parameterisation of the C_2 coefficient in the RT 2005 Model.

probability in going from 100 to 200 lux of daylight is shown using a reduced lux scale in the inset plot. Note that this steep-fall occurs within the UDI-a range, i.e. between 100 and 300 lux. We consider three periods when the lights may be on: 7am to 9am; 9am to 7pm; and, 7pm to 10pm. The configuration of the six spaces for the electric lighting calculation is given in Table 3 below. The occupancy factor vector refers to the three periods, whilst the sensor planes vector refers to the number of calculation planes in the space which varies between one and ten.

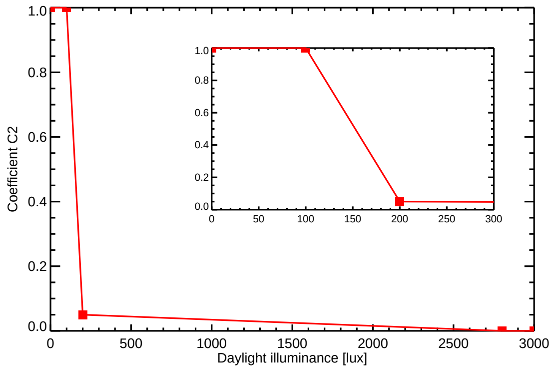

Figure 6: Electric light switch-on probability as a function of daylight illuminance

Space	ID	Installed power [W]	Occupancy schedule (default)	Sensor planes (default)
Living room	wg01	80	[1.00 0.30 1.00]	[0 0 0 0 1 0 0 0 0]
Kitchen	wg02	255	[1.00 0.15 1.00]	[0 1 0 1 0 1 0]
Hallway	wg03	360	[1.00 0.30 0.75]	[1]
Small bathroom	wg04	100	[1.00 0.05 0.20]	[1 1]
Large bathroom	wg05	300	[1.00 0.05 0.20]	[1 1]
Stairs	wg06	80	[1.00 0.30 0.75]	[1 1 1 1 1 1 1 1 1 1]

Table 3: Configuration of the six spaces for the electric lighting calculation.

Rather than present results for particular occupancy patterns, e.g. weekdays and weekends, our intention instead is to delineate overall sensitivities in the model to various input parameters. Here we present results for just the living room (wg01). The basecase occupancy profile for the three periods is $[1, 0.3, 1]$ i.e. [full occupancy, average 30%, full occupancy]. Additionally, we predict for a case where there is full occupancy for all three periods, i.e. $[1, 1, 1]$. Another parameter we investigate is the number and location of 'sensor planes' - the daylight illuminance on these is used as a potential trigger to switch on electric lights. For the living room there are nine possible planes (Figure 1).

The basis of the switching model is that, regardless of the number of sensor planes, the daylight on the sensor plane with the *lowest* illuminance is used in the light switching algorithm. The rationale for this model is that the occupant may switch on the lights even though most of the planes may be receiving sufficient daylight provided that there are one or more less well illuminated planes in the space. Here we consider two extremes, the basecase where it is just the daylight on the central plane in the living room that is active, i.e. which is used is the light switching algorithm. The vector describing this is $[0, 0, 0, 0, 1, 0, 0, 0, 0]$. And another where all nine planes participate in the switching, i.e. $[1, 1, 1, 1, 1, 1, 1, 1, 1]$. Thus there are four combinations of occupancy factor and number/location of sensor planes. We would expect that, with increasing occupancy and having a greater number of sensor planes, both of these would lead to a greater use of electric lighting, and, potentially a greater saving resulting from increased daylight provision (i.e. from the addition of a skylight). A graphic illustrating the occupancy factor and the sensor planes for all six room is given in Figure 7.

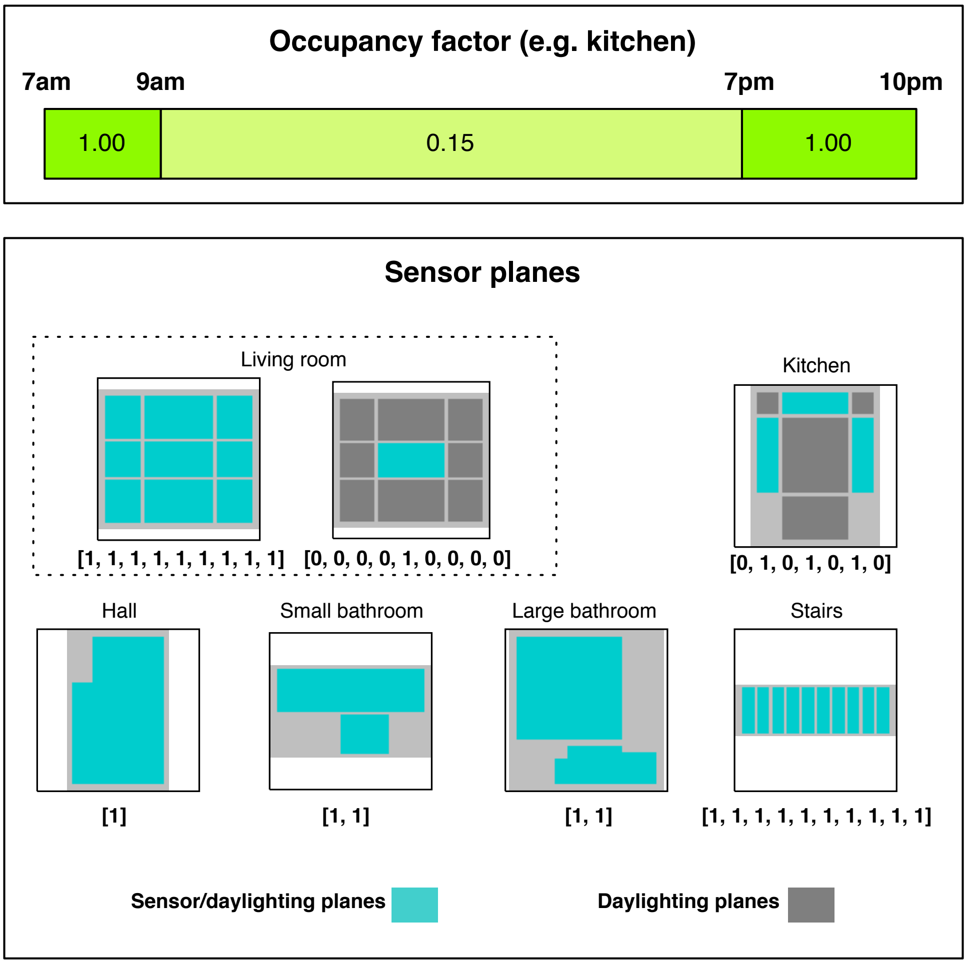

Figure 7: Occupancy factor and sensor planes

4.2 Potential lighting energy savings due to addition of a skylight

The potential for increased daylight provision from a skylight to save electric lighting energy was determined as follows - the example given below is for the living room, but the principle was the same for all six spaces. The distribution in daylight illuminance across the nine calculation planes in the living room was predicted at a 15 minute time-step for a full year. Approximately 10,000 calculation points were used to represent the nine planes. This was done for all 64 combinations of eight climates, four building orientations and two building types (i.e. with and without skylights). At each time-step, the mean daylight illuminance across each calculation plane was determined from the collection of points that comprise each plane. Next, the coefficient C_2 was determined using the smallest of the mean illuminances for all the sensor planes considered, i.e. for the results here, either just the central plane or all nine. The instantaneous electrical power Q_z was determined using Equation 2 and stored. The annual electric power consumption for electric lighting in this space was determined for all 32 combinations of climate and orientation, and for cases with and without skylights. The potential to save electric lighting energy is simply the difference between the with and without skylight cases.

The results are shown in Figure 8. As noted in the previous section, there are four scenarios covering the combinations of two occupancy profiles and two arrangements for sensor planes used in the switching model. For each of these scenarios, there are 32 predictions of energy saving covering all the combinations of climate and building orientation. The energy saving predictions for each scenario are presented as a set of points along a horizontal line. For this stage in the study we are interested primarily in the range of predicted savings rather than wishing to note the identity of any particular case.

For the first profile A (i.e. minimal occupancy profile and using only the central plane for switching), the predicted saving ranges from 11.6 to 28.6 kWh/yr. For profile B the range is 17.6 to 38.8 kWh/yr. For C the range is 25.1 to 55.3 kWh/yr and, lastly, for D it is 39.0 to 77.6 kWh/yr.

The predicted energy saving due to illumination provision from a skylight is shown to be highly sensitive to the occupancy factor and the consideration of surfaces used to trigger light switching (i.e. the number and location of sensor planes). In addition to a consistent pattern showing a steady increase in the overall saving (in progressing from profile A to D), there is also a widening of the range of predictions within each scenario, i.e. a consequence of the variations in daylight provision due to the different climates and building orientations. For profile A the size of the range is 17.0 kWh/yr, but for D it is 38.6 kWh/yr.

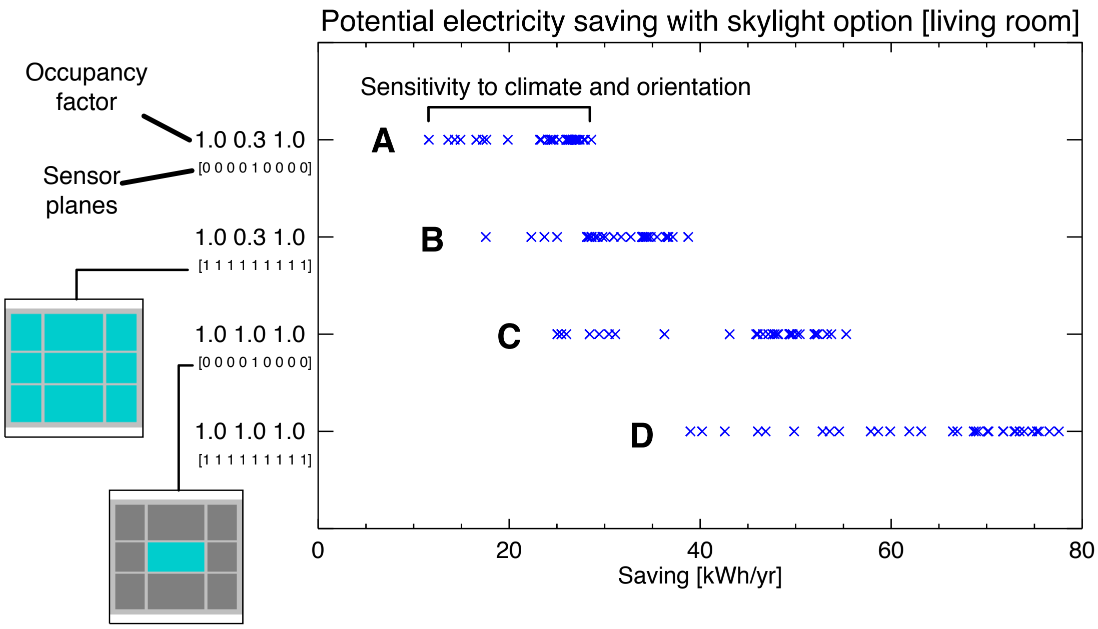

Figure 8: Sensitivity in predicted lighting energy saving (living room) across all combinations of climate and orientation for four profiles. In the inset graphics for the calculation planes, the two combination of sensor planes are illustrated (i.e. 1 = cyan = used).

5 A simulation model for non-visual effects

The daily cycle of day and night plays a major role in regulating and maintaining biochemical, physiological, and behavioural processes in human beings. This cycle is known as the circadian rhythm - the term “circadian” comes from the Latin circa, “around”, and diem or dies, “day”, meaning literally “approximately one day”. Circadian rhythms occur in almost all organisms from bacteria to mammals. The circadian rhythms are endogenous meaning that they are produced from within the organism, i.e. what is commonly referred to as the ‘body clock’. However for many organisms the cycle needs to be adjusted or entrained to the environment by external cues, the primary one of which is light.

The primary circadian “clock” in mammals is located in the suprachiasmatic nucleus (or nuclei) (SCN), a pair of distinct groups of cells located in the hypothalamus. The SCN receives information about illumination through the eyes. The retina of the eye contains not only the well-known photoreceptors which are used for vision (i.e. rod and cones) but also ganglion cells which respond to light and are called photosensitive ganglion cells. The SCN in turn coveys signals to the pineal gland, which, in response, controls the secretion of the hormone melatonin. Secretion of melatonin peaks at night and ebbs during the day; its presence modulates the wake/sleep patterns [27, 28].

The failure to maintain circadian rhythms that are firmly entrained to the natural 24 hour cycle of daylight results in many negative health outcomes for humans, though not all are fully understood. The degree and severity of the outcomes usually depends on the period over which the cycle is disturbed. A transitory disturbance to the circadian system familiar to many who have experienced a long-haul flight is jet-lag. When traveling across a number of time zones, the body clock will be out of synchronisation with the destination time, as it experiences daylight and darkness contrary to the rhythms to which it has grown accustomed. Depending on the individual it can take a few days to re-set the body clock to the local day - night cycle [29].

Less immediately obvious in its effects than jet-lag is the chronic persistence of poorly entrained circadian rhythms[29, 30]. This was first noticed in shift-workers, however it is believed to be one of the factors in the increasing occurrence of sleep-disturbance and related conditions in the wider population of the developed world [31]. Whilst the symptoms of sleep-disturbance can be at first mild, e.g. sleepiness, fatigue, decreased mental acuity, etc., the long term persistence of the condition may result in significant impacts on both health and worker productivity [32, 33, 34, 35, 36, 37].

The duration, intensity and spectrum of the light received at the eye are the principal factors determining the suppression in the production of melatonin by the pineal gland, and thus a key factor in the entrainment of the circadian cycle, Figure 10(a). Another important factor is the time of day when the light is applied. Inadequate light exposure can disrupt normal circadian rhythms and have a negative effect on human performance, alertness, health or safety.

Daylight often provides illuminances significantly higher than the design level, though this is only in close proximity to windows and perhaps also highly daylit spaces such as atria. If the typical illuminances in these zones are high - but not so great that blinds are needed - then those building users that regularly occupy the well-daylit spaces may perhaps experience stronger and more regular circadian entrainment stimuli than those users away from windows who are habitually exposed to lower illuminance levels at the eye. These considerations have resulted in the notion that a building through its daylighting may possess a *circadian efficacy* [38]. Given the current state of knowledge, it needs to be understood that the process of determining this 'circadian efficacy' is more one of carefully considered judgement than commonly agreed procedure. Notwithstanding this caveat, a workable schema was devised by Pechacek under the supervision of Andersen (then at MIT) together with the assistance of Lockley from the Division of Sleep Medicine, Harvard Medical School, Boston [38].

Given the evident limitations in delivering significant amounts of daylight from vertical windows more than a few metres into a deep-plan space, it is plausible that residential dwellings and low-rise buildings with some form of top-lighting (e.g. skylights) have a greater potential to achieve the daylight illuminance levels at the eye required for non-visual effects. While no actual recommendations can - or should - yet be made because of our limited understanding of the effects of exposure to light on human health and circadian organisation, especially during daytime, the relevance of some critical design parameters on the perceived light spectrum, intensity and duration is certainly a topic of investigation. Now is also the right time to start developing calculation methods and simulation workflows that would allow us to extract circadian-relevant information from traditional, vision-based building simulation results. From there, the light exposure and timing influenced by design and environmental factors such as opening size and orientation, climate type, or dominant view directions can be evaluated prospectively. The components of a model to predict non-visual effects for daylight exposure are given in the schematic shown in Figure 9.

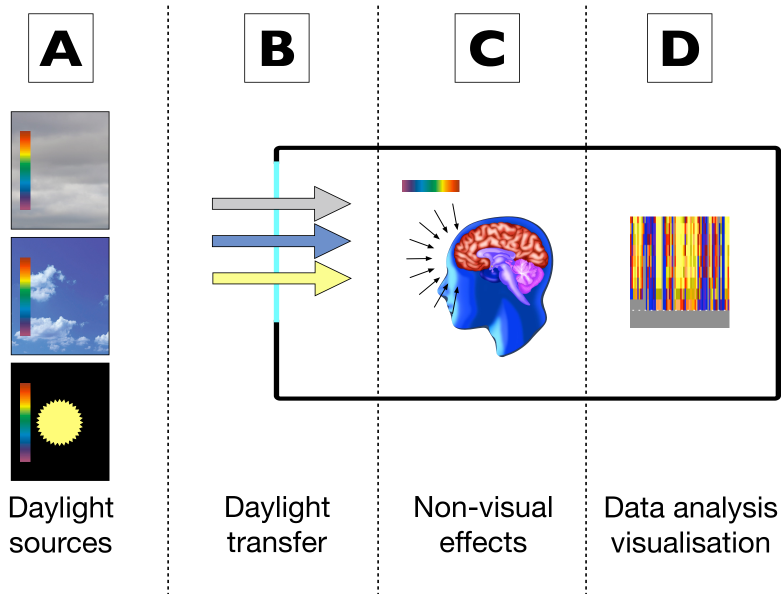

Figure 9: Components of a simulation model for non-visual effects

The first two components of the model have already been largely covered in previous sections. The daylight sources are the standardised climate files. However, their application in a model for N-VE requires that the spectral characteristics of the various sources (i.e. direct beam, overcast skylight and light from a clear blue sky) are inferred from values in the basic climate data. It is possible to approximate the spectral composition for these daylight sources - this will be described shortly. The light transfer component of the model is that which determines the vertical illuminance at the eye resulting from instantaneous sky and sun conditions derived from the climate data. This is achieved using a modified version of the climate-based daylight simulation approach already described.

The following sections will expand on the other two components: the model for non-visual effects and the data analysis/visualisation procedures required to meaningfully present and interpret the results. A journal paper by Andersen, Mardaljevic and Lockley describing the model for non-visual effects has recently been published by Lighting Research & Technology [1].

5.1 Relevant findings from photobiology research

Our approach uses outcomes of photobiology research to define threshold values for illumination in terms of spectrum, intensity, and timing of light at the human eye, and translates these into goals for simulation – and perhaps, ultimately, into goals for building design.

Compared to the luminous efficiency function of the eye which has a peak value at 555 nm, the action spectrum for the suppression of melatonin is known to be shifted to the blue end of the spectrum [39]. This is illustrated in Figure 10(b). The C(λ) curve is based on that derived by Pechacek, Andersen & Lockley [38].

On the other hand, threshold photon densities (photons/cm^{2}s^{-1} on the retinal surface) have been found to be necessary to have a significant effect on circadian photoreception, and a dose-response curve was determined by Cajochen *et. al.* in 2000 for subjective alertness during night-time exposure to polychromatic light [40] (most other studies were based on monochromatic light exposure). This particular study found that a (visual) illuminance of about 300 lux was required to achieve a 100% subjective alertness effect when the light source was fluorescent lighting (4100K)[2].

As of yet, very few alertness studies for polychromatic light are available during daytime exposure and none provides a dose-response curve. One daytime study of reference is that conducted by Phipps-Nelson *et. al.* in 2003 [41] which compares the effect of daytime bright (1000 lux) and dim (<5 lux) light on alertness. The latter was assessed through measures of subjective and objective sleepiness for subjects slightly sleep-deprived, and also used fluorescent lighting. Unlike previous related studies [42] [43] that used higher 'dim' light levels (50 lux e.g.), this one reported a significant effect of bright light exposure during daytime, probably due to the combination of having particularly dim comparison levels and sleep-deprived subjects.

The next sections describe how these selected findings in the photobiology field have been applied to building simulation and the prospective assessment of the 'circadian potential' of a space.

5.1.1 Illumination spectrum

To determine light levels relevant to our circadian photoreception system (as opposed to our visual system), we need to convert climate-based vertical illuminance calculations, that are derived from our visual system's sensitivity curve $V(\lambda)$, into their equivalent 'circadian-lux', based on the $C(\lambda)$ action spectrum illustrated in Figure 10. In other words, assuming one can calculate the illuminance at the eye - expressed in (visual) lux - independently for overcast sky light, sunlight and clear sky light (which is how the climate-based simulation used here operates), then one can also determine an equivalent

[2] Based on a visual reading of Fig 5 (left), p. 81 in [40]

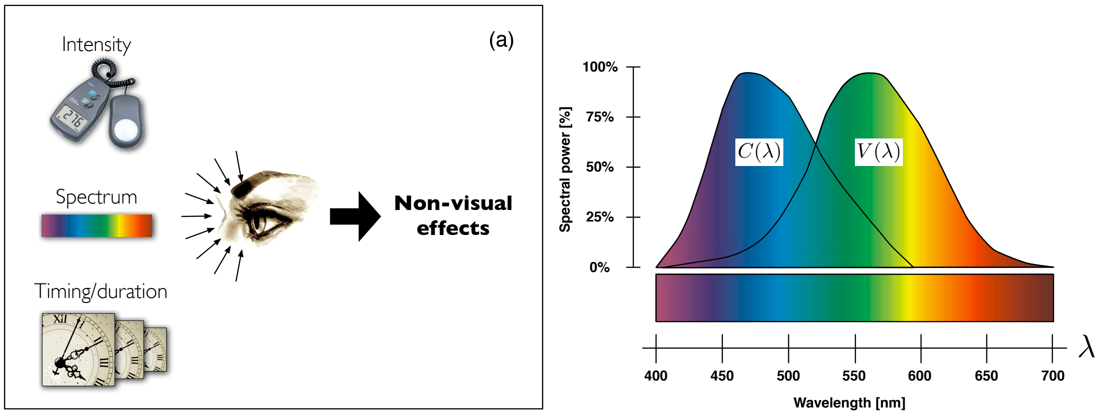

Figure 10: Factors influencing the non-visual effects of daylight (a), and the spectral responses of visual system, i.e. photopic curve $V(\lambda)$, and circadian system, i.e. melanopsin action spectrum $C(\lambda)$ (b).

'circadian' illuminance using the approach described by Pechacek *et. al.* [38] and illustrated in Figure 11. This conversion comes down to determining the 'circadian' efficacy of light, starting from a known illuminance and relative spectral distribution and thus being able to define an absolute radiometric spectrum. By multiplying the latter by the 'circadian' sensitivity curve $C(\lambda)$ discussed above, one can extract a 'circadian-lux' value. The normalization factor (683 lm/W for photometry) is considered equal to 1 for lack of a standardized value.

As a result, one can account for the greater 'circadian' efficacy of, say, 1000 lux of diffuse light from a clear blue sky compared to 1000 lux of light from the sun. As already noted, it is possible to infer sky model type (e.g. overcast, intermediate, clear) from diffuse horizontal and direct normal illuminance in the climate data. It then becomes possible to categorise the daylight into three distinct sources and approximate each of these to a CIE standard illuminant. Thus solar beam radiation is approximated to D55, overcast sky to D65 and light from a clear blue sky to D75. For the analysis reported here, we consider the reflecting surfaces (e.g. walls, floor, ceiling, ground, etc.) and the glazing elements to be achromatic, i.e. the spectral properties of the light are not modified by reflection or transmission. This seems a reasonable approximation for spaces with a neutral decor.

5.1.2 Intensity of illumination

Figure 12 shows the number of lux that, based on the $C(\lambda)$ efficacy curve and the method described above, a given value of (visual) illuminance for a specific source would correspond to for another source: for example, 190 lux of Daylight Illuminant D65 would correspond to 700 lux of 555nm LED light in terms of circadian effectiveness. This figure also shows how subjective alertness would correlate with illuminance thresholds (based on the night-time study by Cajochen *et. al.* [40]), depending on the light source. Figure source is Pechackek 2008 [44].

While it is too early to derive any reliable illuminance threshold for alertness from the night-time and daytime studies published so far, we already know that daytime 'circadian-lux' thresholds are likely to be determined in the future in association with subjective and objective alertness, as well as other physiological and health effects.

Until these more reliable thresholds are determined we can prospectively use the dose

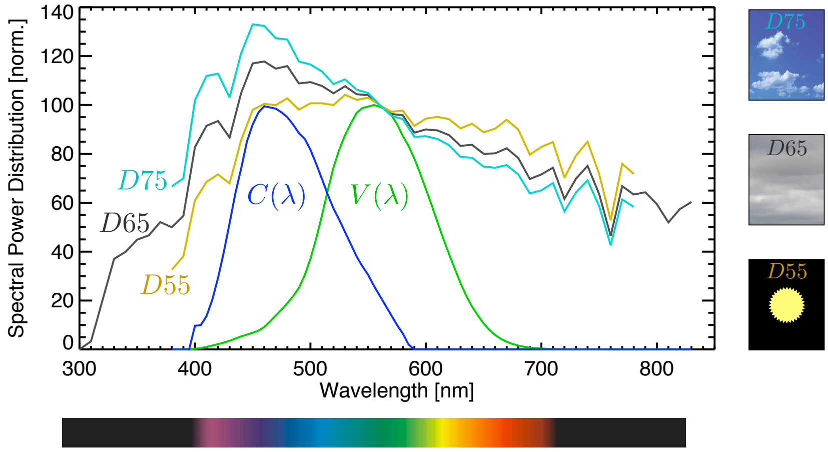

Figure 11: Spectral power distribution for CIE daylight illuminants associated to the three daylight sources alongside normalised photopic and circadian sensitivity curves $V(\lambda)$ and $C(\lambda)$.

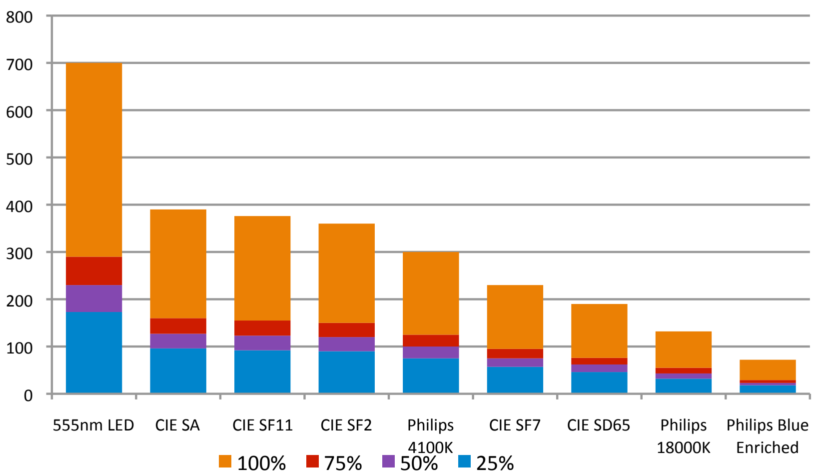

Figure 12: Circadian-equivalent illuminances for a selection of light sources

response curve from the night-time Cajochen study [40] in combination with the daytime Phipps-Nelson results [41] as a lower and an upper bound, respectively, for alertness effects: one can reasonably assume that the illuminance threshold required to have a significant effect on alertness during daytime will be at least as high as what was found out during night-time. On the other hand, one can also reasonably assume that if an effect was found during daytime with a given illuminance, those effects will also be observed with a higher illuminance. Light timing and exposure history also have a critical influence on how the circadian system is stimulated. Research in this area indicates that light exposure thresholds will be strongly dependent on the duration of the light exposure. This discussion being beyond the scope of the present report and not advanced enough to provide more tangible hypotheses, we will consider these thresholds as indicative exposure levels for which one might expect a non-visual effect (alertness increase e.g.) during nighttime and daytime, respectively. One should note that the Phipps-Nelson study was run with slightly sleep-deprived subjects but the argument for now is more on the method than the exact values. In both cases, fluorescent tubes were used as the light source: Philips Color 840 4100K fluorescent tubes in the former study and Thorn 2L (36 W) tubes in the latter.

We find out that the threshold for initiating an alerting effect would be equivalent to an illuminance at the eye of 210 lux, 190 lux, and 180 lux for Illuminant D55 (used for sunlight), D65 (used for overcast sky light) and D75 (used for clear (blue) sky light) respectively [38]. As one would expect, the bluer spectrum corresponds to the lowest equivalent illuminance threshold.

The Phipps-Nelson study used a mean eye illuminance of 1056 lux as the bright light condition to evaluate daytime alerting effects. We do not have spectral data for the particular fluorescent tubes that were used but can assume that they approximate the Illuminant F7 (Daylight Fluorescent) reasonably well (given that the thresholds themselves require further photobiology research, it actually does not really matter how precise the spectrum is). We then have all the data necessary to determine the 'circadian' illuminance with daylight that would be equivalent to 1056 lux of fluorescent (F7) light [45]: we find 960 lux, 870 lux and 830 lux for Illuminants D55, D65 and D75.

To avoid having to calculate the equivalent circadian illuminance, and then apply the relevant alertness thresholds independently for overcast sky light, clear sky light and sunlight, we will arbitrarily choose a single light source of reference, and thus consider 210 lux as the lower bound 'circadian' threshold E_{low}^{D55} and 960 lux as the upper bound 'circadian' threshold E_{up}^{D55} for the Illuminant D55 used to approximate sunlight. Given the noted uncertainties, a simple ramp-function appears as a reasonable proxy to represent the likelihood that the vertical illuminance at a given point in time and for a given view direction is sufficient to affect the circadian system and have either circadian entrainment and/or subjective alertness effects: low likelihood (0%) below 210 lux and high likelihood (100%) above 960 lux with a linear interpolation between these, as illustrated in Figure 13. Note that the illuminance is in terms of D55 equivalent, as noted above. These and other parameters will be refined with advances in measurements from photobiology studies.

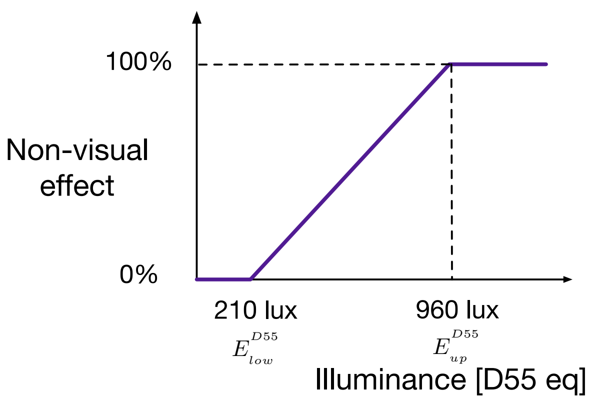

Figure 13: Schematic showing ramp-function for non-visual effect.

5.1.3 Timing factors for illumination

The timing of the exposure determines the type of effect and whether it is beneficial or detrimental. Given our incomplete knowledge, the boundaries are 'fuzzy', but nevertheless it is possible to delineate three distinct periods: early to mid-morning; mid-morning to early evening; and the rest as notional night-time, Figure 14 [46]. In the early to mid-morning period, sufficient daylight illuminance (e.g. ∼1,000 lux or greater at the eye) can serve to 'lock' and maintain a preferred (i.e. healthy) sleep - wake cycle. From mid-morning to early evening high levels of daylight illuminance (e.g. ∼1,000 lux or greater at the eye) may lead to increased levels of subjective alertness. For the remainder of the day (mostly hours of darkness) daylight exposure that might trigger the N-VE is to be avoided so as not to disrupt the natural wake-sleep cycle. The timing factor includes not only the duration and time of occurrence but also the history, i.e. recent exposure. However we do not know enough yet to warrant the additional complexity of including this factor, so we consider only time of occurrence in isolation of the duration and history of the exposure.

We present the cumulative N-VE occurring in these three periods using a simple graphical device that we have called the 'sombrero'. The boundaries for the periods were set as follows: 06h00 to 10h00 (inner circle of the 'sombrero'); 10h00 to 18h00 (middle circle of the 'sombrero'); and, 18h00 to 06h00 (outer circle of the 'sombrero'). The use of the sombrero plot is further explained below.

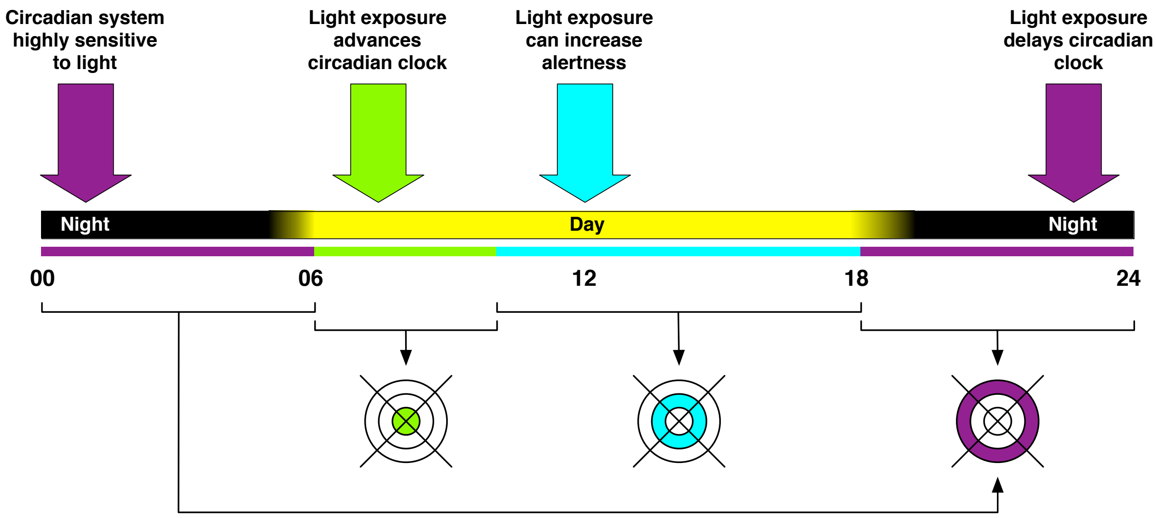

Figure 14: The day is divided into three periods according to type of non-visual effect. The cumulative occurrence of the degree of N-VE determined for each of these periods is represented using the 'sombrero' plot.

5.2 Example output

Using the model described above, the magnitude of the non-visual effect produced by daylight illumination at the eye was predicted at a number of locations in the living room for the entire year at a 15 minute time-step, and for four horizontal view directions at 90° increments. This was done for all 64 combinations of climate, building orientation and building type. Example output showing both the time-series (temporal maps) and cumulative occurrence (sombrero) plot for one location in the living room is given in Figure 15. The small inset graphic in the figure shows the position in the room of the calculation plane (red square) and the arrangement of the four temporal maps corresponds to the view directions illustrated by the green arrows.

In the temporal maps, the instantaneous magnitude of N-VE is shown as a percentage, i.e. 0% = zero N-VE (black shade), 100% = full N-VE (white shade) and false colour for values between 0 and 100%. The lower and right-hand temporal maps represent views away from the corner and directed towards the opposing walls, i.e. 'right' and 'down'. These views look in part towards the window wall and the centre of the room which in this case is illuminated by a skylight (Figure 1). These directions show a much greater occurrence of N-VE than the other two view directions which look away from the middle of the room and into one corner. The pattern is what we might expect. The 'sombrero' plot shows the percentage of the cumulative occurrence of N-VE across the year for each of the three periods described in the previous section.

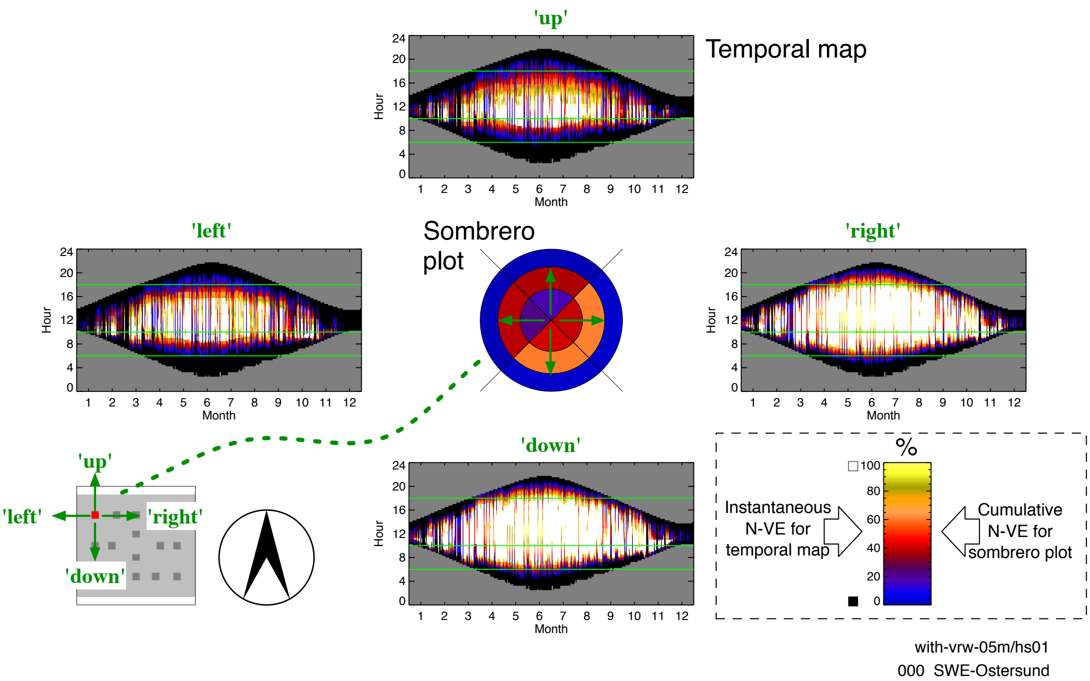

Figure 15: Example output showing both the time-series (temporal maps) and cumulative occurrence (sombrero) plot for the living room with skylight. The Ostersund (Sweden) climate file was used and the building had the default orientation 000 (i.e. north at the 'top').

The same 0-100% false-colour scale as for the temporal maps is used to shade the 'sombrero' plot. The following can be determined from the plot. For the 06h00 to 10h00 period (inner circle - syncing of circadian clock), the cumulative N-VE at this location was approximately 40% for the views 'right' and 'down'. Because the shaded value in the 'sombrero' plot is a cumulative measure, it could represent a full N-VE occurring for 40% of the time, a 40% N-VE occurring for all of the time, or, as is more likely, something in between. For the other two view directions the cumulative N-VE is around 20% each for both.

For the 10h00 to 18h00 period (middle circle), the cumulative N-VE for illuminances that promote subjective alertness is around 60% for the views 'right' and 'down', and just under 40% for the other two view directions. For the 18h00 to 06h00 period, the cumulative N-VE is less than 3% for the views 'right' and 'down' and less than 1% for the other two views.

We shall not dwell on small numerical differences in predicted cumulative N-VE, rather our intention in this initial paper is to reveal using graphical means significant differences in cumulative N-VE due to various factors, e.g. the addition of a skylight. For example, in Figure 16 we compare the predicted cumulative N-VE for the cases without and with skylights for the Ostersund (Sweden) climate (building orientation as indicated in the figure). Comparison of the two cases gives an immediate impression of the potential of the space to produce illuminances which have a non-visual effect. For the case without skylights, the degree of N-VE is greatest for those view points/directions located closest to and directed towards the (external) window. The case with skylight shows a greater cumulative N-VE for all locations, and with less of a preference for those views directed towards the window.

A few illustrative plots showing the change in predicted non-visual effect for a small number of cases are given in the Appendix (Section 8.2).

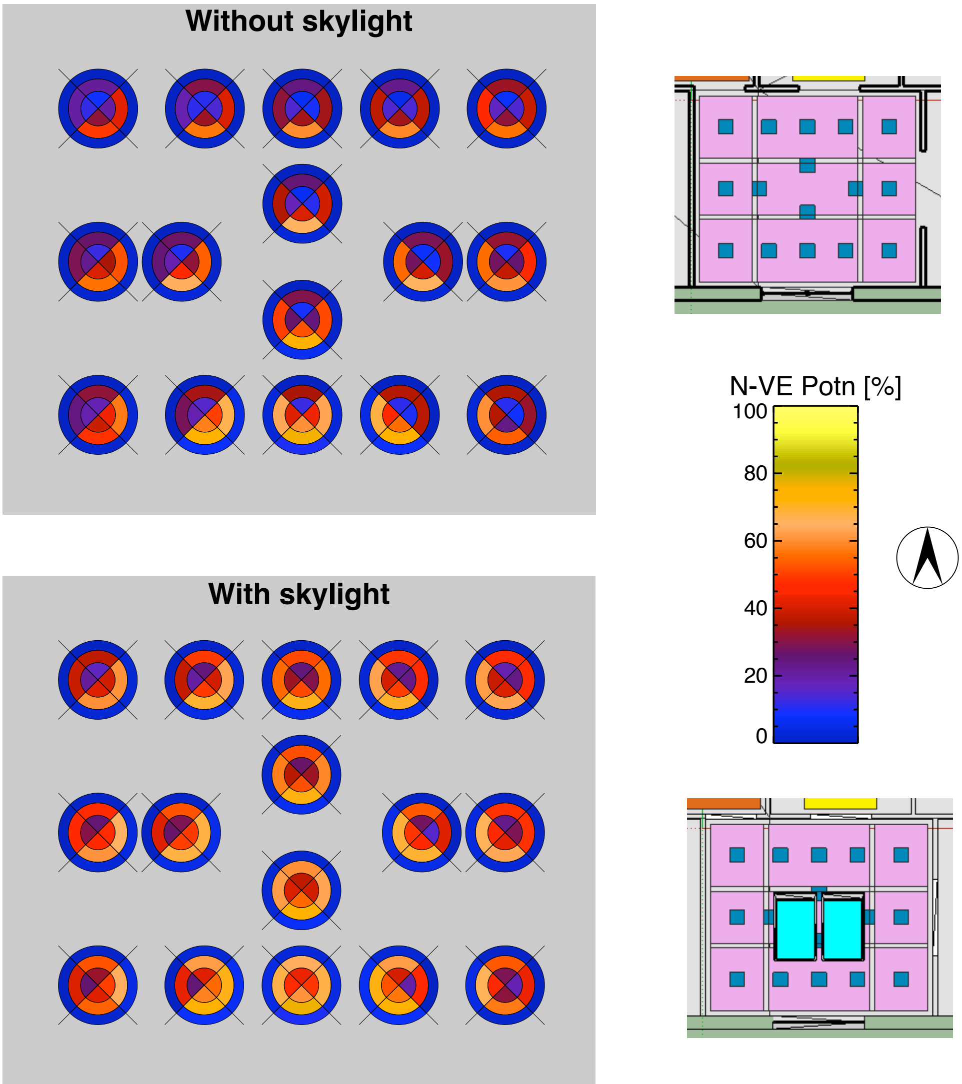

Figure 16: Predicted cumulative N-VE for case without and with skylights (Ostersund/000).

6 Summary of All Results

Here we present the results for all three analyses, i.e. daylighting, energy saving and non-visual effect, using a common graphical scheme for each one. We show the change in the various metrics (e.g. UDI-a) by plotting the difference in the achieved value for the case with and without the skylight. The results are clustered in groups of four (i.e. the four building orientations) for each of the eight climates, Figure 17. For example, the illustration in Figure 17 shows the change in the UDI-a metric (300 to 3,000 lux) for the living room space a whole, for the Hamburg (Germany) climate. For each orientation there is an increase - the value with the skylight is marked by a box at the end of the line. The orientation showing the greatest increase is that with north pointing 'downwards' (blue compass arrow), i.e. the living room window (which is at the 'bottom' in this floor plan) is facing north. For this orientation, the UDI-a metric increases from ∼45% to ∼65% of the year, i.e. illuminances in the UDI-a range occur for an additional ∼20% of the year [08h00-20h00].

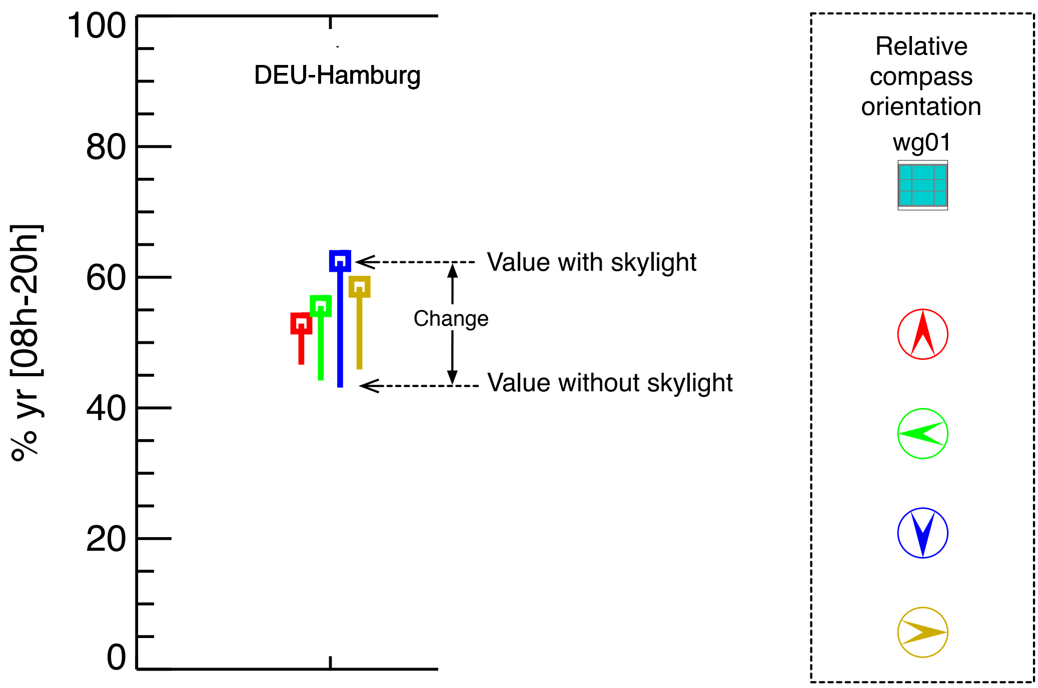

Figure 17: Illustration of common graphical scheme to show the performance for all three analyses, i.e. daylighting, energy saving and non-visual effect.

To aid interpretation and understanding of these plots, it helps to consider the orientation of the main perimeter glazing for the space rather the the orientation for the building *per se*. This is because the various daylight measures can be sensitive to the ingress of sunlight - both direct and indirect - which depends to a large degree on the aspect (i.e. orientation) of the glazing. The orientation of the vertical glazing - for those spaces that have it - with respect to the four compass points is illustrated in Figure 18. Note also that, the horizontal component of the direction of the (sloped) skylight glazing will be the same as the (perimeter) vertical glazing.

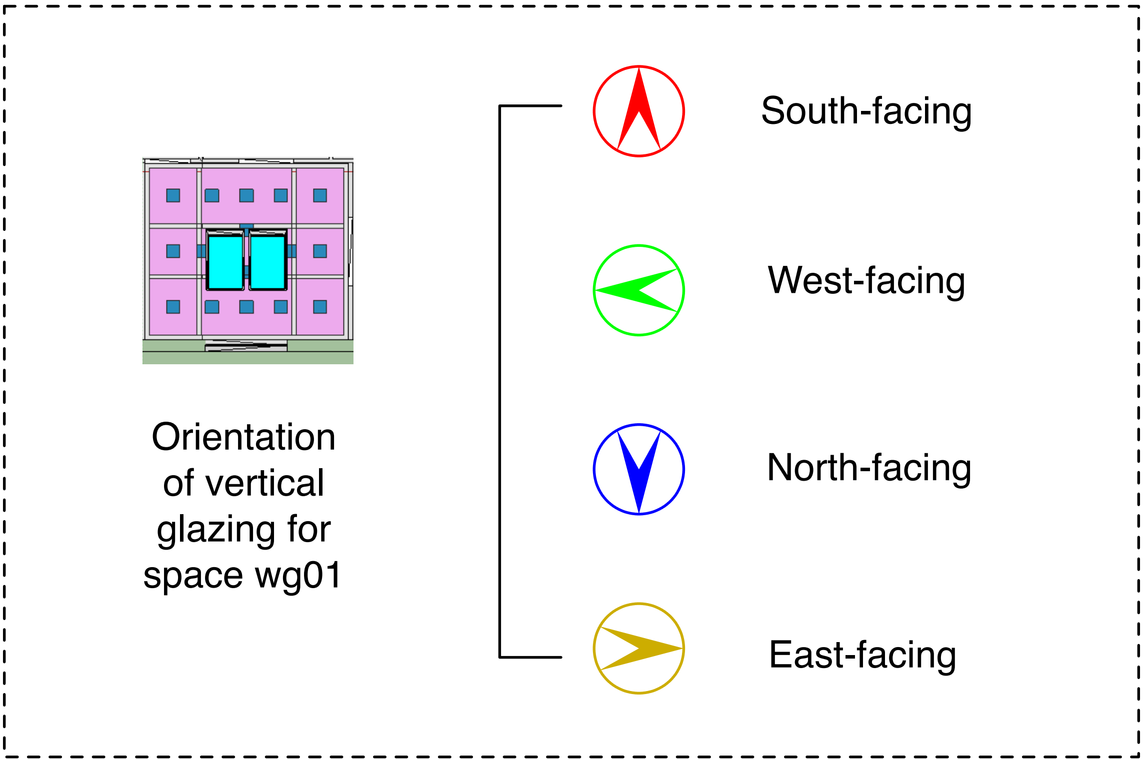

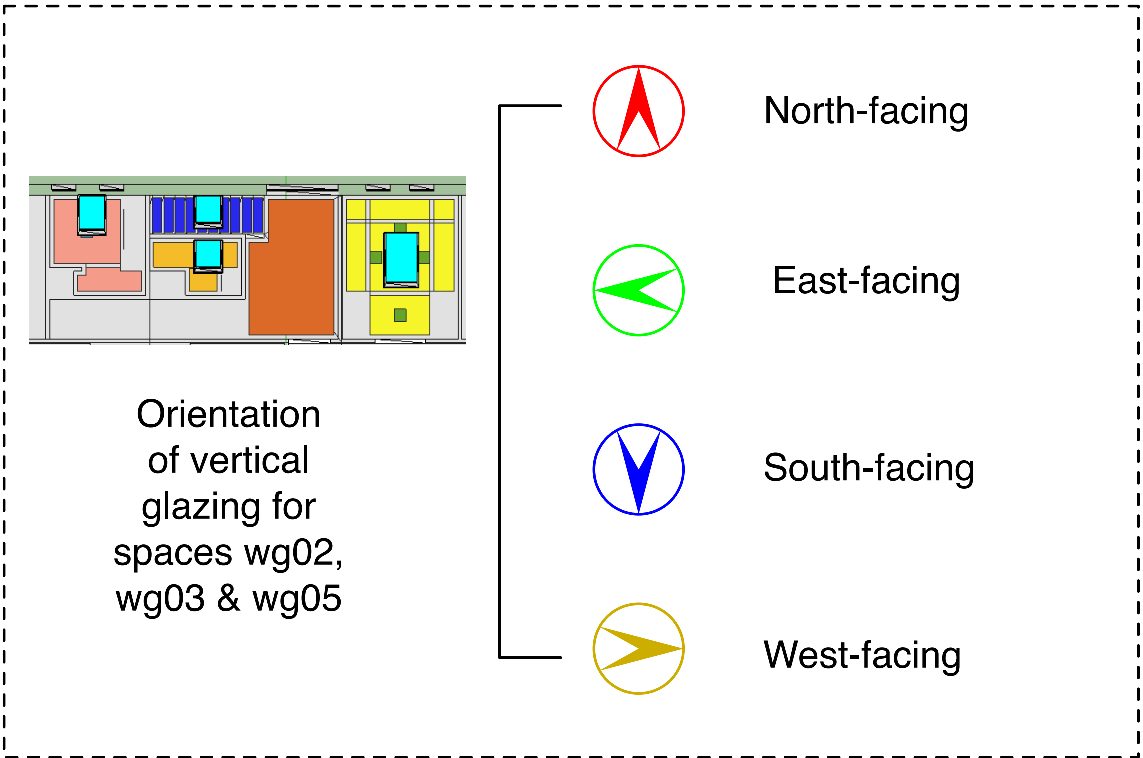

Figure 18: Illustration showing orientation of the vertical glazing (where present) with respect to the four compass icons showing the relative orientation of the building to due north (i.e. arrow direction in the icon).

6.1 Daylighting Performance

The daylight performance of the six spaces was assessed using the useful daylight illuminance scheme. The summary charts that follow show the values for the five UDI metrics:

- UDI-s (UDI-supplementary) - illuminances in the range 100 to 300 lux.
- UDI-a (UDI-autonomous) - illuminances in the range 300 to 3,000 lux.
- UDI-c (UDI-combined) - illuminances in the range 100 to 3,000 lux.
- UDI-f (UDI-fell-short) - illuminances less than 100 lux.
- UDI-e (UDI-exceeded) - illuminances greater than 3,000 lux.

We summarise the performance of the space by showing the area-weighted mean value for the UDI metric across the considered sensor planes – these are shaded cyan in the image of the plan area that accompanies each page of plots. With the addition of a skylight, the following trends in changes for the UDI metrics are observed on a space by space basis.

6.1.1 The living room - wg01

For this space (wg01) there is a marked decrease in the occurrence of UDI-s across all climates and orientations, Figure 19. This is largely due to increases in UDI-a, i.e. illuminances that were in the range 100 – 300 lux are 'bumped-up' to the 300 – 3,000 lux range. There is a decrease in the occurrence of illuminances less than 100 lux (i.e. UDI-f) though this is smallest for the sunniest climates, i.e. Madrid and Rome. There is an increase in the occurrence of illuminances greater than 3000 lux, particularly for those orientations that allow the ingress of direct sun, i.e. all but when the glazing is facing north (i.e. compass ( )). All nine sensor planes at table height were used in the evaluation.

6.1.2 The kitchen - wg02

For this space (wg02) we see a pronounced improvement in the overall daylighting with the introduction of the skylight, Figure 20. The occurrence of illuminances in the range 100 – 300 lux decreases by up 35% of the annual period. Whilst the occurrence of illuminances in the desired 300 – 3,000 lux range increases by up to 40% or even more. For all but Madrid and Rome, the decrease in the annual occurrence of illuminances less than 100 lux is around 20%. There is a slight increase in the occurrence of illuminances greater than 3,000 lux, which is largely for those orientations where the kitchen glazing faces either south ( ) or west ( ). The three main worktop sensor planes were used for the evaluation of the summary UDI metrics.

6.1.3 The hall - wg03

The hall (wg03) does not have a dedicated skylight and so the effect here is solely due to light spillage from adjacent spaces, which we expect to be small. Nonetheless, even here we see decreases in UDI-s and corresponding increases in UDI-a of up to ∼10%, Figure 21. Illuminances in the range 300 – 3,000 lux occur between ∼20% and ∼50% depending on the climate (i.e. location) and orientation. A single sensor plane – the entire floor of the floor area – was used for the evaluation.

6.1.4 Small bathroom - wg04

The small bathroom (wg04) does not have a pre-existing vertical window, so the only daylight results from the introduction of the skylight. Thus we see illuminances in the UDI-c range (100-3,000 lux) occurring for between ∼65% and nearly 80% of the year, Figure 22. The two sensor planes that comprise the majority of the floor area of the bathroom were used for the evaluation.

6.1.5 Large bathroom - wg05

The large bathroom (wg05) has two small windows positioned at a high level for privacy which provide only moderate amounts of daylight. The overall daylighting is again greatly improved by the addition of the skylight: increases in UDI-a range from ∼25% to ∼50% depending on the climate and orientation, Figure 23. The two sensor planes that comprise the majority of the floor area of the bathroom were used for the evaluation.

6.1.6 Staircase - wg06

The staircase (wg06) to the basement receives moderate light spillage from the hall. The introduction of the skylight greatly improves the daylight provision for this space. Because the key task here is simply using the stairs, the availability of daylight should be assessed using the UDI-c metric, i.e. the range that extents from 100 to 3,000 lux. The introduction of the skylight leads to an increase in the occurrence of illuminances in the UDI-c range of between ∼30% and ∼40% of the year, depending on the climate and orientation. Note also that there is a correspondingly large decrease in the occurrence of illuminances less than 100 lux (i.e. UDI-f). All of the ten sensor planes that make up the horizontal steps were used for the evaluation.

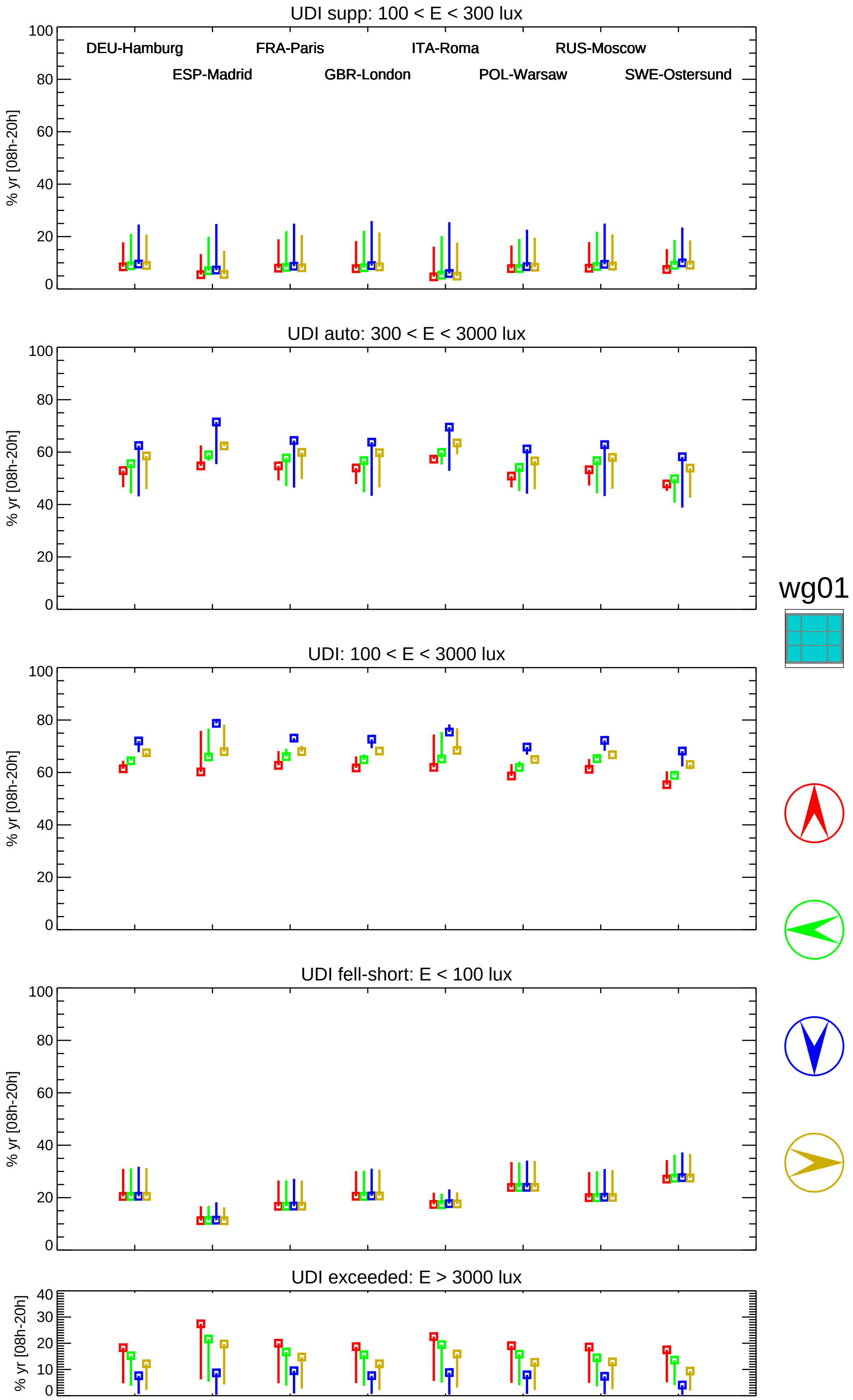

Figure 19: UDI metrics for the living room (wg01)

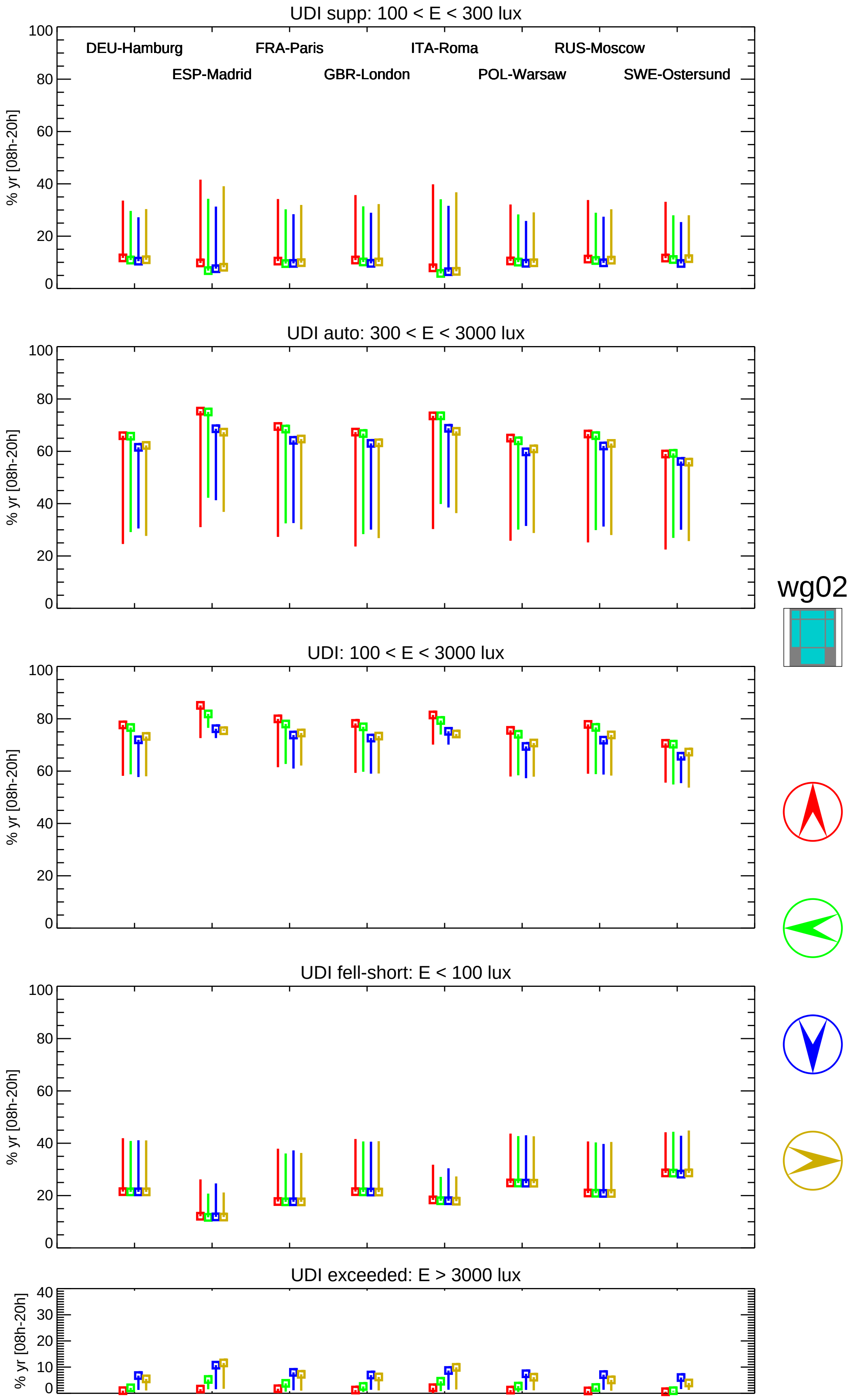

Figure 20: UDI metrics for the kitchen (wg02)

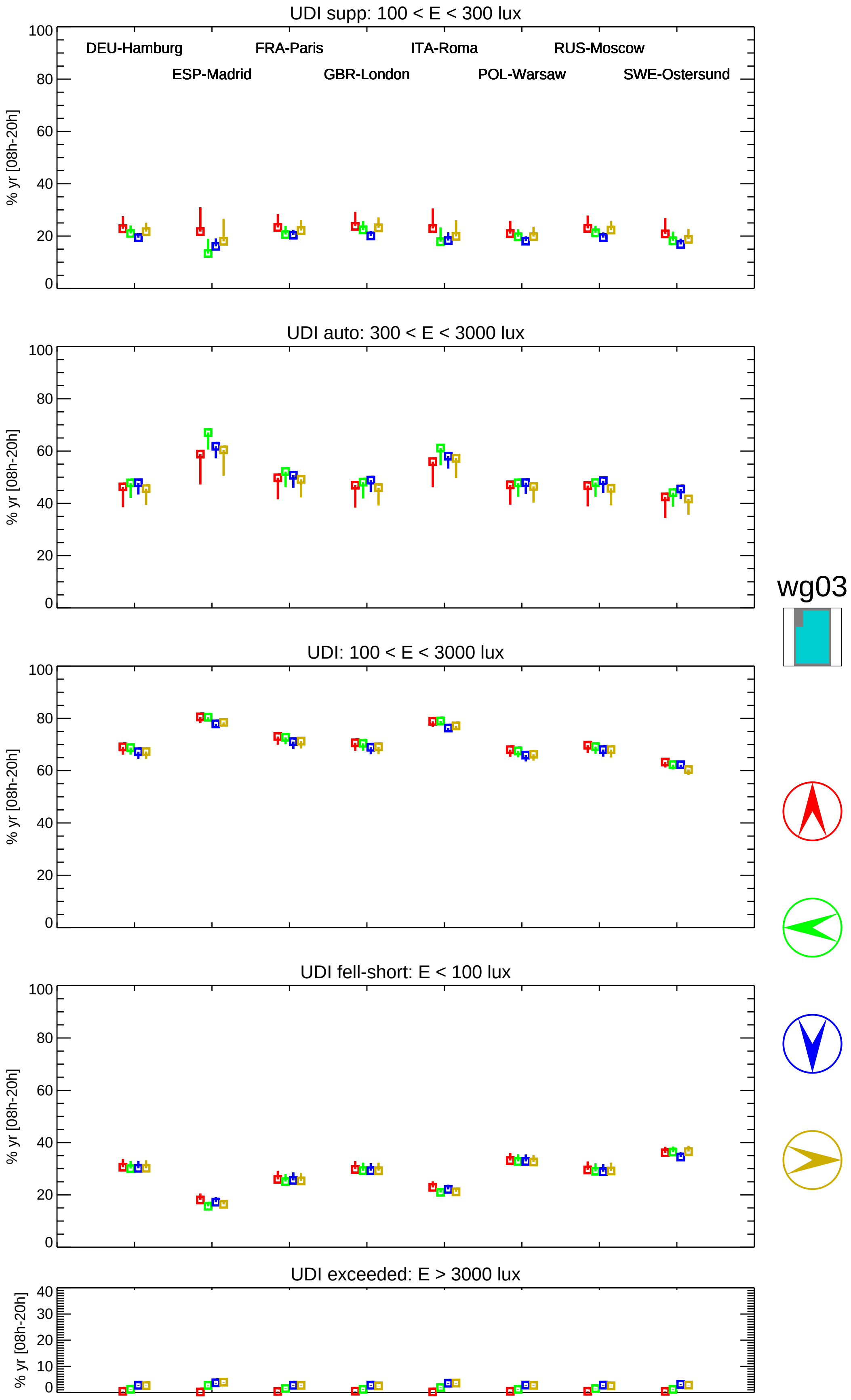

Figure 21: UDI metrics for the hall (wg03)

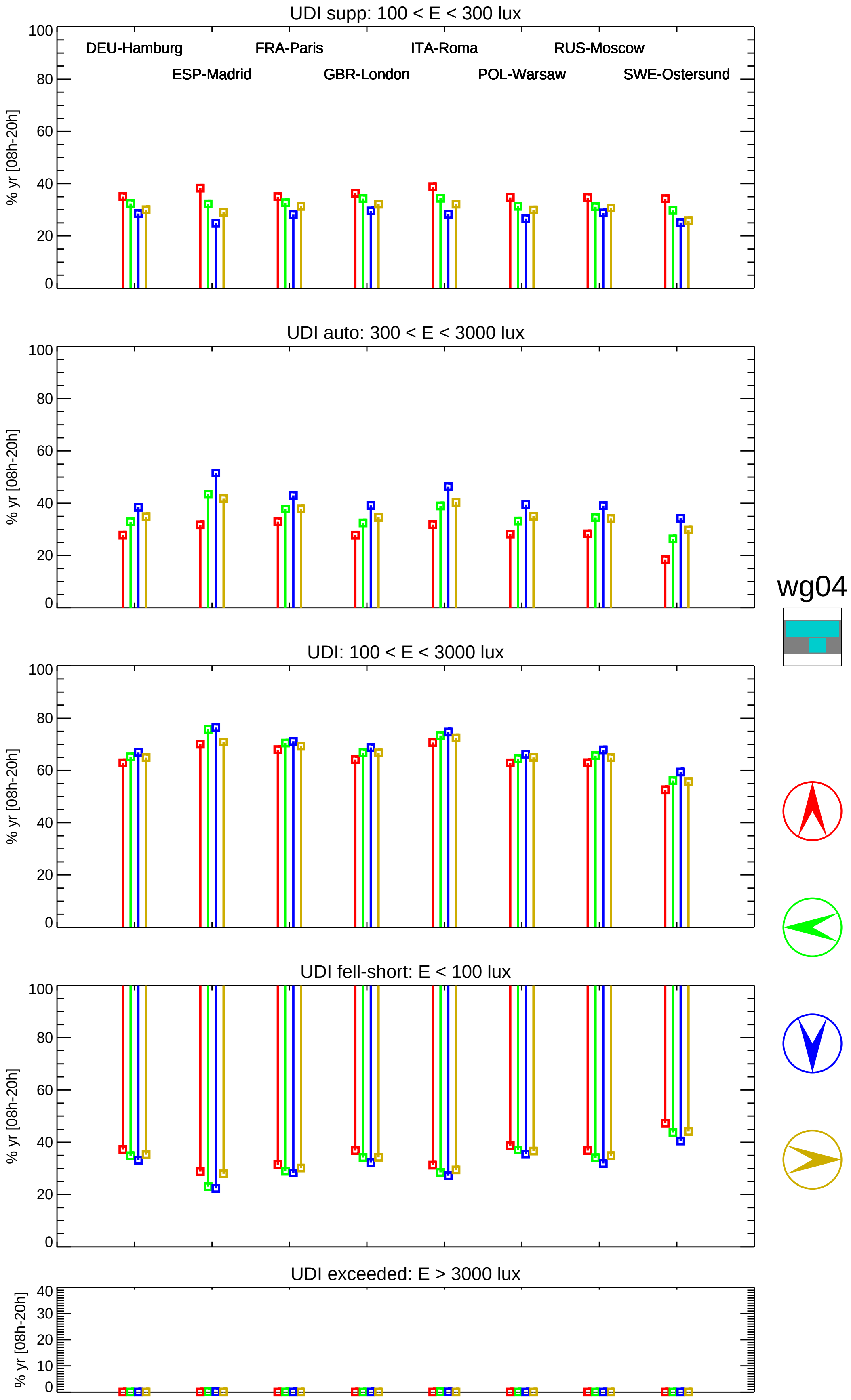

Figure 22: UDI metrics for the small bathroom (wg04)

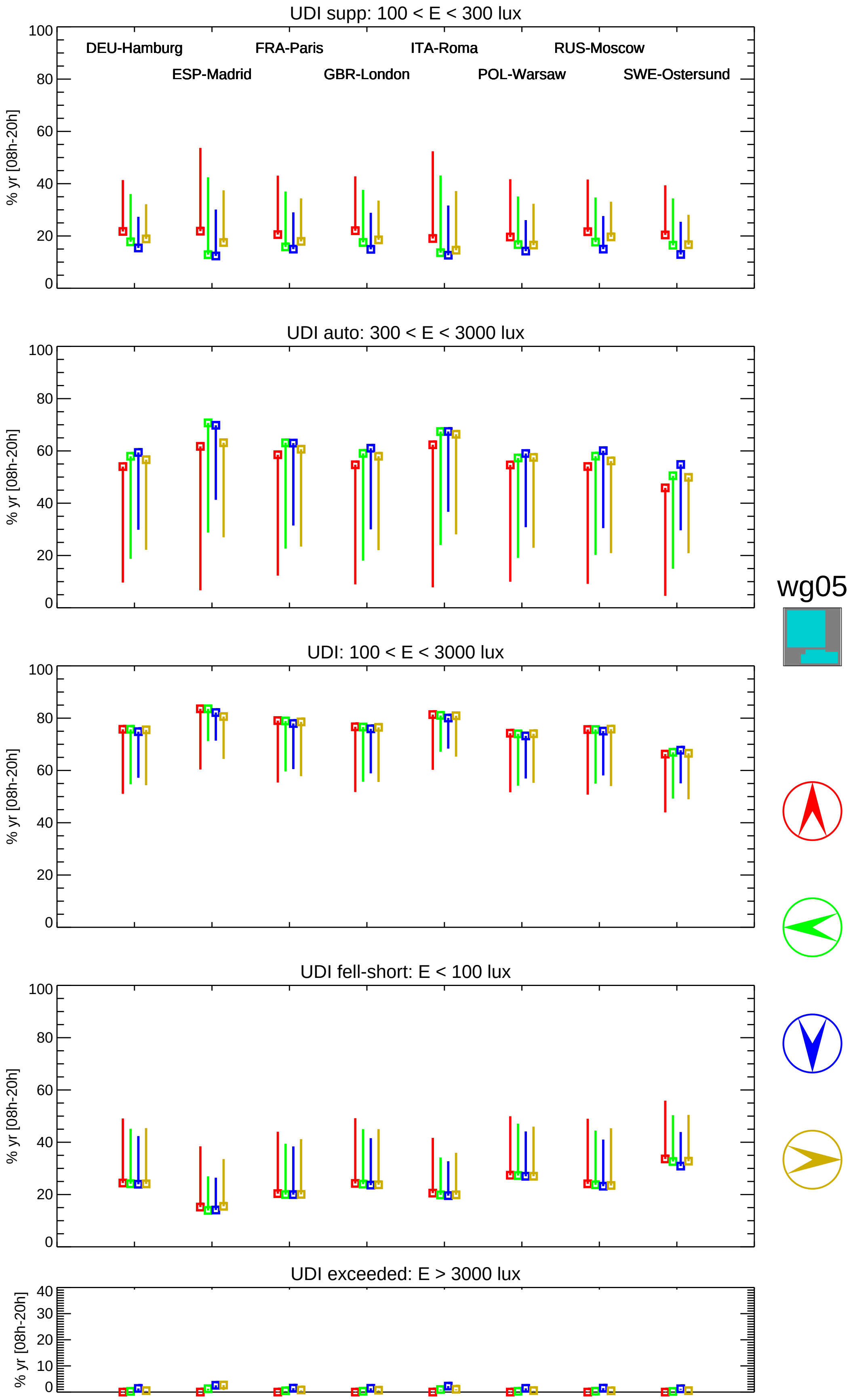

Figure 23: UDI metrics for the large bathroom (wg05)

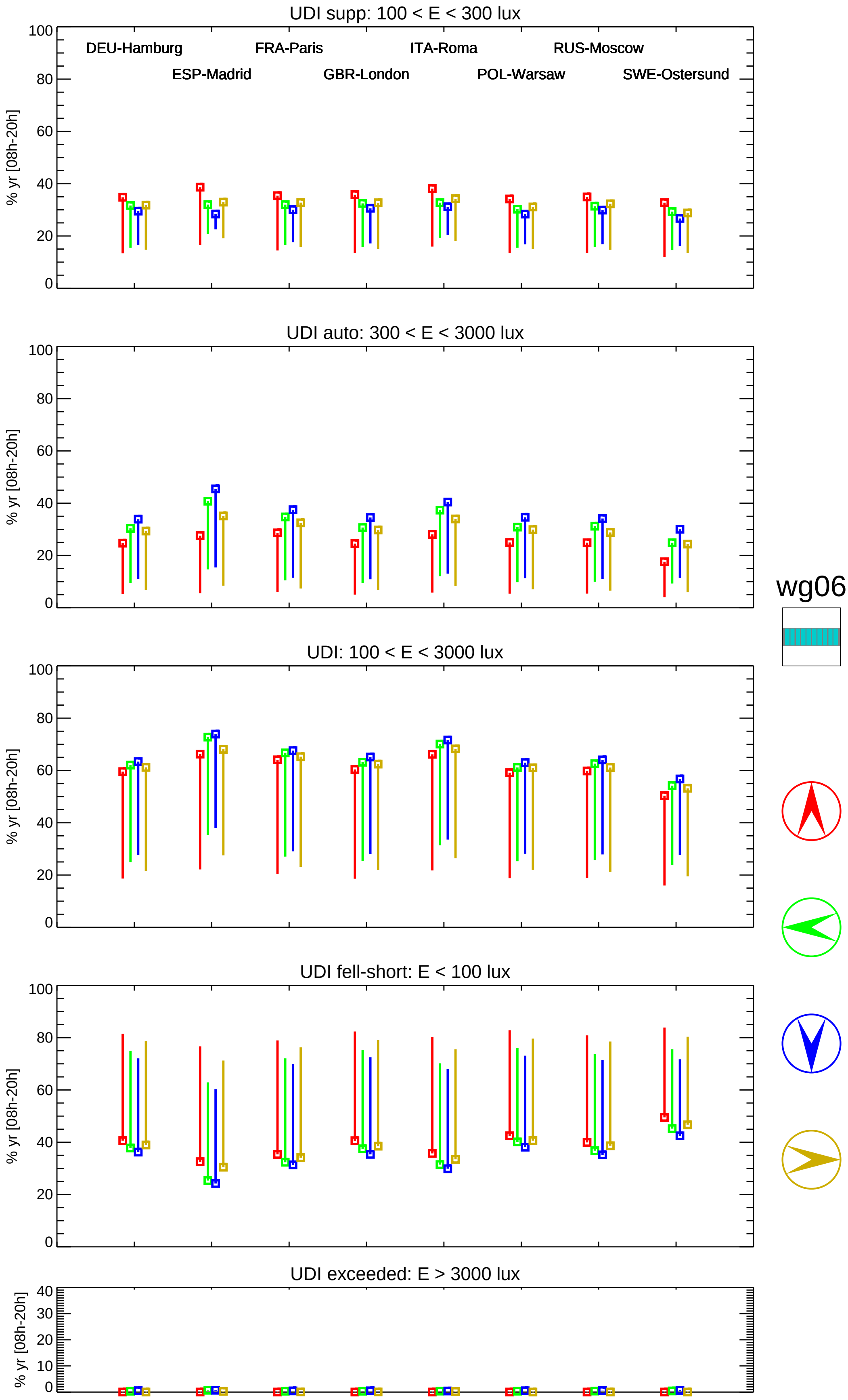

Figure 24: UDI metrics for the stairs (wg06)

6.2 Lighting Energy Use and Savings

The lighting energy use was predicted using the RT 2005 residential model described in Section 4.1. A similar graphical presentation to that used for daylighting is employed. The summary charts show the following on a per space basis:

- The annual lighting energy use in kWh/yr for the case without and with the skylight.
- The saving in kWh/yr resulting from the introduction of the skylight.
- The saving as a percentage.

As with the daylighting plots, the case with the skylight is marked by a box at the end of the line.

6.2.1 The living room - wg01 (80W LP)

As shown in Section 4.2, the predicted lighting energy use is highly dependant on the occupancy factor and sensitive also to the number and location of sensor planes that can trigger the switching on of the light(s). To further illustrate this, for the living room (wg01) we show results for four combinations of two occupancy factors and and two sensor plane configurations. The occupancy factors are default $[1, 0.3, 1]$ and continuous $[1, 1, 1]$, and the sensor plane configurations are centre plane only $[0, 0, 0, 0, 1, 0, 0, 0, 0]$ and all nine planes $[1, 1, 1, 1, 1, 1, 1, 1, 1]$ (see Section 4.2).

For the default occupancy factor and the centre sensor plane, the annual electric lighting consumption drops from ∼125 kWh/yr to ∼100 kWh/yr for all but the Madrid and Rome climates, Figure 25. This corresponds to a saving of ∼25 kWh/yr or ∼20%. Although savings for Madrid and Rome are noticeably less, the performance across the remaining six climates is remarkably consistent and insensitive also to orientation. This is largely because the switch-on probability (as a function of daylight illuminance) drops off steeply from a maximum of 1 for 0 to 100 lux to 0.05 for 200 lux. These relatively low illuminances inside the building will often occur when overcast sky conditions prevail. Thus, the electric lighting condition will, under this switching model, be largely insensitive to building orientation. This is seen for all spaces and occupancy profiles, etc.

Using the same occupancy factor but now having all 9 sensor planes considered in the switching results in higher overall consumption (up by about ∼15%) and a similar increase in savings due to introduction of the skylight, Figure 26.

Returning now to the single sensor plane case, but now with a continuous occupancy factor, we see a marked increase in both the consumed lighting energy and the savings due to introduction of the skylight, Figure 27. The lighting energy saving is now ∼50 kWh/yr or ∼30% of the total for all locales except Madrid and Rome – as before, the savings here are less.

The combination of continuous occupancy and all nine sensor planes results in the higher electricity consumption and greater savings with the skylight in both relative and absolute terms, Figure 28. Savings are now in the 60 to 80 kWh/yr range, and the percentage savings often greater than 30% (for all but Madrid and Rome).

The real living room space had relatively low power lighting (i.e. 80W), which is probably atypical for rooms of this type or similar. Accordingly, all the absolute values given here could be simply scaled to determine the consumption and savings for spaces with different installed power. For example, if the living room had installed power similar to the hallway (i.e. 360W), the absolute values shown in Figures 25 to 28 would be 4.5× greater, e.g. ∼100 kWh/yr saving for the default occupancy factor and the centre sensor plane, up to ∼280 kWh/yr for the case with continuous occupancy using all nine sensor planes.

6.2.2 The kitchen - wg02 (255W LP)

Here we see a marked savings in consumed lighting energy due to the introduction of the skylight: typically ∼100 kWh/yr, which corresponds to a relative saving of ∼20 to 25% in most cases, Figure 29. Sensitivity due to building orientation is a little more evident, though still not very great.

6.2.3 The hall - wg03 (360W LP)

As noted previously, the hall (wg03) did not have a dedicated skylight and so the effect here is solely due to light spillage from adjacent spaces, which we expect to be small. Nonetheless, because of the high installed power the savings are not insignificant: ∼20 kWh/yr in absolute terms which equals around ∼5% of the consumption without skylights, Figure 30.

6.2.4 Small bathroom - wg04 (100W LP)

As noted previously, the small bathroom (wg04) did not have a pre-existing vertical window, so the lighting consumption for all cases was the same, i.e. just over 100 kWh/yr, Figure 31. Here the savings were largely in the range 20 to 40 kWh/yr, in relative terms the savings were in the range 20 to 45%, Figure 31.

6.2.5 Large bathroom - wg05 (300W LP)

As noted previously, the large bathroom (wg05) has two small windows positioned at a high level for privacy which provide only moderate amounts of daylight. Climate and orientation effects are more evident in this space than others, this it seems is due to the size and positioning of the windows which results in illumination at the sensor planes being very sensitive to the narrow "views" of the sky luminance pattern in this arrangement. This, together with the higher installed lighting power, results in absolute savings in the range 40 to 120 kWh/yr, in relative term the savings were in the range 20 to 45%, Figure 32.

6.2.6 Staircase - wg06 (80W LP)

The staircase (wg06) does receive a little light spillage from the hall, but not enough affect the switching of the lights. So, all the cases without the skylight have the same lighting energy consumption: 190 kWh/yr, Figure 33. With the skylight, the savings are largely in the range 10 to 35 kWh/yr, or 5 to 15% in relative terms. The savings may well be underestimated because it is likely that, in actual use, the occupants might find that illuminances at the lowest steps of around 100 lux are sufficient for safe use of the stairs, and so switch-on may be less than predicted using the RT 2005 model.

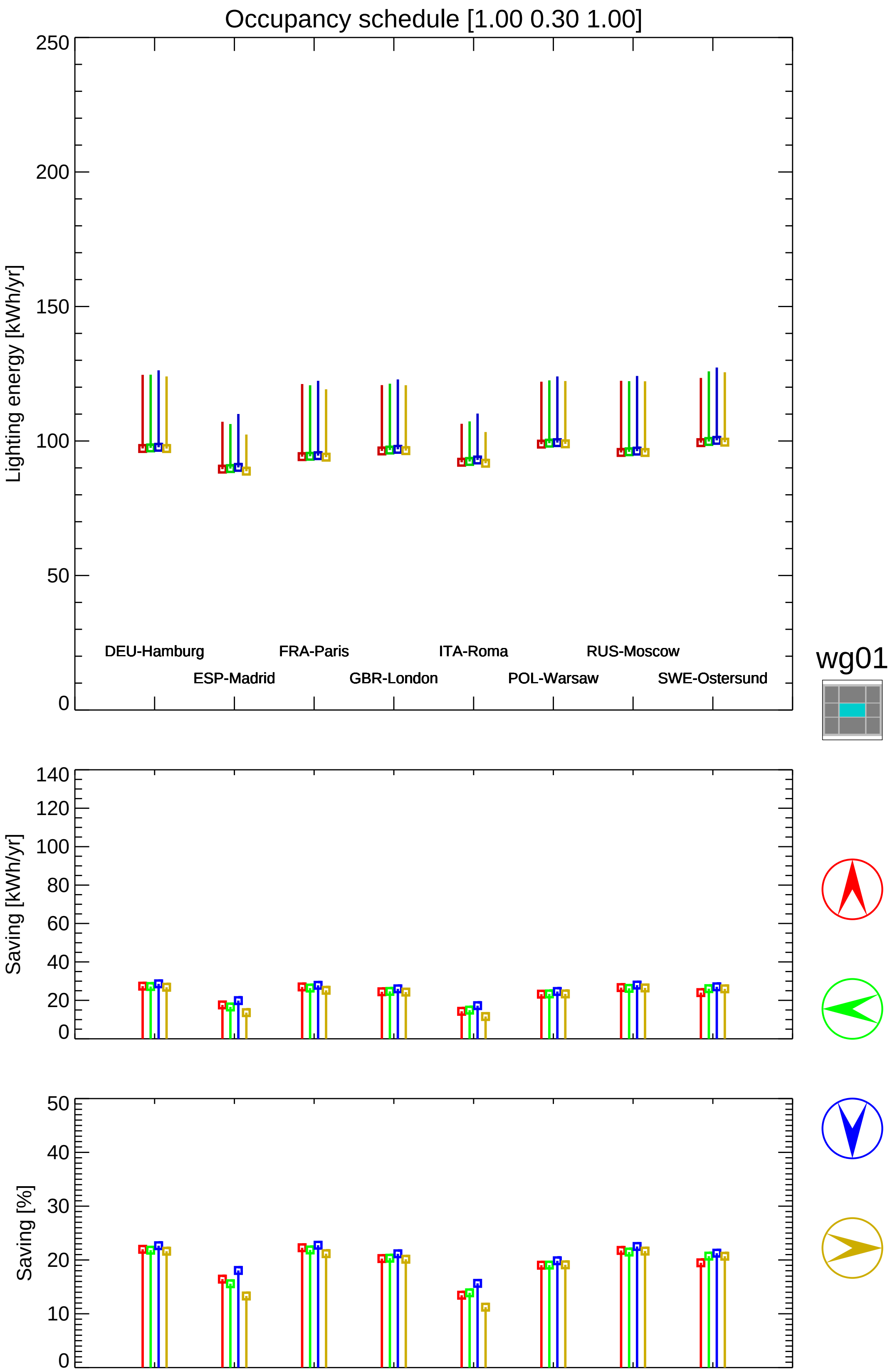

Figure 25: Lighting energy use / saving for the living room (wg01)

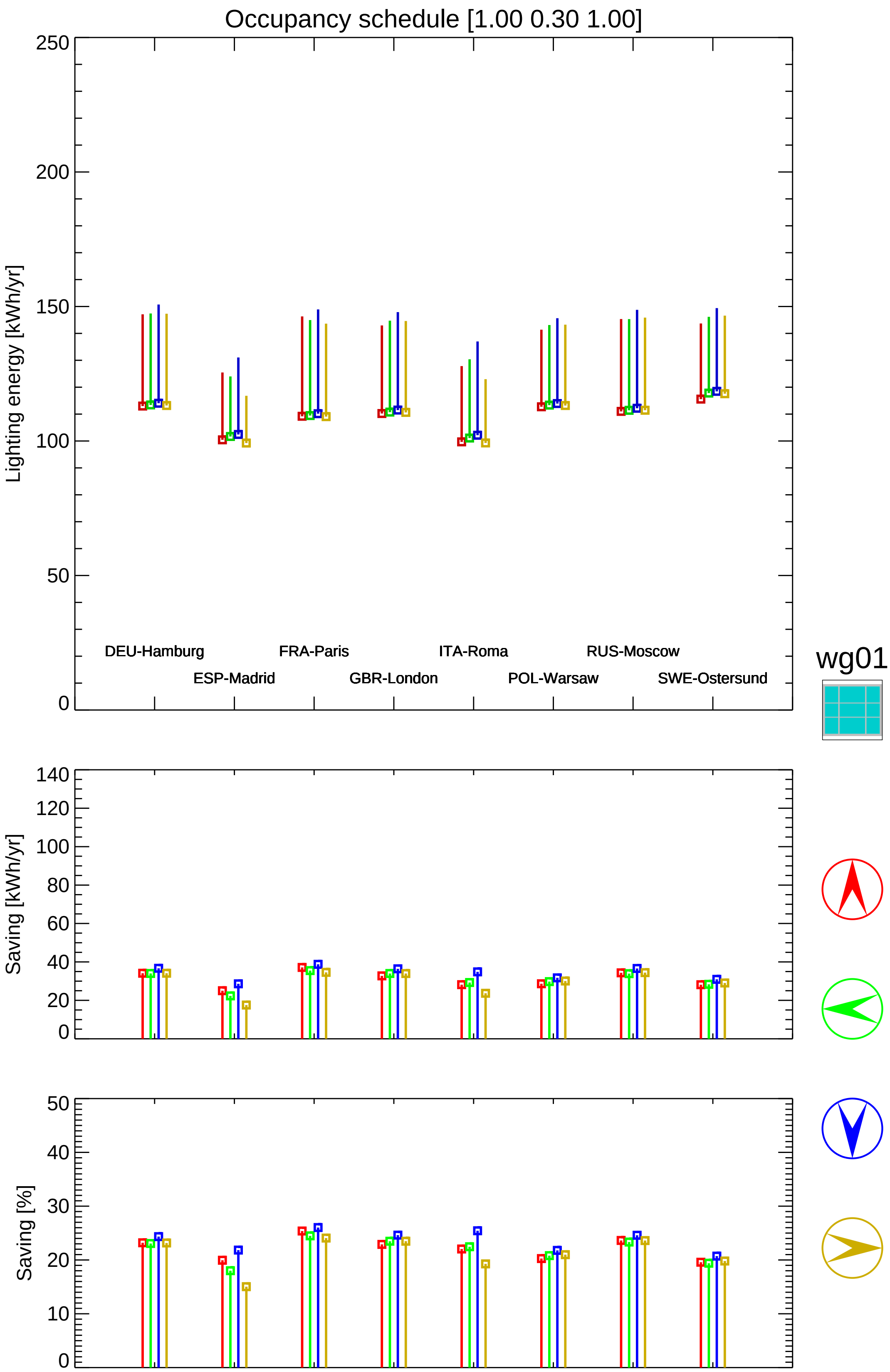

Figure 26: Lighting energy use / saving for the living room (wg01)

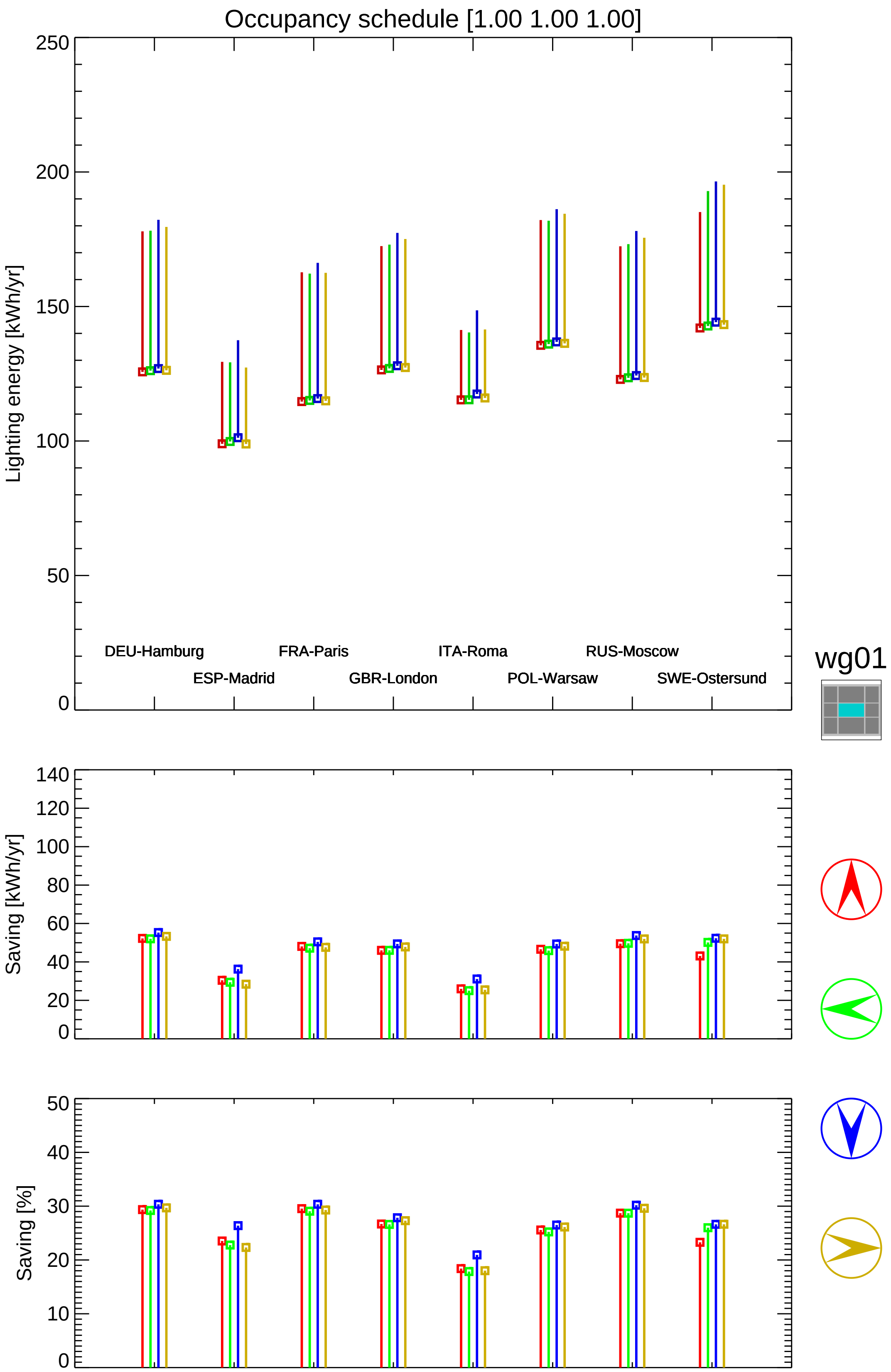

Figure 27: Lighting energy use / saving for the living room - continuous occupancy (wg01)

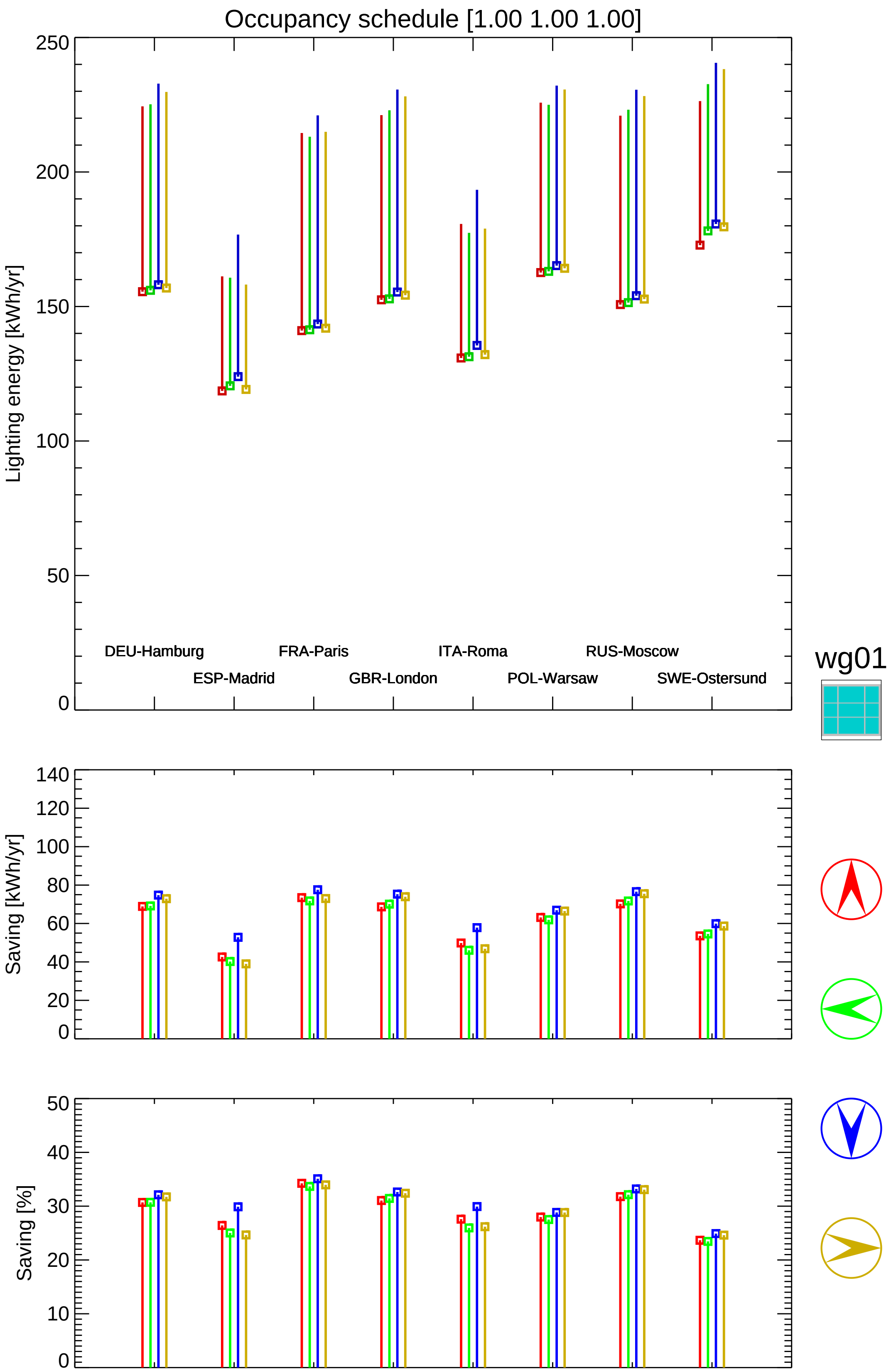

Figure 28: Lighting energy use / saving for the living room - continuous occupancy (wg01)

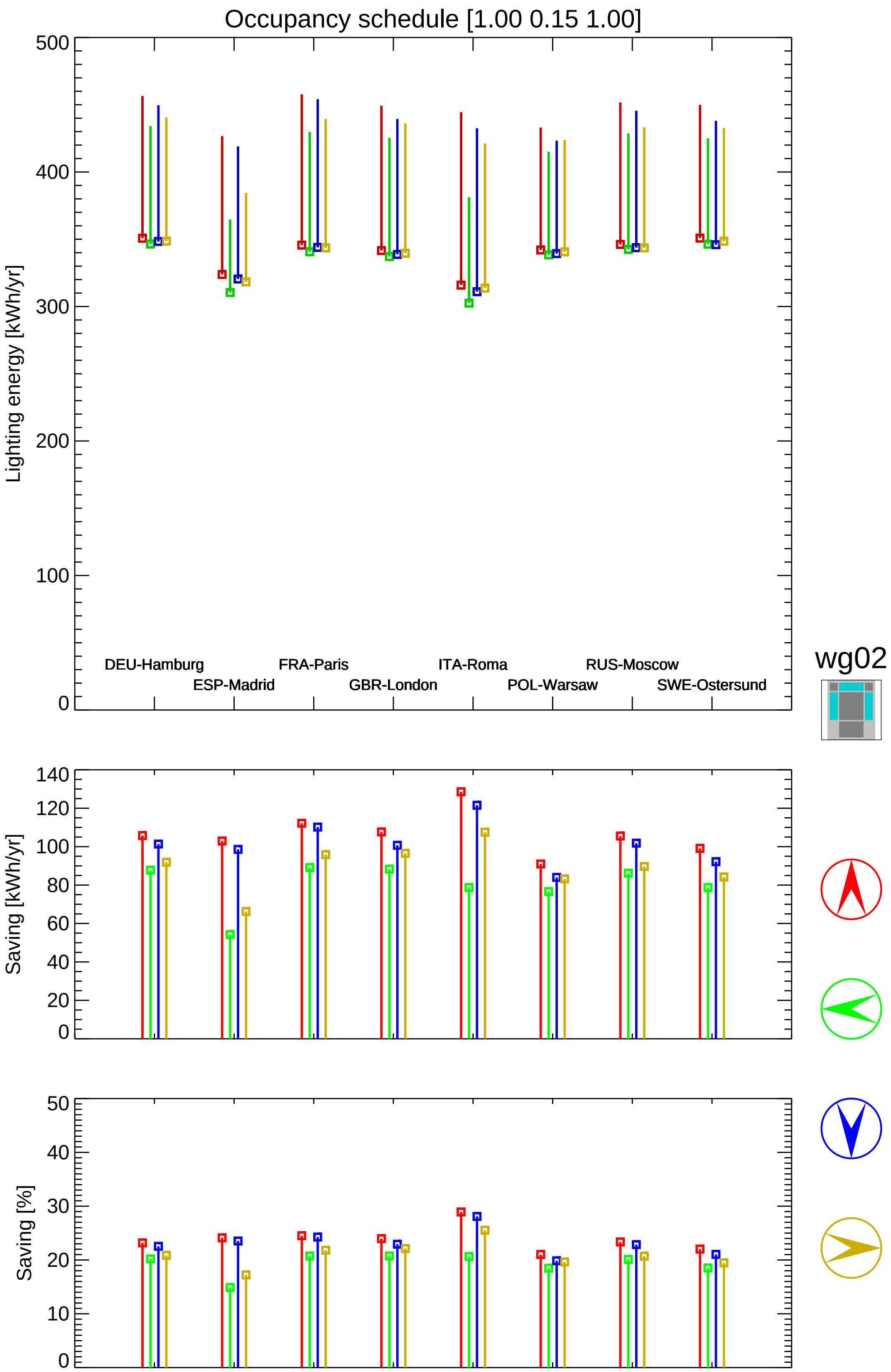

Figure 29: Lighting energy use / saving for the kitchen(wg02)

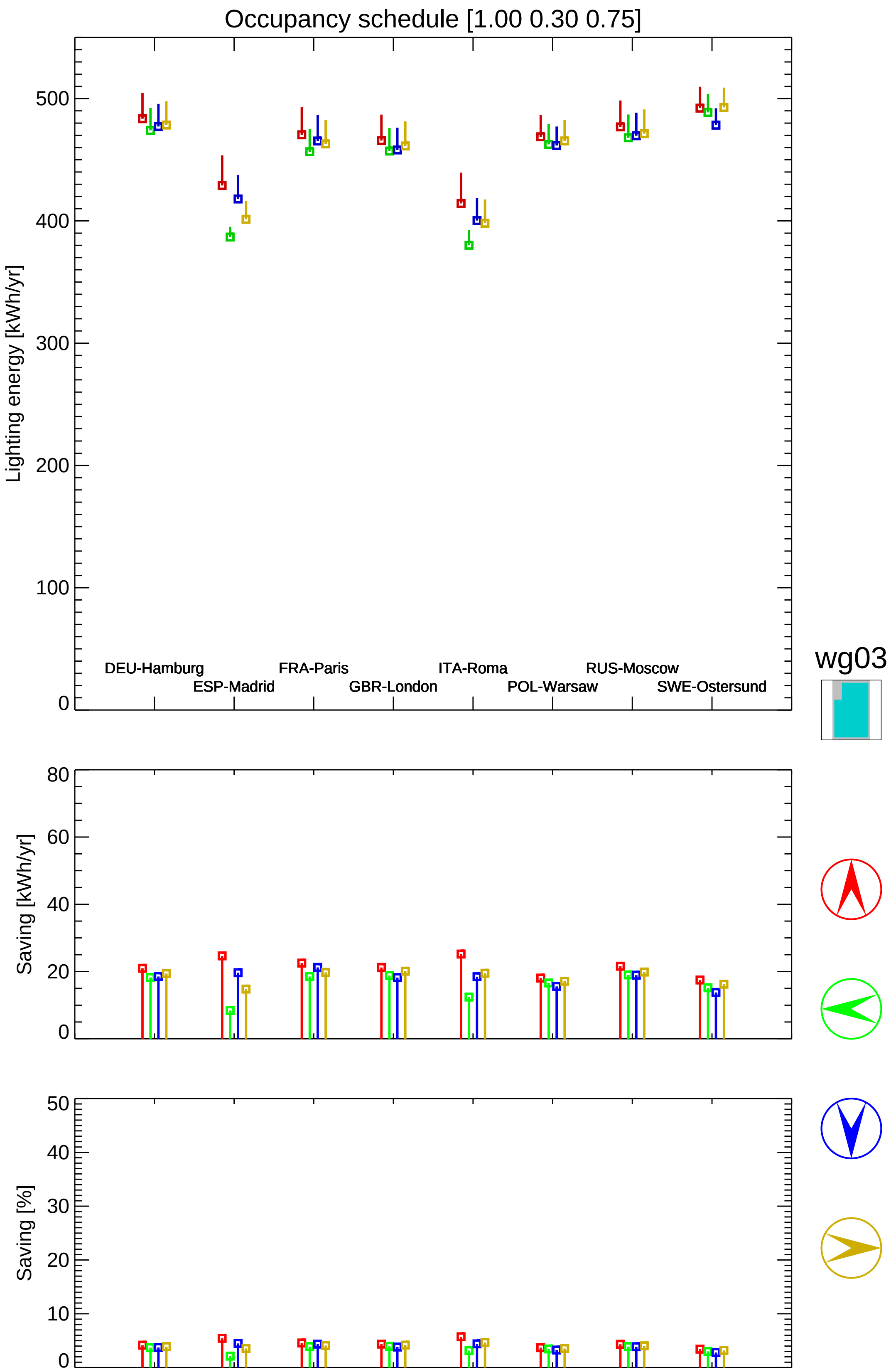

Figure 30: Lighting energy use / saving for the hall (wg03)

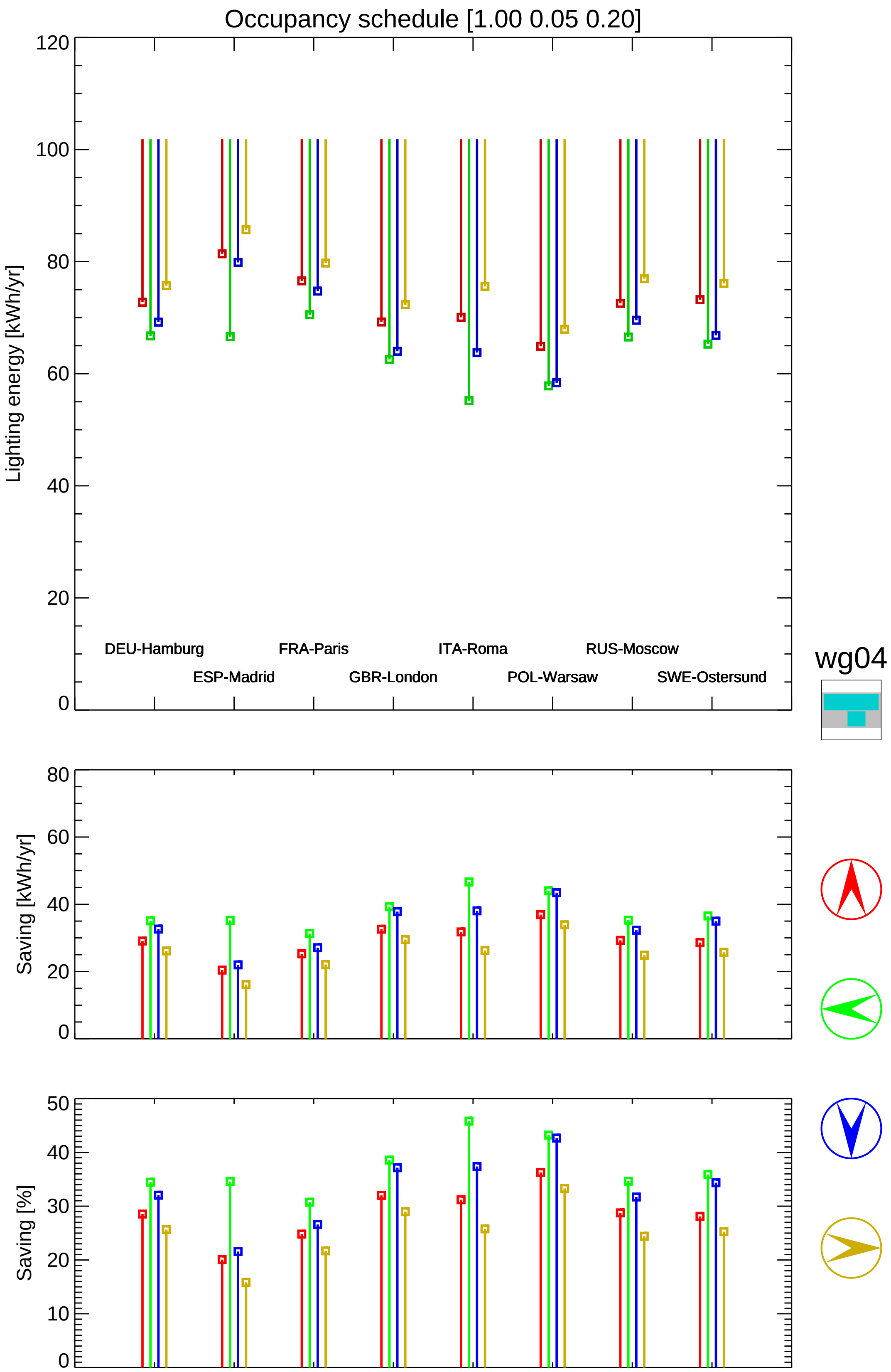

Figure 31: Lighting energy use / saving for the small bathroom (wg04)

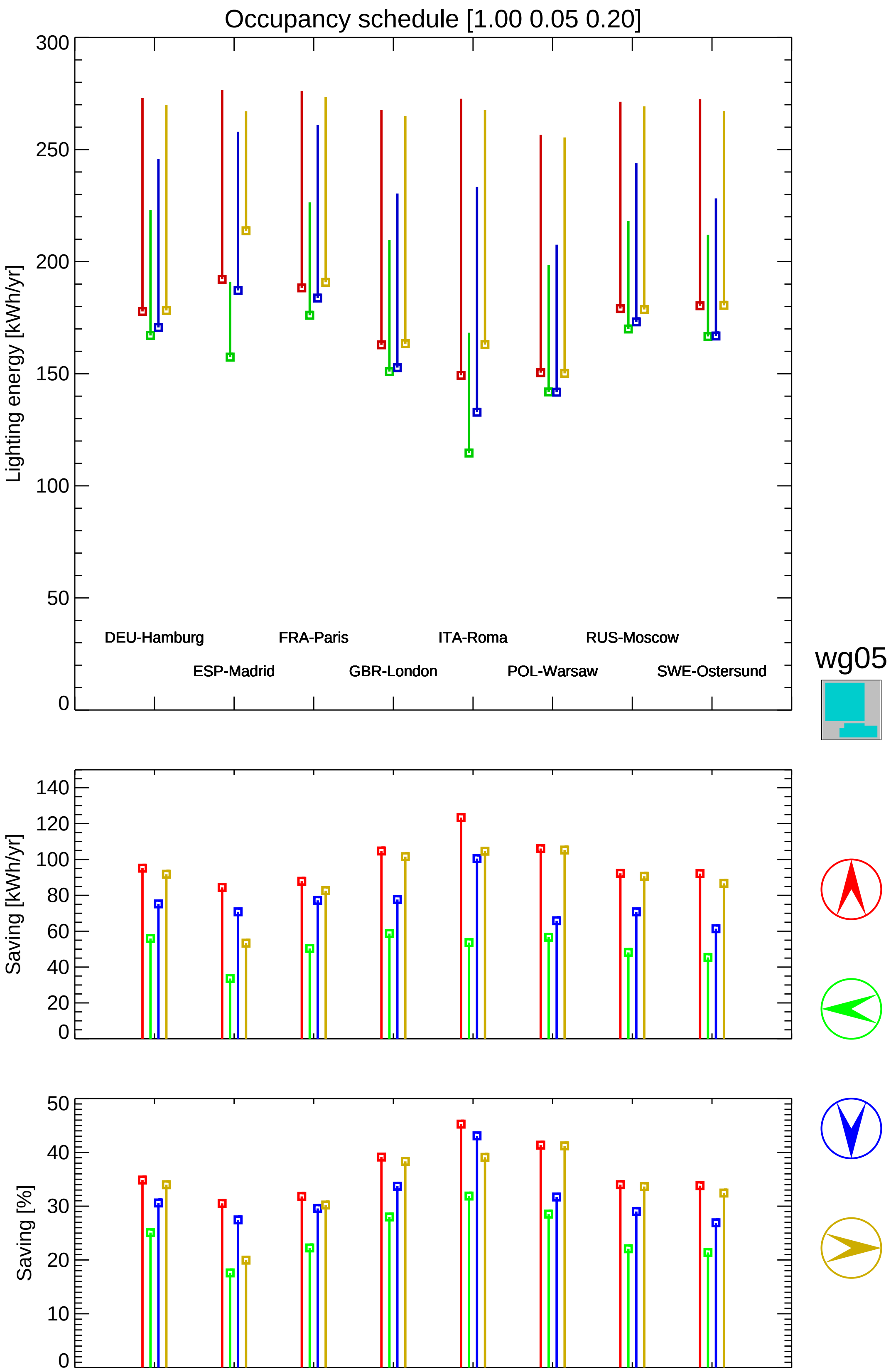

Figure 32: Lighting energy use / saving for the large bathroom (wg05)

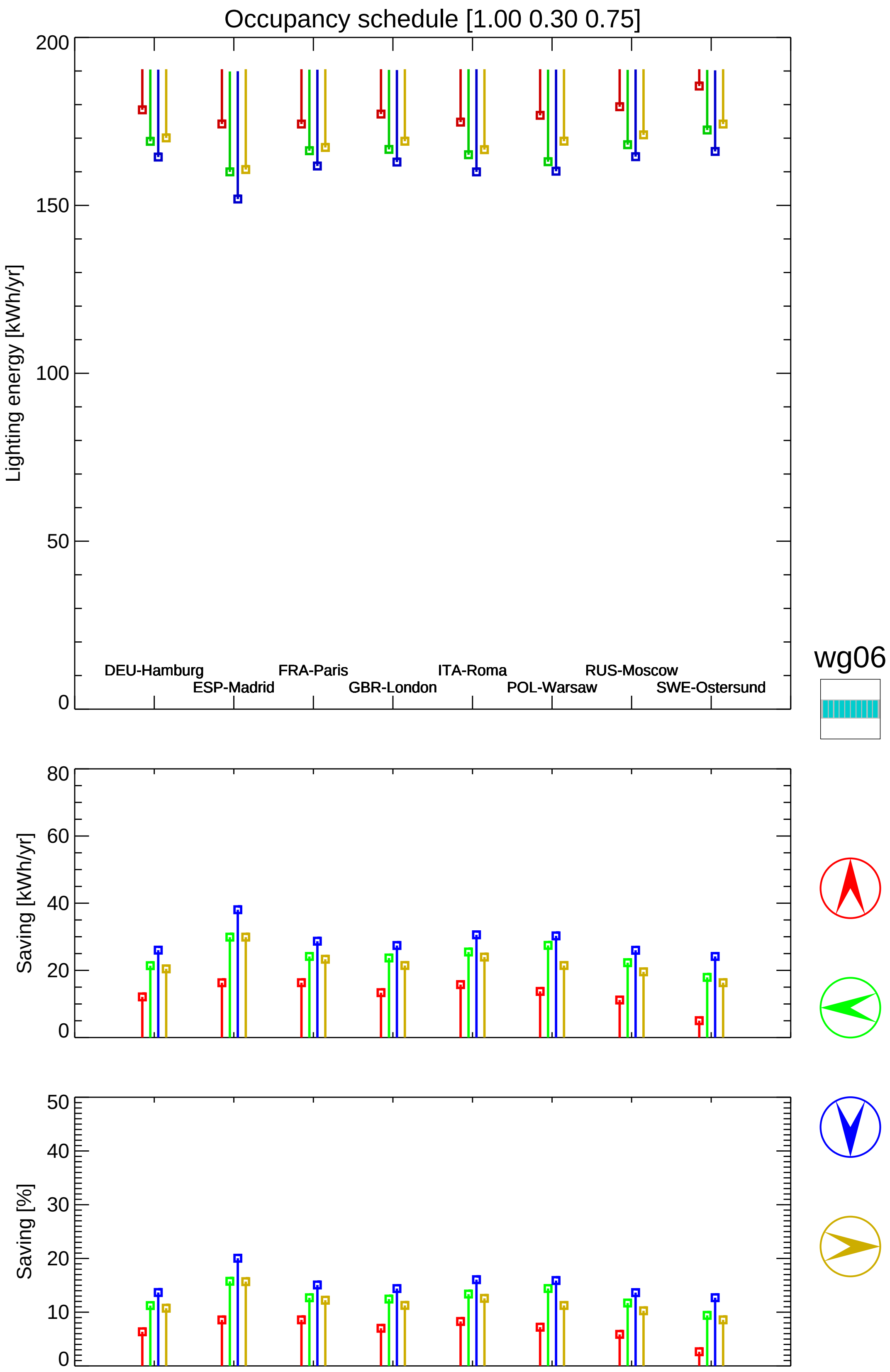

Figure 33: Lighting energy use / saving for the stairs (wg06)

6.3 Non-Visual Effects

The potential for daylight to induce non-visual effects was determined for three of the spaces: the living room (wg01), the kitchen (wg02) and the large bathroom (wg05). A similar graphical presentation to that used for daylighting (Section 6.1) is employed. The three summary charts show the following on a per space basis for cases without and with the skylight:

- The predicted cumulative annual non-visual effect for the period 06h00 to 10h00, i.e. associated with circadian entrainment.
- The predicted cumulative annual non-visual effect for the period 10h00 to 18h00, i.e. associated with subjective alterness.
- The predicted cumulative annual non-visual effect for the notional night-time period (18h00 to 06h00).

We summarise the performance of the space by showing the (arithmetic) mean value for the predicted non-visual effect across all the considered (eye-height) sensor planes: 16 for the living room; 4 for the kitchen; and, 1 for the large bathroom. As with the daylighting plots, the case with the skylight is marked by a box at the end of the line. Unlike the UDI metrics, in all cases there will be either an increase in the predicted non-visual effect caused by the introduction of the skylight, or no significant change as is often the case for the night-time period. The effect of climate and building orientation is quire pronounced, especially for the 'circadian' period in the morning. This is because the effect is quite strong when the building orientation is such that the space receives sunlight illumination in the morning, i.e. when the windows face east. With the addition of a skylight, the following trends in the changes for the predicted non-visual effect are observed on a space by space basis. Note it may be helpful to refer to Figure 18 to be reminded of the relation between the compass orientation of the vertical glazing for the space and the relative orientation of the building with respect to the compass icons ↑, →, ↓ and ← shown on the plots.

6.3.1 The living room - wg01

For any one location there is often a factor two difference in predicted non-visual effect for the 'circadian period' across the four orientations, Figure 34. The preferential orientation with the highest 'circadian period' effect for any one locale is when the glazing faces east (i.e. compass legend →). To maximise the non-visual effect for the 'alertness period', the preferred orientation is usually that with the glazing facing south (↑). Note that Madrid shows lower non-visual effect for the circadian period than perhaps one might expect given the high occurrence of clear skies. This is because Spain uses Central European Time and so, given its longitude, solar time is markedly later than clock time for much of the country.

The addition of a skylight results in a marked increase in predicted non-visual effect for the circadian and alertness periods. Typical increases for the circadian period were from ∼10% to ∼25%, though there is a lot of variation resulting from climate and orientation. Recall that spectral properties of the daylight are also a factor in the prediction of non-visual effect (Section 5.1.1). For the alertness period the typical increases were from ∼25% to ∼55%, though once again there was marked sensitivity to climate and orientation.

For the notional night-time period the small predicted effect was that due evening daylight and is generally not a consideration for this study for any of the spaces – it will not be remarked upon further. Note, for the same reasoning given above re: solar time and clock time for Spain, the night-time value for Madrid – though still small – is noticeably greater than for the other cities.

6.3.2 The kitchen - wg02

As was the case with the living room, orientation effects were particularly evident for the circadian period. As expected, the building orientation that had the kitchen windows facing east resulted in the greatest predicted non-visual effect (i.e.). This was so without and with skylights, Figure 35. For all climates, the patterns in non-visual effect for the alertness period with respect to orientation were the same: highest when the window faces south () and lowest for the window facing north ().

As was the case with the living room, the addition of a skylight results in a marked increase in predicted non-visual effect for the circadian and alertness periods. Typical increases for the circadian period were from ∼5% to ∼25%, with consderable variation resulting from climate and orientation. The typical increases for the alertness period were from ∼20% to 50% or more.

6.3.3 Large bathroom - wg05

The patterns in predicted non-visual effect for the large bathroom are similar to those for the kitchen, but with greater variation with respect to orientation, Figure 36. This is most likely because a single head position was used for this space (i.e. facing the bathroom mirror). As was the case with the kitchen, the greatest effect for the circadian period was when the window faced east (). And for the alertness period when the window faced south ().

The increase in predicted non-visual effect for both periods resulting from the introduction of a skylight was marked. For the circadian period the typical increases were from ∼5% to ∼20% in many cases. Typical increases for the alertness period were from ∼20% to ∼50%.

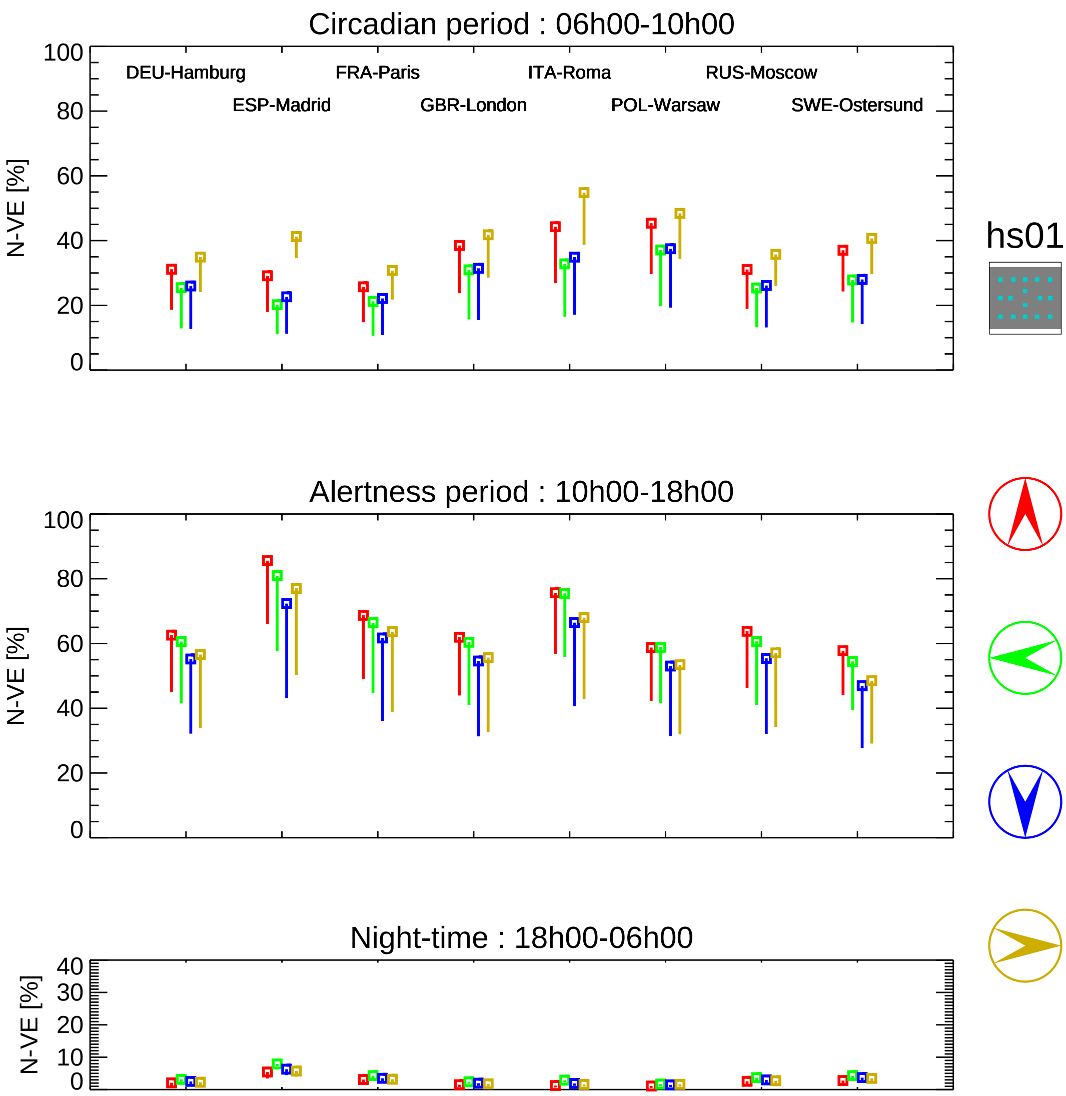

Figure 34: Cumulative non-visual effects for the living room (wg01)

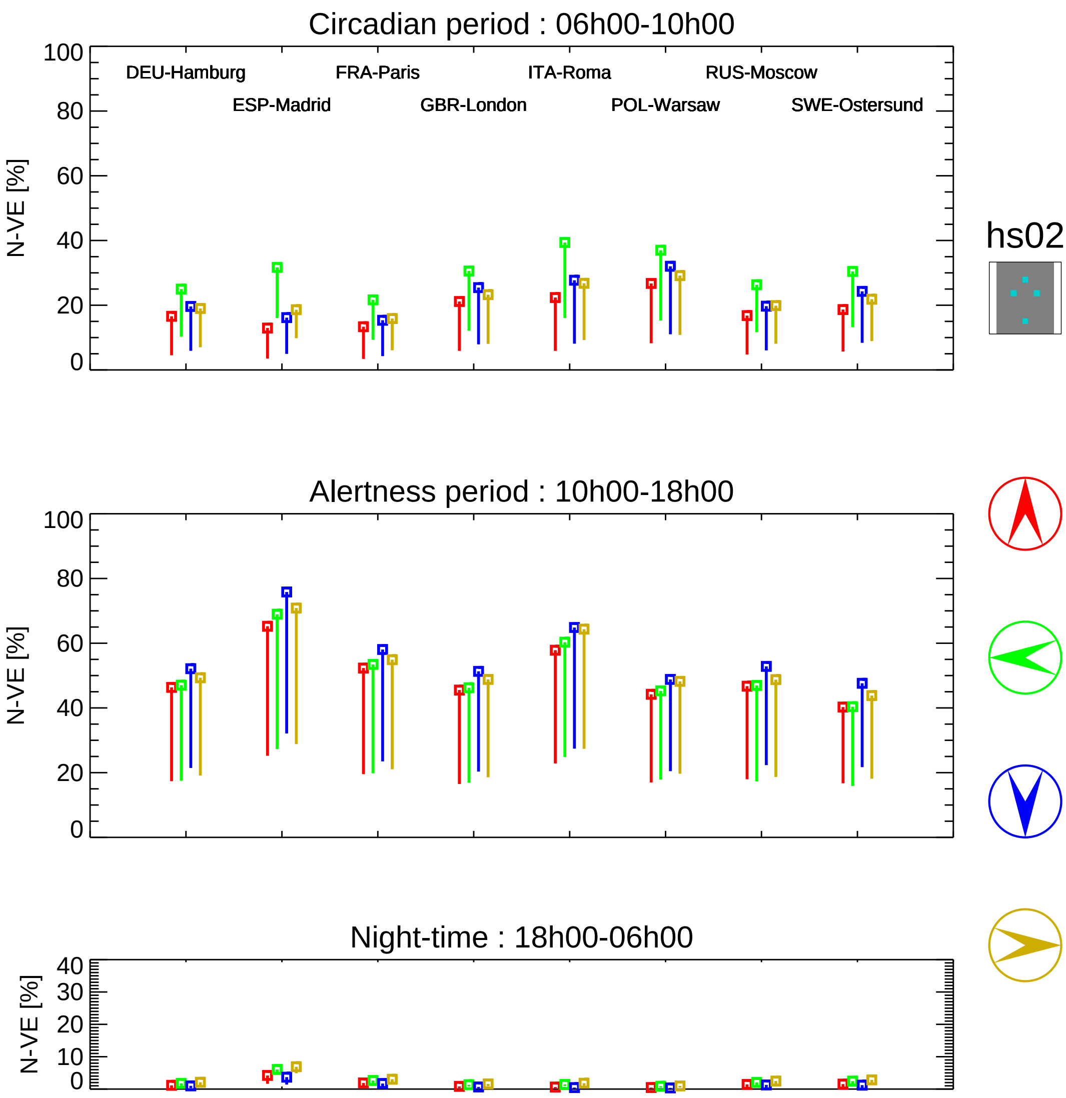

Figure 35: Cumulative non-visual effects for the kitchen (wg02)

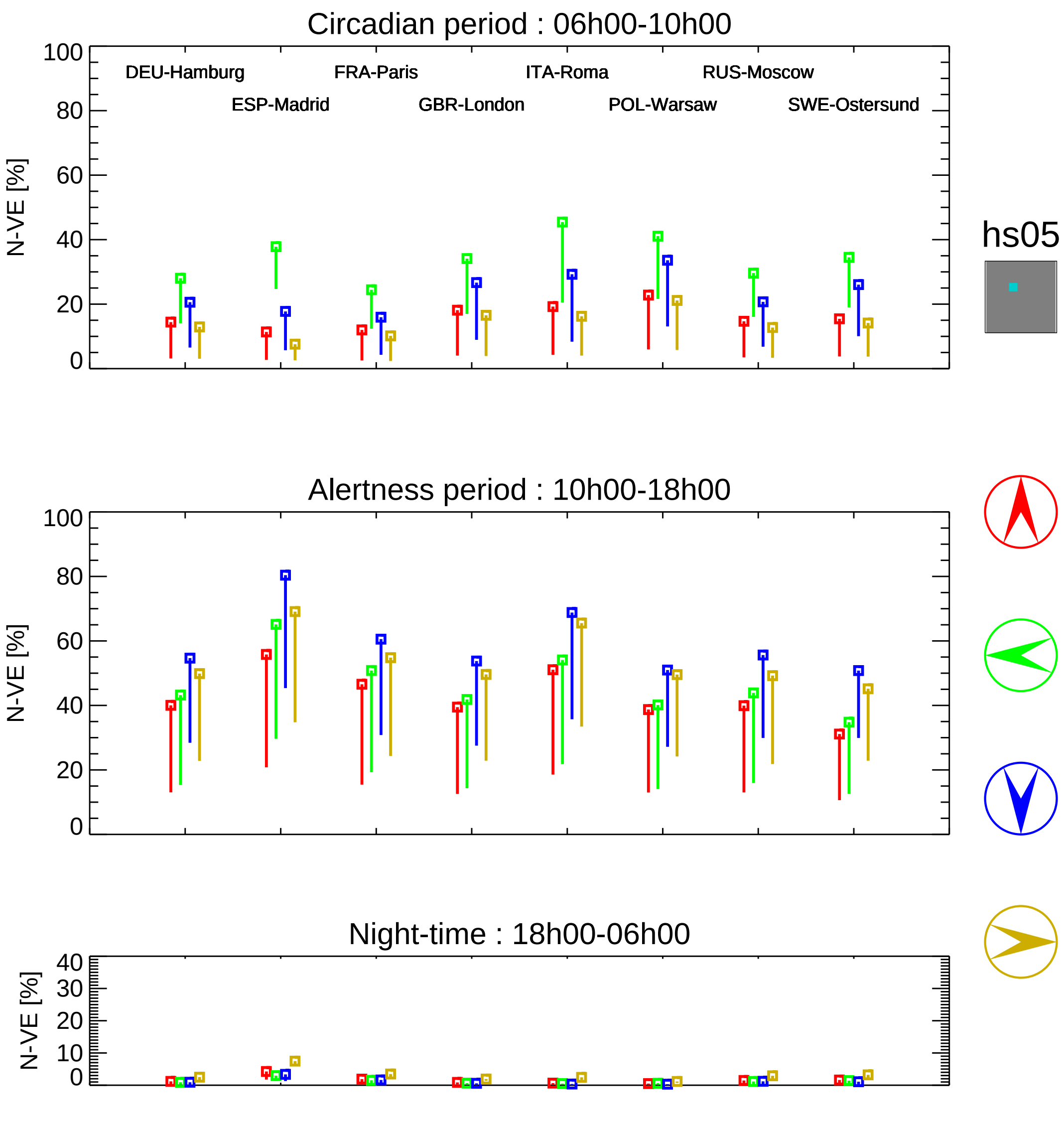

Figure 36: Cumulative non-visual effects for the large bathroom (wg05)

7 Discussion

The methodology and summary findings from this study of three aspects of daylight in residential building have been described. The overall daylight provision for task was assessed using the useful daylight illuminance scheme. Originally devised using data from studies of non-domestic buildings, the UDI approach is effective in disclosing the consequence of daylight design interventions such as the addition of skylights. The boundary values for UDI are not fixed and it is possible that, for residential dwellings, the tolerated upper limit may be higher than that indicated from studies of office buildings. Also, it is quite likely for residential buildings that overheating rather than excessive daylight might be the more common trigger that results in the closing of blinds. An exception may be when the watching of TVs, home cinema screens, etc. causes the blinds to be closed on largely visual considerations.

The most comprehensive set of results presented in this paper are for the potential lighting energy saving due to the addition of a skylight. The results show a marked sensitivity to assumptions regarding the occupancy profile and the selection of sensor planes to trigger the switching of lights. Regardless of those assumptions, the effect of climate and building orientation for any one scenario accounts for approximately a factor two difference between the highest and lowest predicted energy saving.

The model of non-visual effects presented here is an extension of that described by Pechacek *et. al.* [38]. Key enhancements of the previous implementation include the concept of a ramp-function from a lower to an upper vertical illuminance threshold, based on photobiology findings, that expresses the increasing potential for circadian effects. Another enhancement is the ability to treat independently light from the sun and sky, thereby accounting for the varying circadian efficacy of the light according to its spectral type, i.e. D55, D65 or D75. And, in terms of data visualization, we introduce the sombrero plot as a simple graphical device to display the cumulative non-visual effect at a point in space and as a function of view direction. The sombrero plot provides a means of representing cumulative data which has properties of position (i.e. multiple plots can be used to show the distribution across a space) and view direction, in addition to showing the effect for the three different periods over a full year.

The field of circadian daylighting in architecture is a new one. Because photometric quantities such as lumens are keyed to visible light rather than circadian-sensing blue-shifted-light, they are not useful to determine if a space has sufficient light of the correct spectrum for circadian realignment without considerable calculations. The proposed approach aims to lead to a better understanding of the relative effect of certain design decisions on the overall ‘circadian potential’ of a space. One must however keep in mind that given the very early developmental stage of photobiology in this field, any finding has to be considered as a possible approach to solve the problem rather than as a design guideline.

The next stage in developing the analysis begun here is to determine what, if any, relation exists between the three measures predicted here. Here are some of the questions/issues that will be addressed in follow-on work:

- Is it possible for one measure to act as a proxy for others? For example, could the UDI schema be refined to act as a proxy for lighting energy usage, or even N-VE?
- As far as broad trends are concerned, do the measures work in concert or in conflict? For example, is it desirable to select building designs that offer the potential of high

levels of N-VE for occupants, or might that result in the over-provision of daylight causing undue visual discomfort and overheating?

- Because the N-VE model requires the prediction of vertical illuminance at the eye, it will be a relatively straightforward matter to predict measures of visual discomfort that rely only on this quantity. Furthermore, it may be possible to use the individual components of vertical illuminance at the eye to estimate (directly visible) source luminance, and so allow computation of glare metrics such as DGP [47].

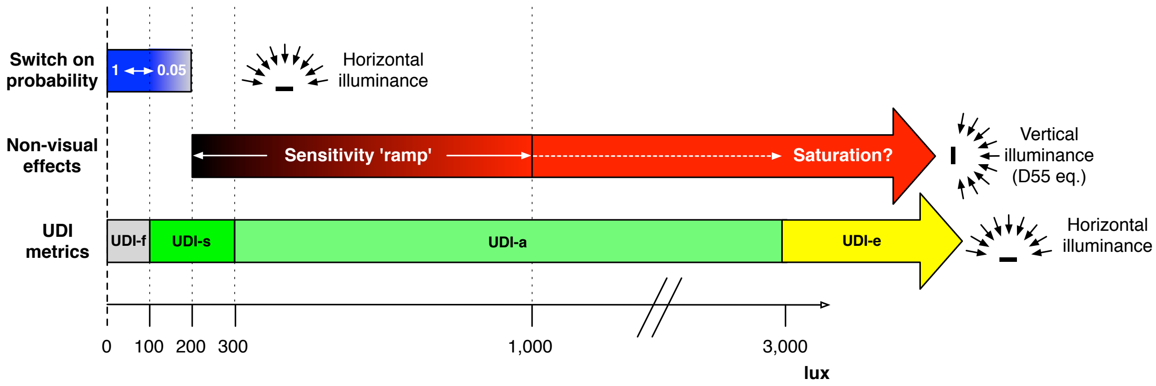

Figure 37: Significant ranges for: electrical light switching; non-visual effects; and, useful daylight illuminance bands.

8 Appendix

8.1 UDI plots - Ostersund, orientation 180

Example UDI plots for Ostersund climate, orientation 180, i.e. living room windows face north, windows (where present) for other rooms face south. Here we present the full set of twelve UDI plots for one climate and orientation. The pages for these plots are landscape orientated – toggling between them when in full-screen mode efficiently conveys the essential change in the UDI metrics that result from the addition of a skylight.

Living room

Figure 38 (without skylight) and Figure 39 (with skylight).

Kitchen

Figure 40 (without skylight) and Figure 41 (with skylight).

Hall

Figure 42 (without skylight) and Figure 43 (with skylight).

Small bathroom

Figure 44 (without skylight) and Figure 45 (with skylight).

Large bathroom

Figure 46 (without skylight) and Figure 47 (with skylight).

Stairs

Figure 48 (without skylight) and Figure 49 (with skylight).

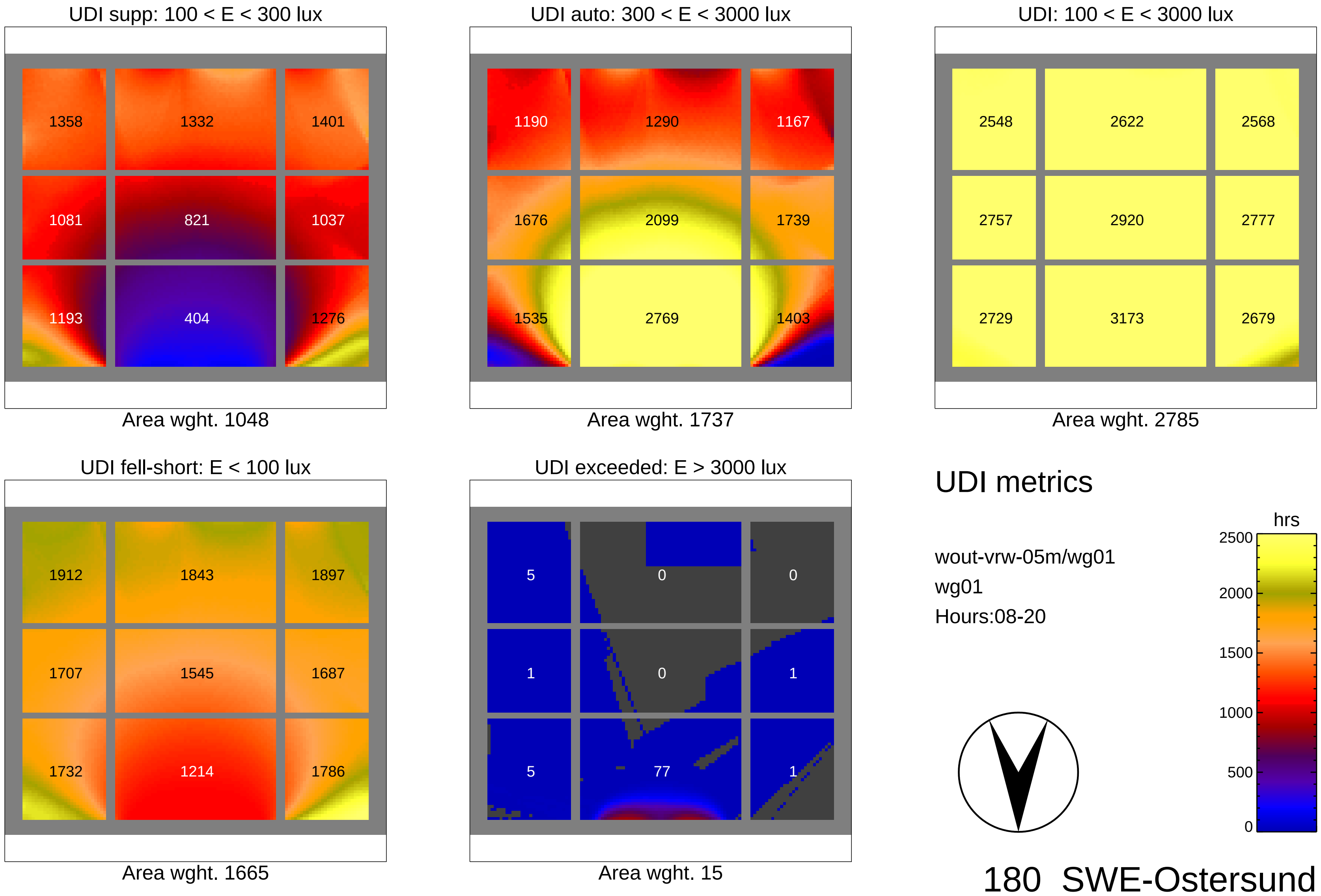

Figure 38: UDI plots for the living room without skylights (Ostersund climate).

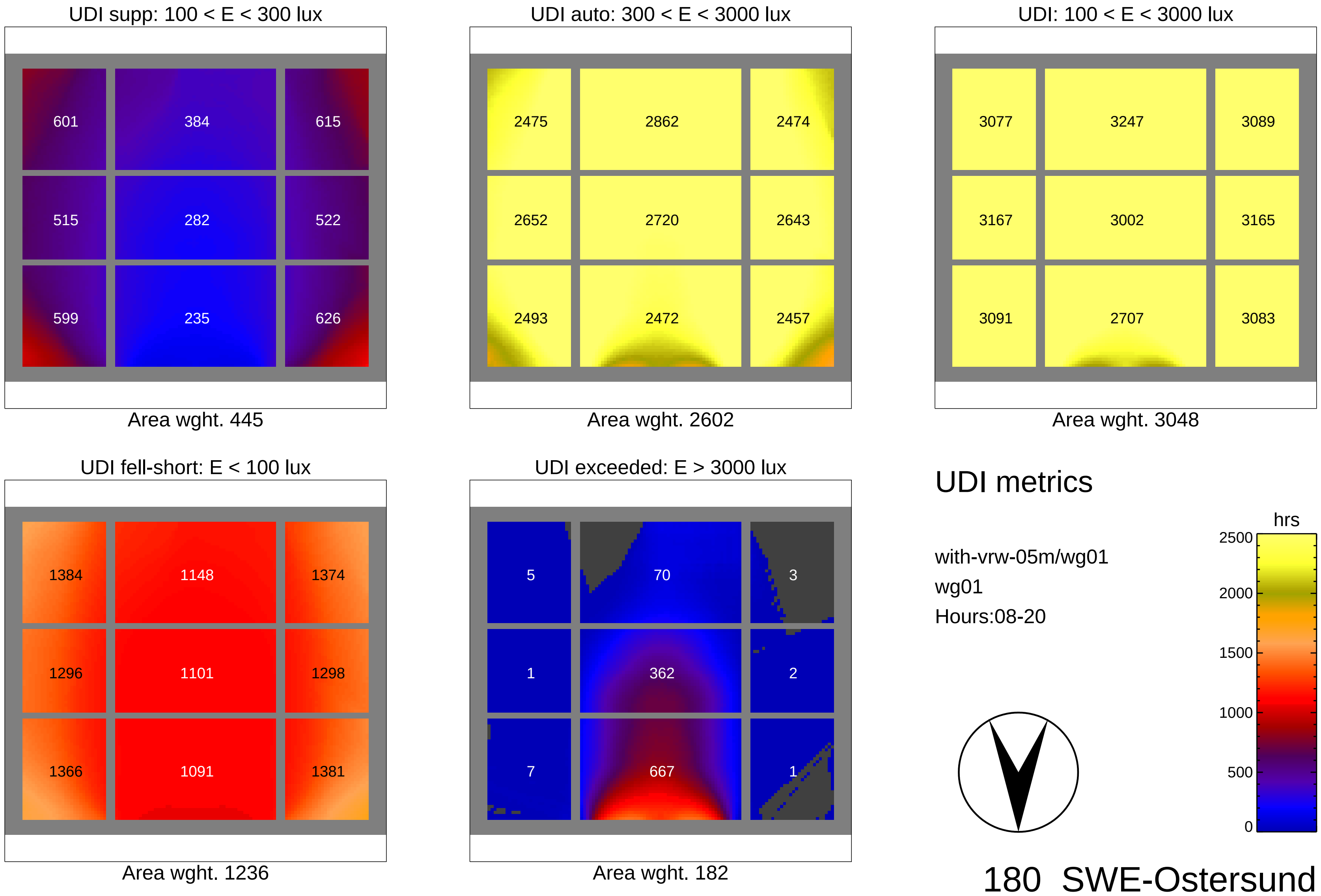

Figure 39: UDI plots for the living room with skylights (Ostersund climate).

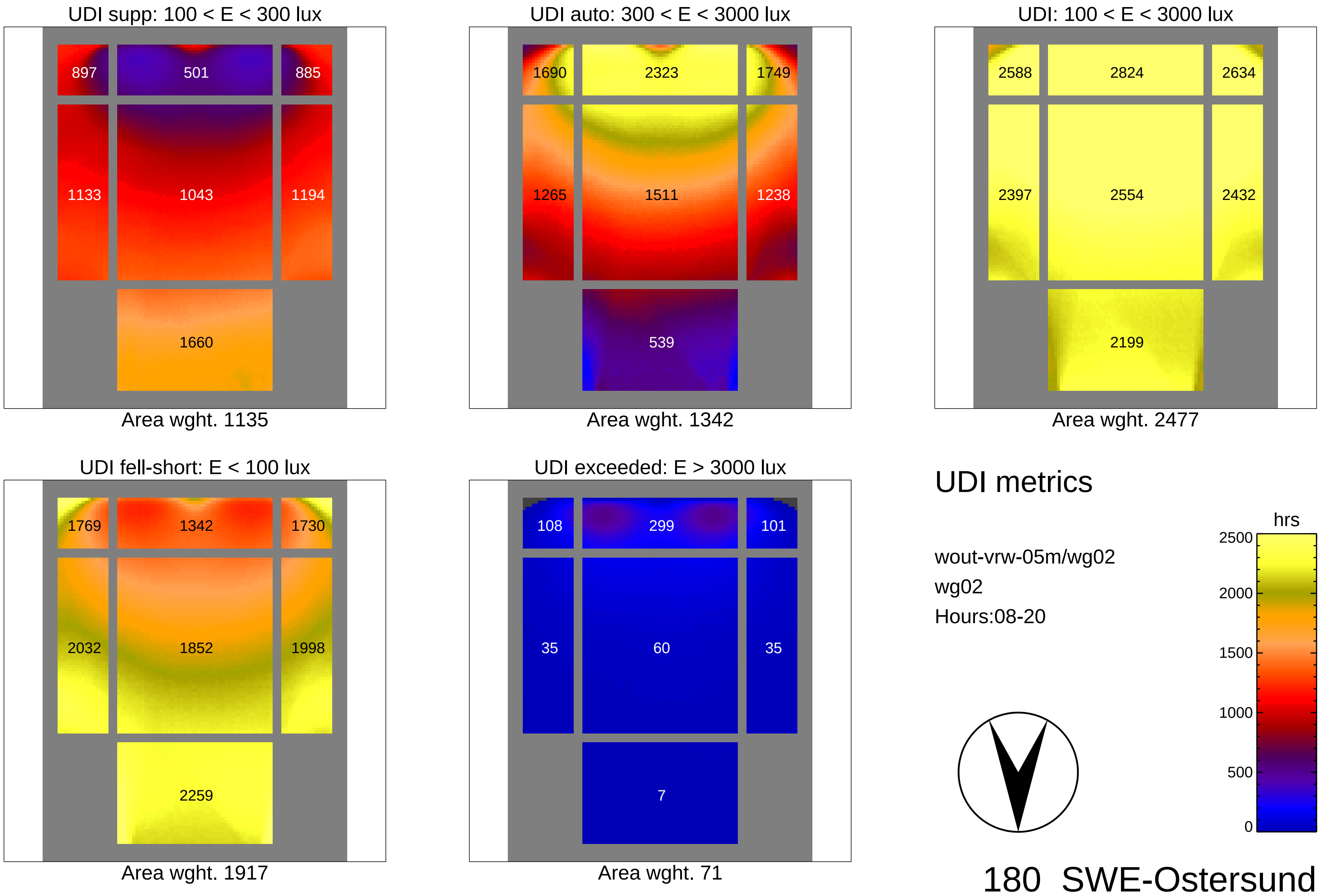

Figure 40: UDI plots for the kitchen without skylights (Ostersund climate).

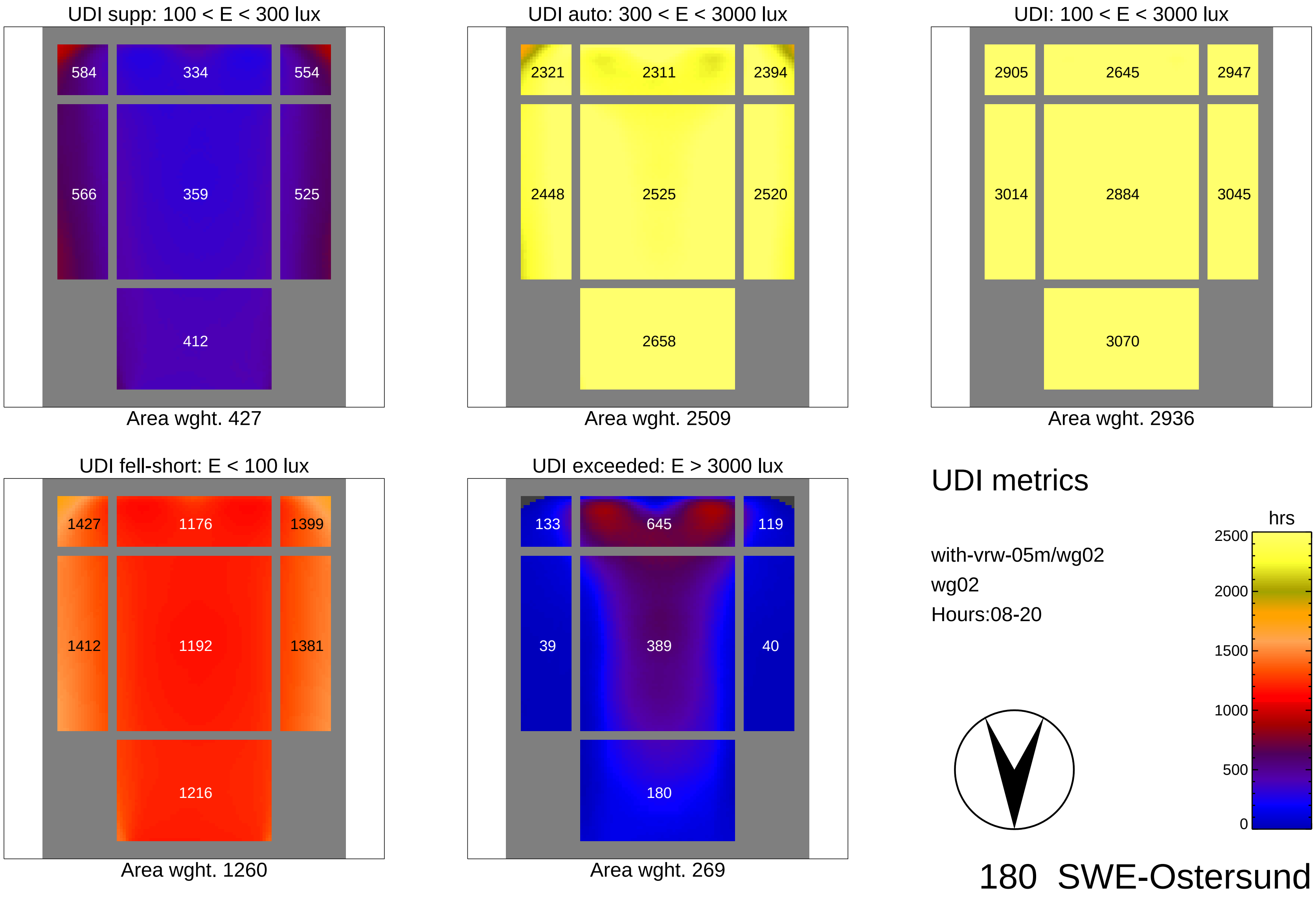

Figure 41: UDI plots for the kitchen with skylights (Ostersund climate).

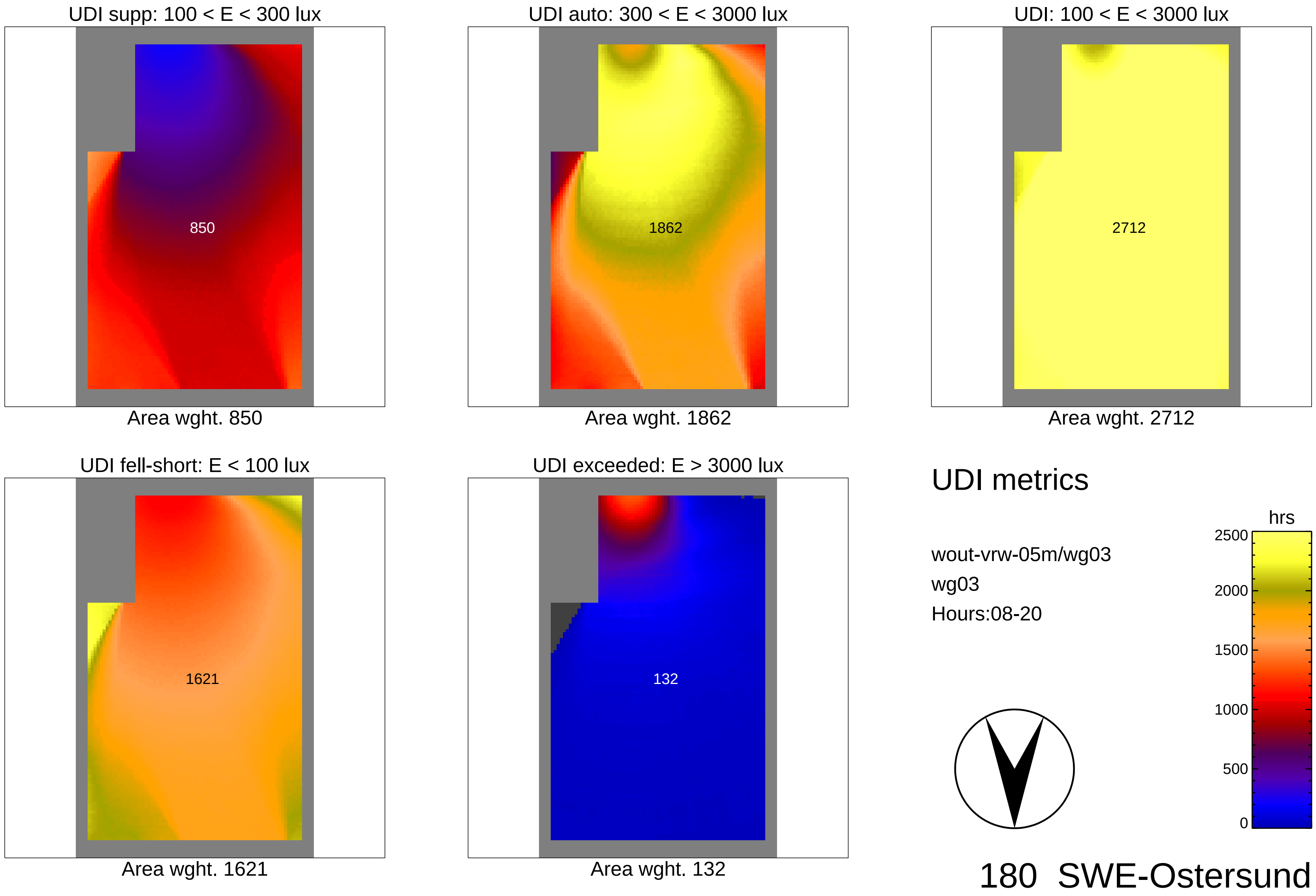

Figure 42: UDI plots for the hall without skylights (Ostersund climate). Note, this space did not have a skylight, and so additional daylight here is due to light 'spillage' from adjacent spaces.

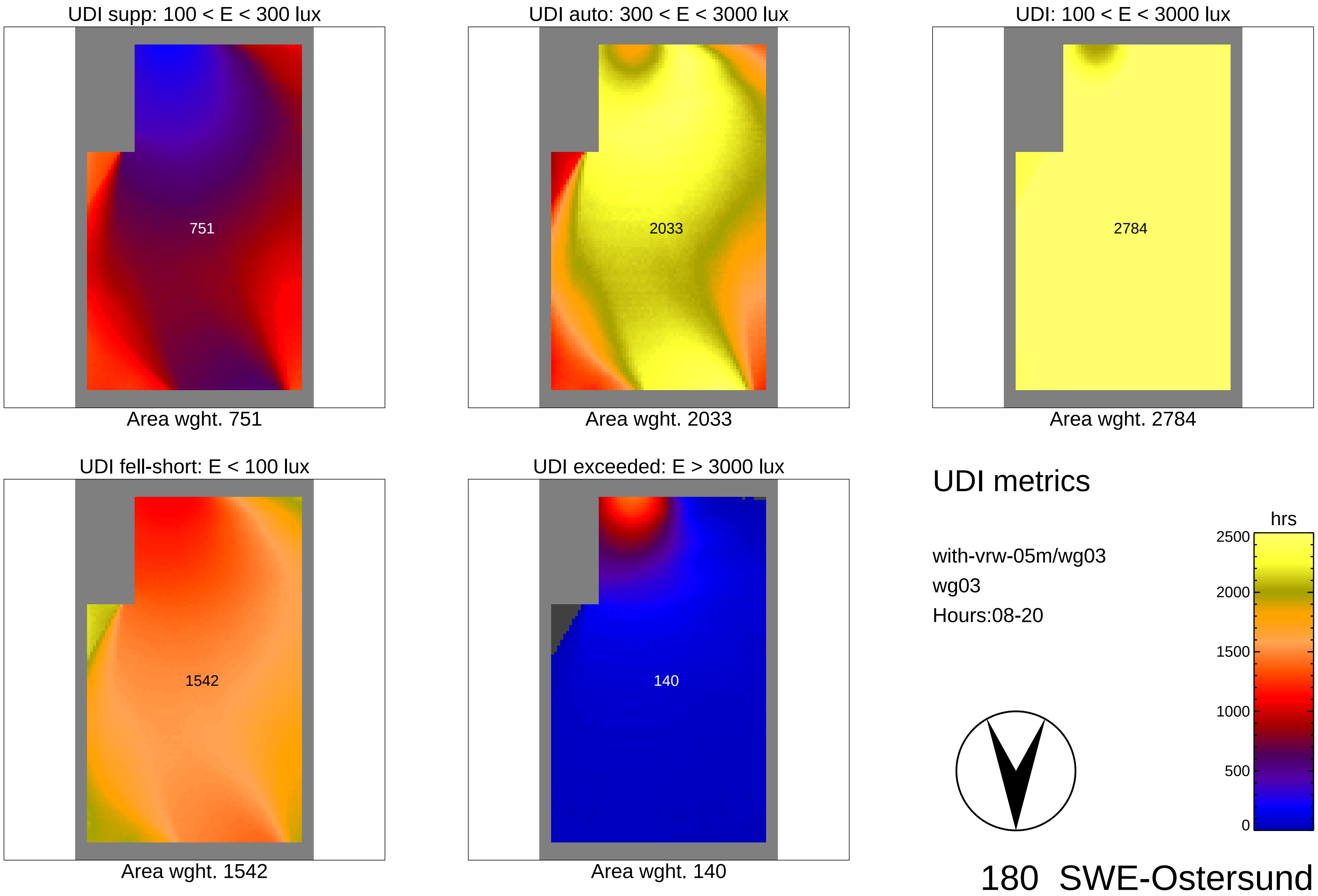

Figure 43: UDI plots for the hall with skylights (Ostersund climate). Note, this space did not have a skylight, and so additional daylight here is due to light 'spillage' from adjacent spaces.

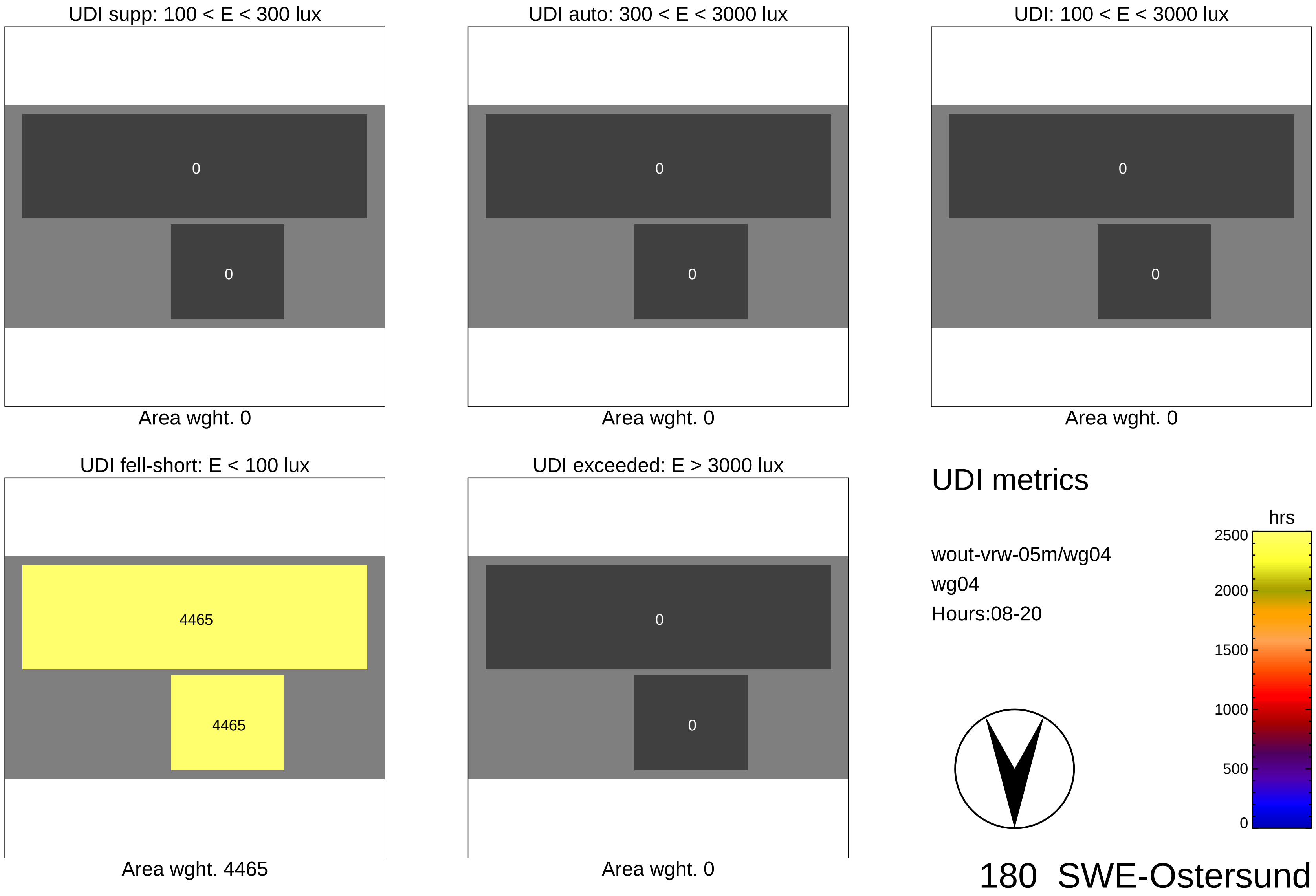

Figure 44: UDI plots for the small bathroom without skylights (Ostersund climate). Note, this space does not have any vertical windows.

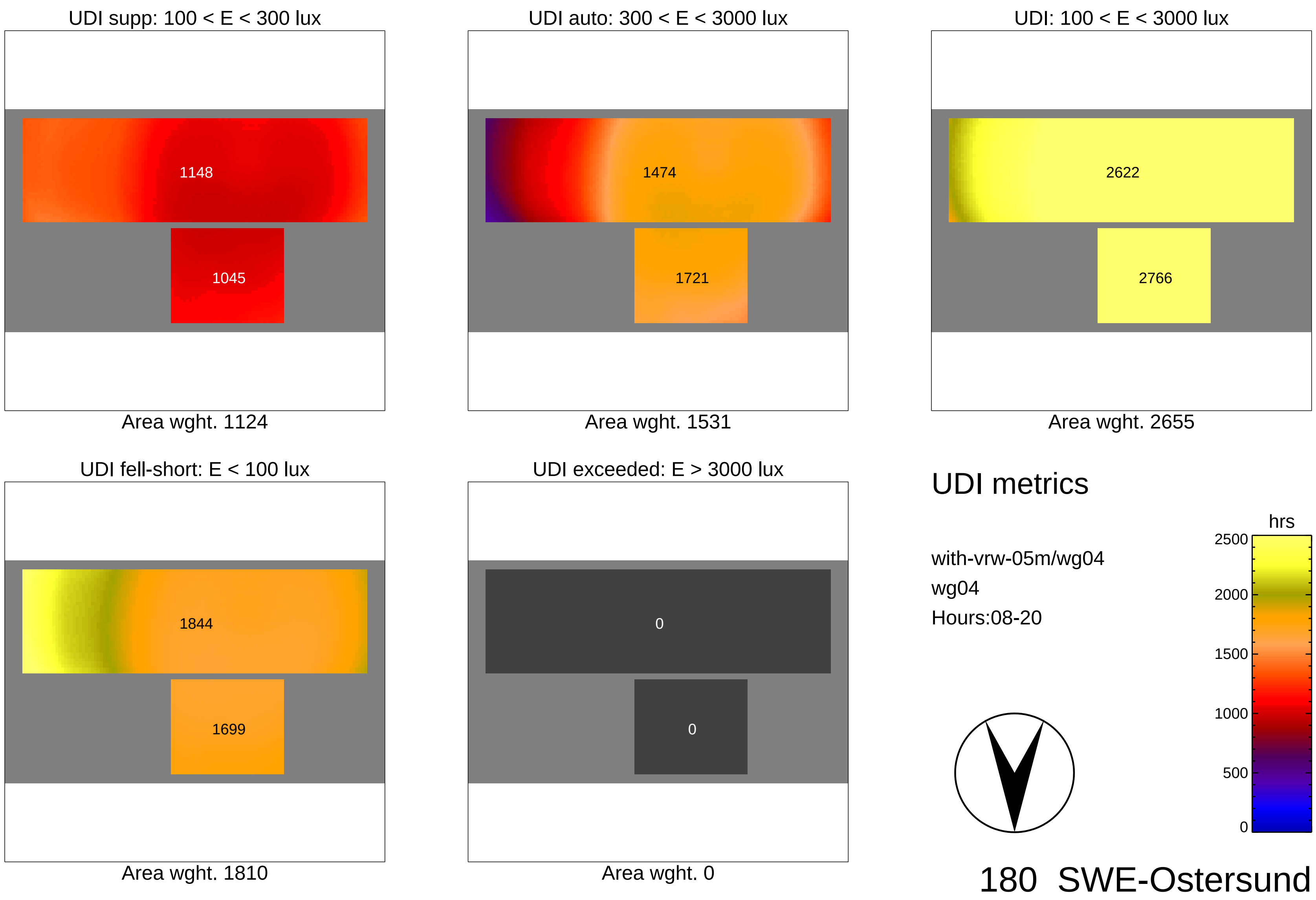

Figure 45: UDI plots for the small bathroom with skylights (Ostersund climate). Note, this space does not have any vertical windows.

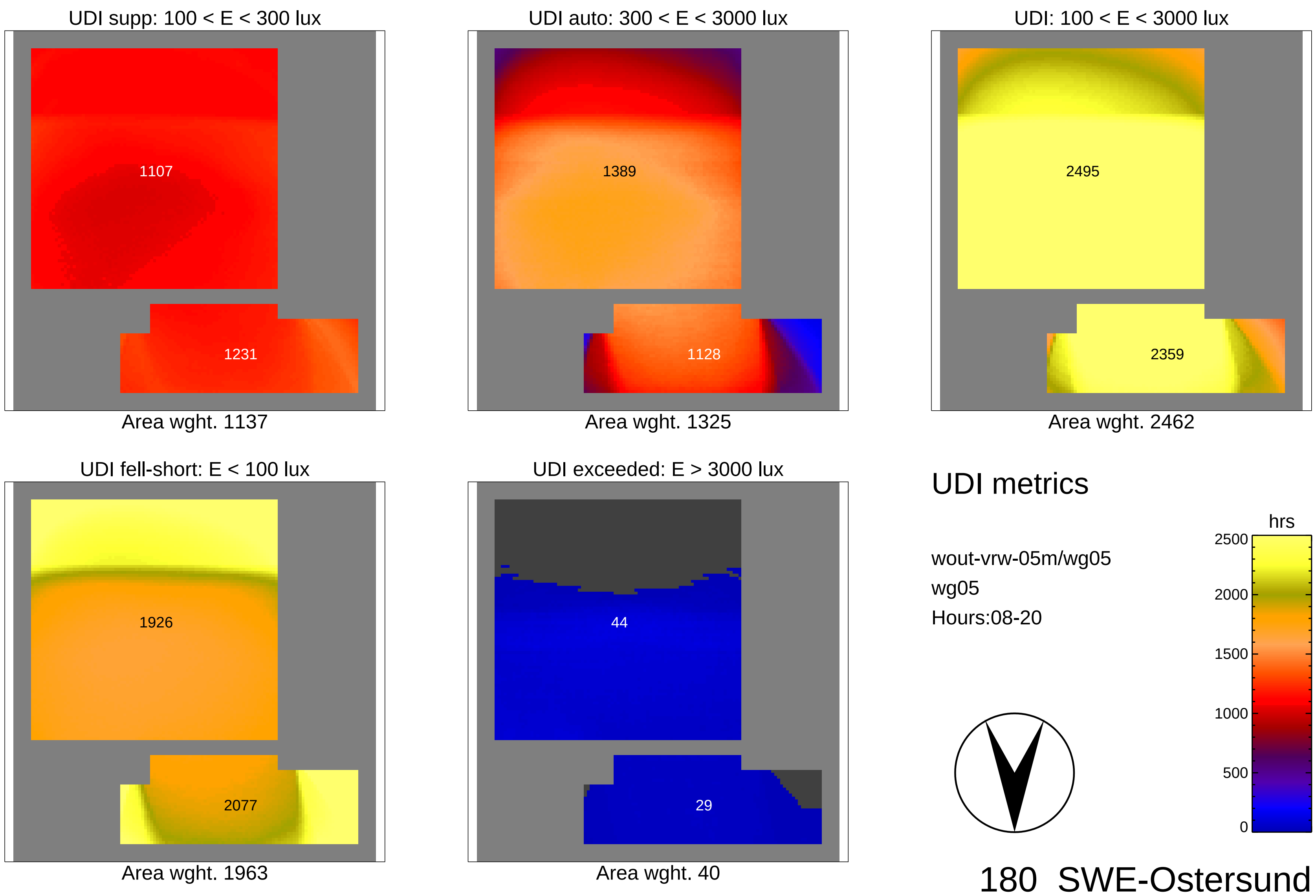

Figure 46: UDI plots for the large bathroom without skylights (Ostersund climate).

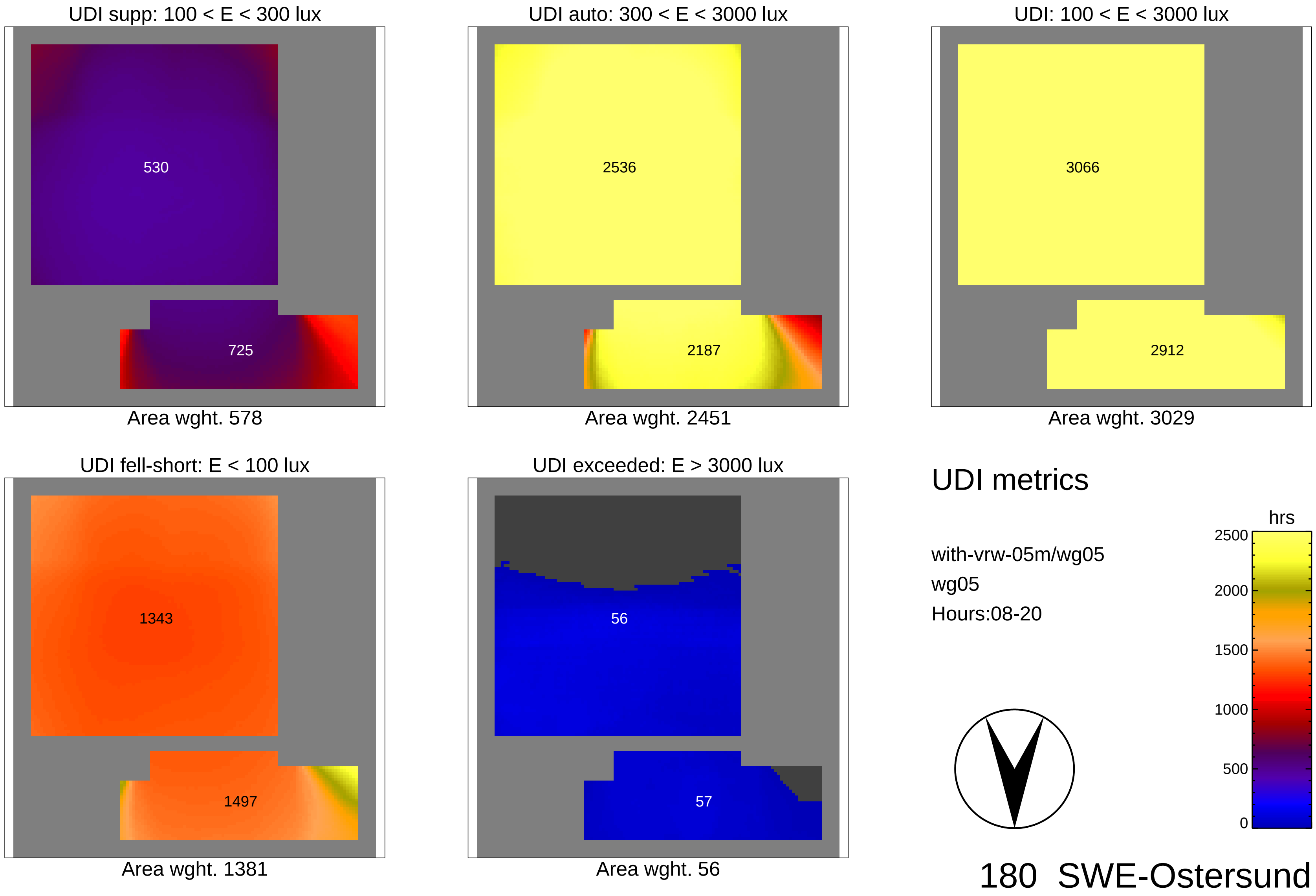

Figure 47: UDI plots for the large bathroom with skylights (Ostersund climate).

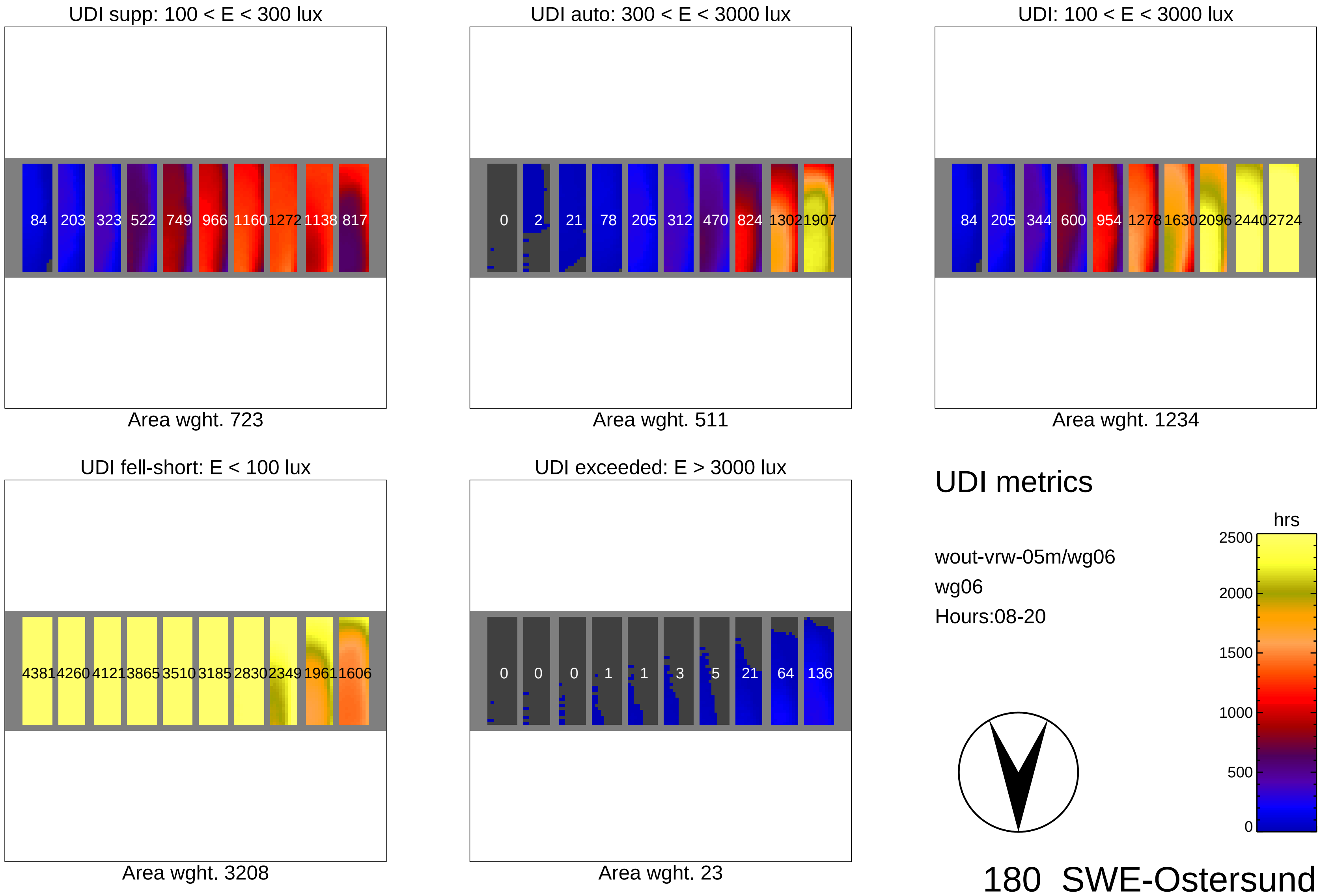

Figure 48: UDI plots for the stairs without skylights (Ostersund climate).

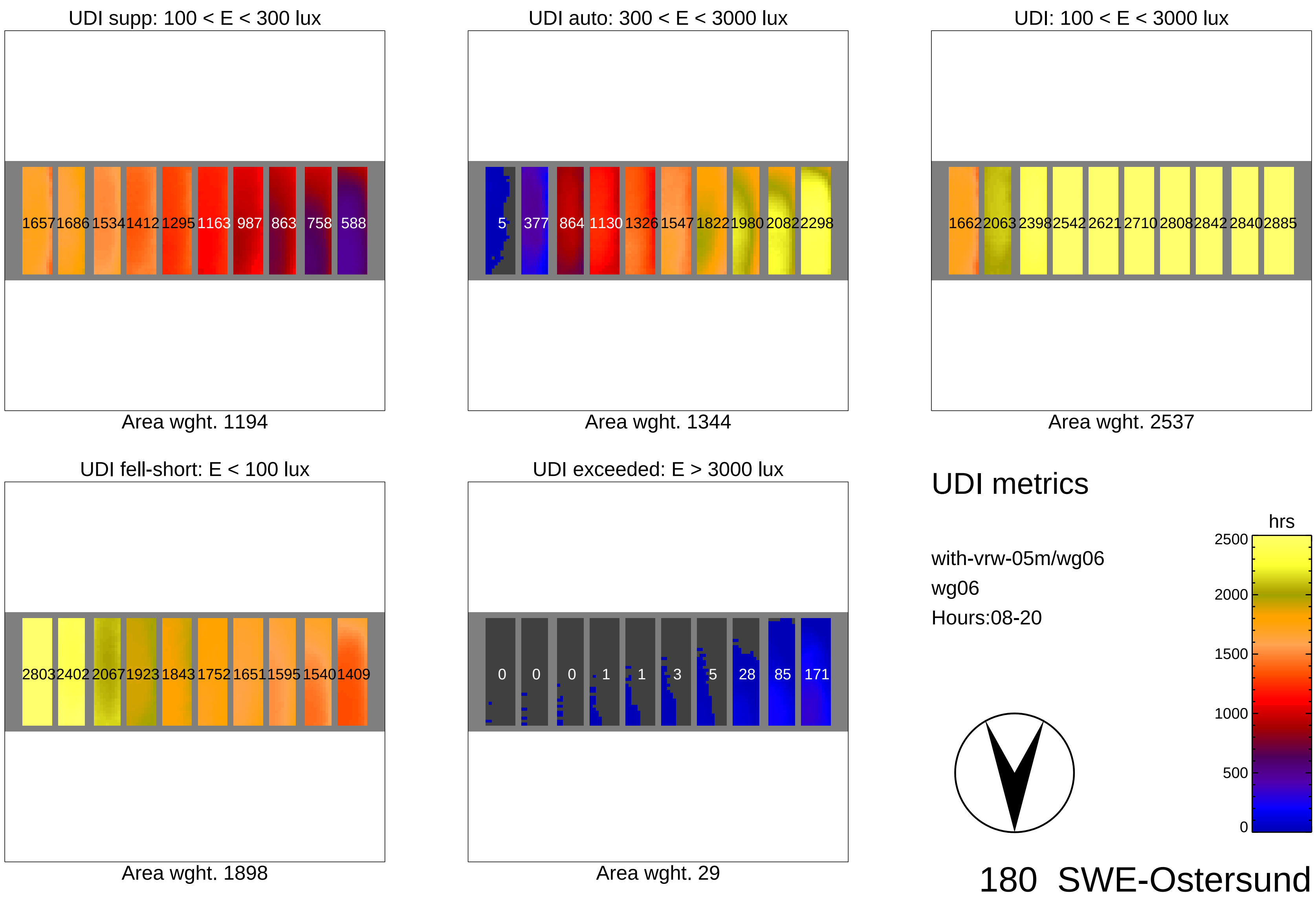

Figure 49: UDI plots for the stairs with skylights (Ostersund climate).

8.2 Example sombrero plots

As with the UDI plots, the pages for these plots are landscape orientated – toggling between them when in full-screen mode efficiently conveys the essential change in the predicted non-visual effects that result from the addition of a skylight. The figure is annotated with median, average, maximum and minimum non-visual effect (i.e. across all positions in space and the four view directions) for the three individual time periods.

Living room - Ostersund, 180

Figure 50 (without skylight) and Figure 51 (with skylight).

Kitchen - Madrid, 090

Figure 52 (without skylight) and Figure 53 (with skylight).

Living room - Rome, 270

Figure 54 (without skylight) and Figure 55 (with skylight).

Large bathroom - Rome, 090

Figure 56 (without skylight) and Figure 57 (with skylight).

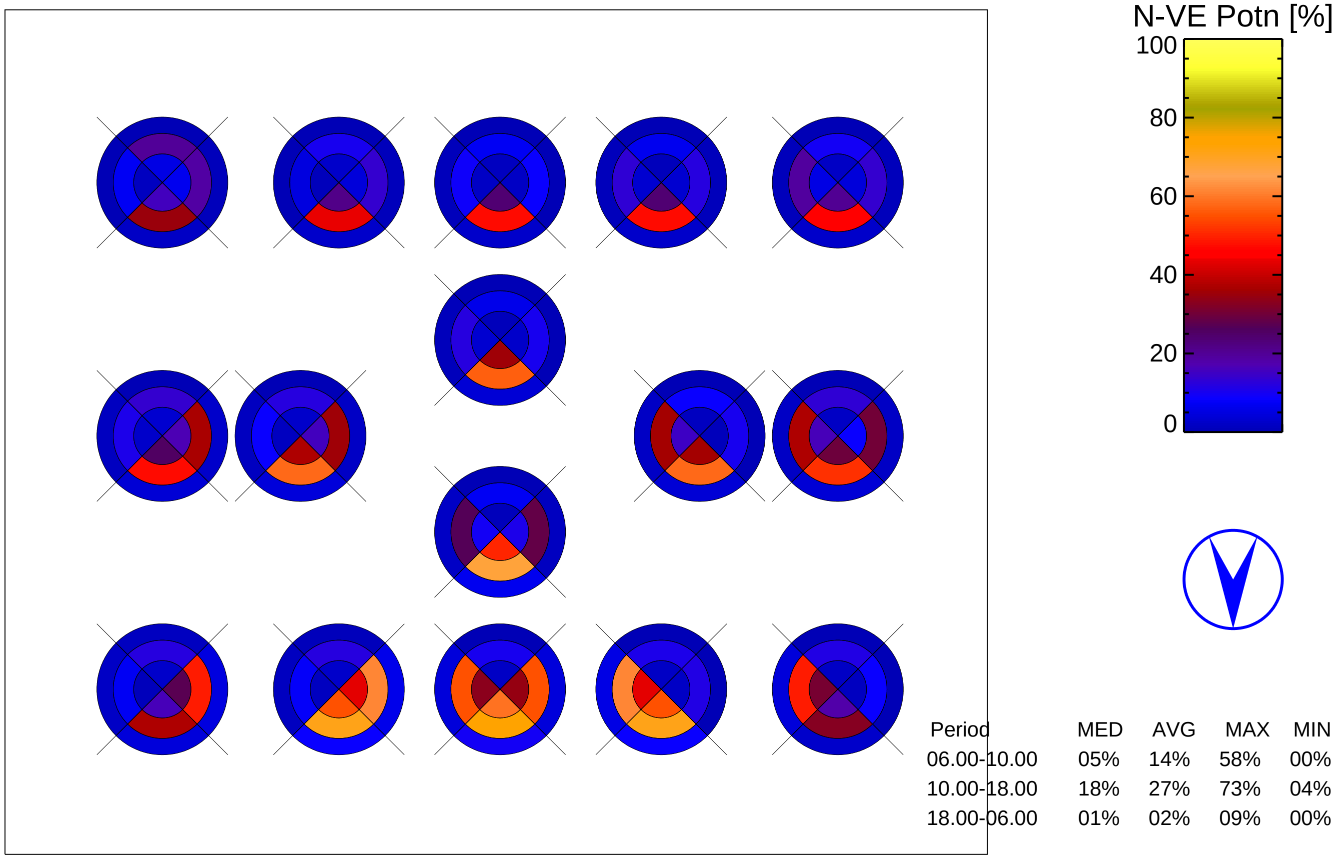

Period	MED	AVG	MAX	MIN
06.00-10.00	05%	14%	58%	00%
10.00-18.00	18%	27%	73%	04%
18.00-06.00	01%	02%	09%	00%

wout-vrw-05m/hs01

180 SWE-Ostersund

Figure 50: Predicted cumulative N-VE for case without skylights (Ostersund/180).

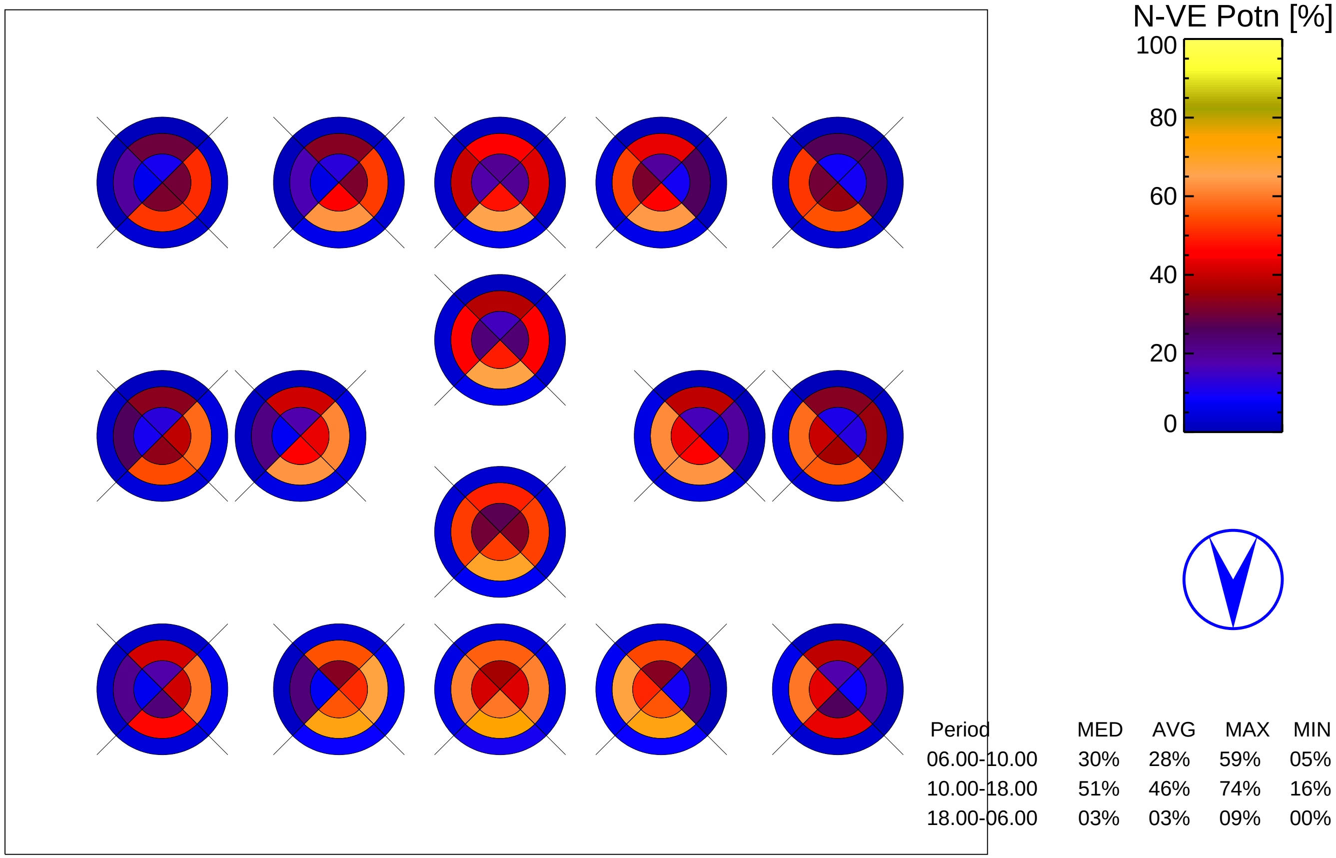

Period	MED	AVG	MAX	MIN
06.00-10.00	30%	28%	59%	05%
10.00-18.00	51%	46%	74%	16%
18.00-06.00	03%	03%	09%	00%

with-vrw-05m/hs01

180 SWE-Ostersund

Figure 51: Predicted cumulative N-VE for case with skylights (Ostersund/180).

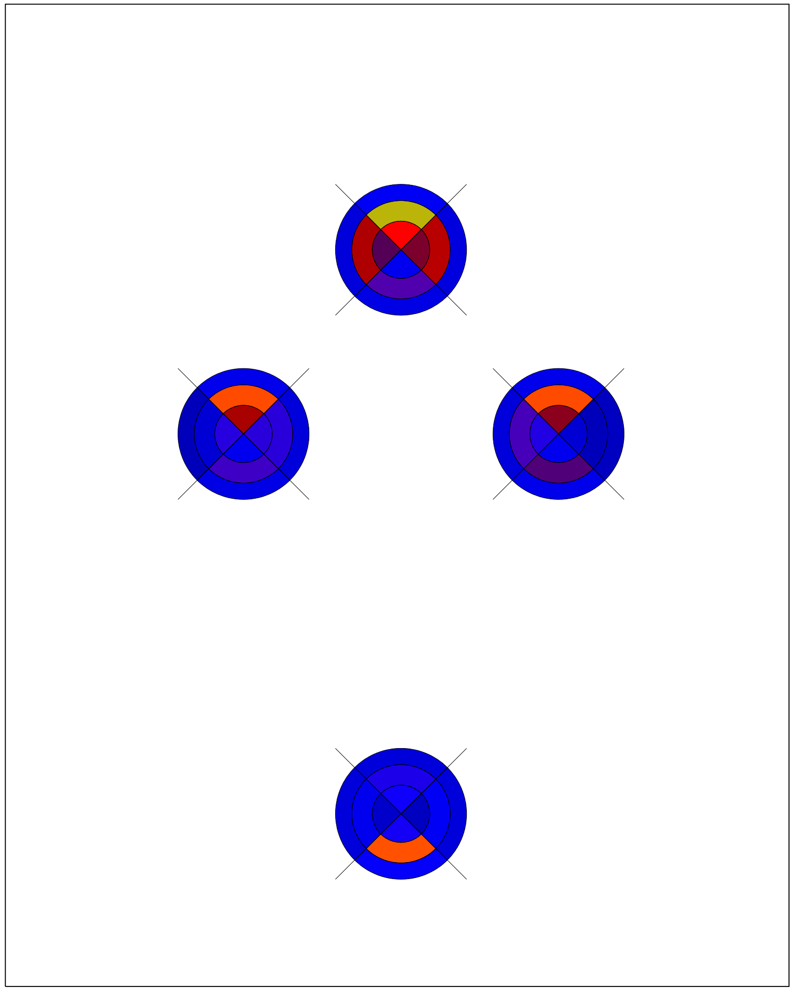

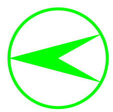

Period	MED	AVG	MAX	MIN
06.00-10.00	11%	16%	45%	01%
10.00-18.00	17%	27%	84%	00%
18.00-06.00	04%	04%	07%	01%

wout-vrw-05m/hs02

090 ESP-Madrid

Figure 52: Predicted cumulative N-VE for case without and with skylights (Madrid/090).

www.TheDaylightSite.com

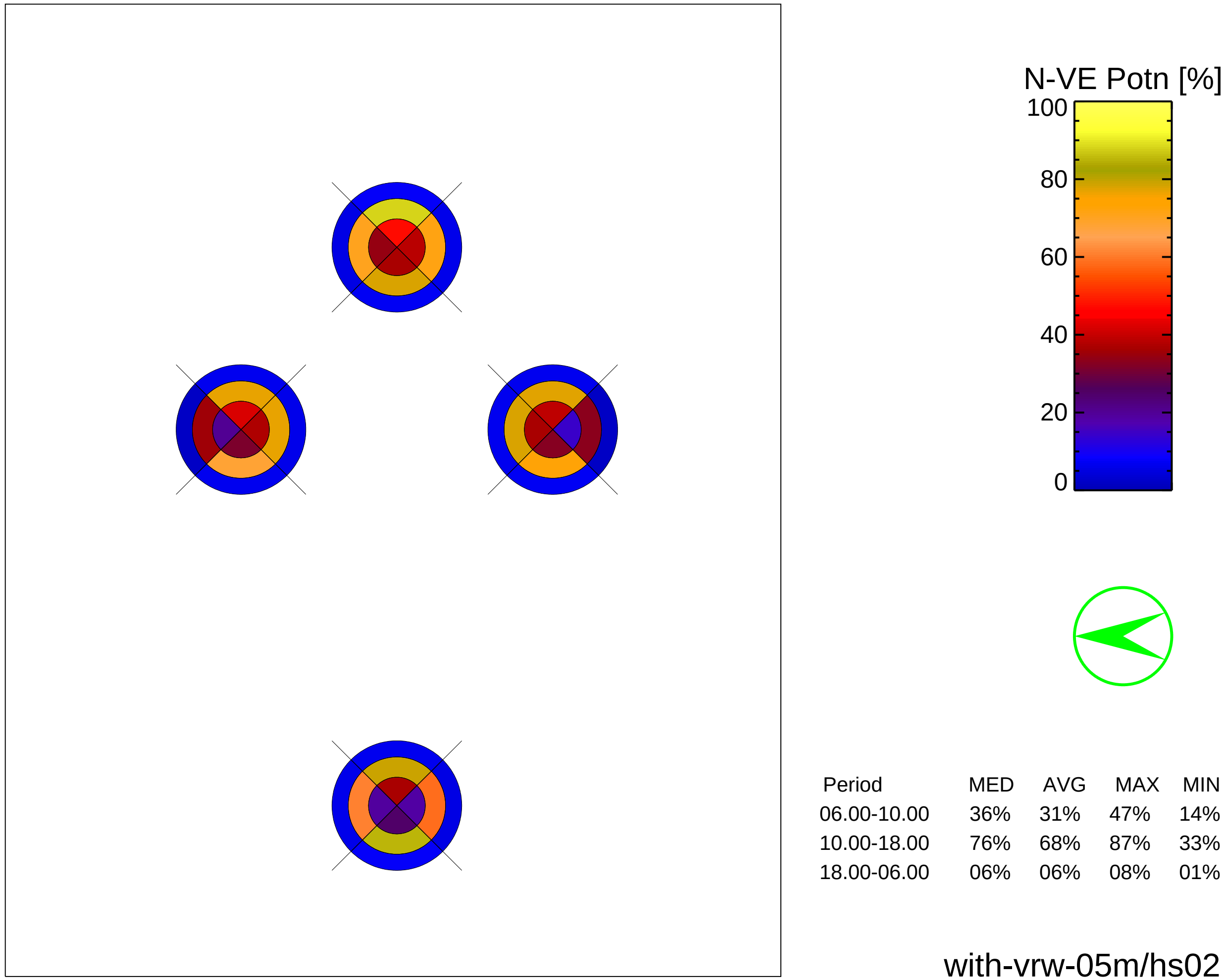

Period	MED	AVG	MAX	MIN
06.00-10.00	36%	31%	47%	14%
10.00-18.00	76%	68%	87%	33%
18.00-06.00	06%	06%	08%	01%

Figure 53: Predicted cumulative N-VE for case without and with skylights (Madrid/090).

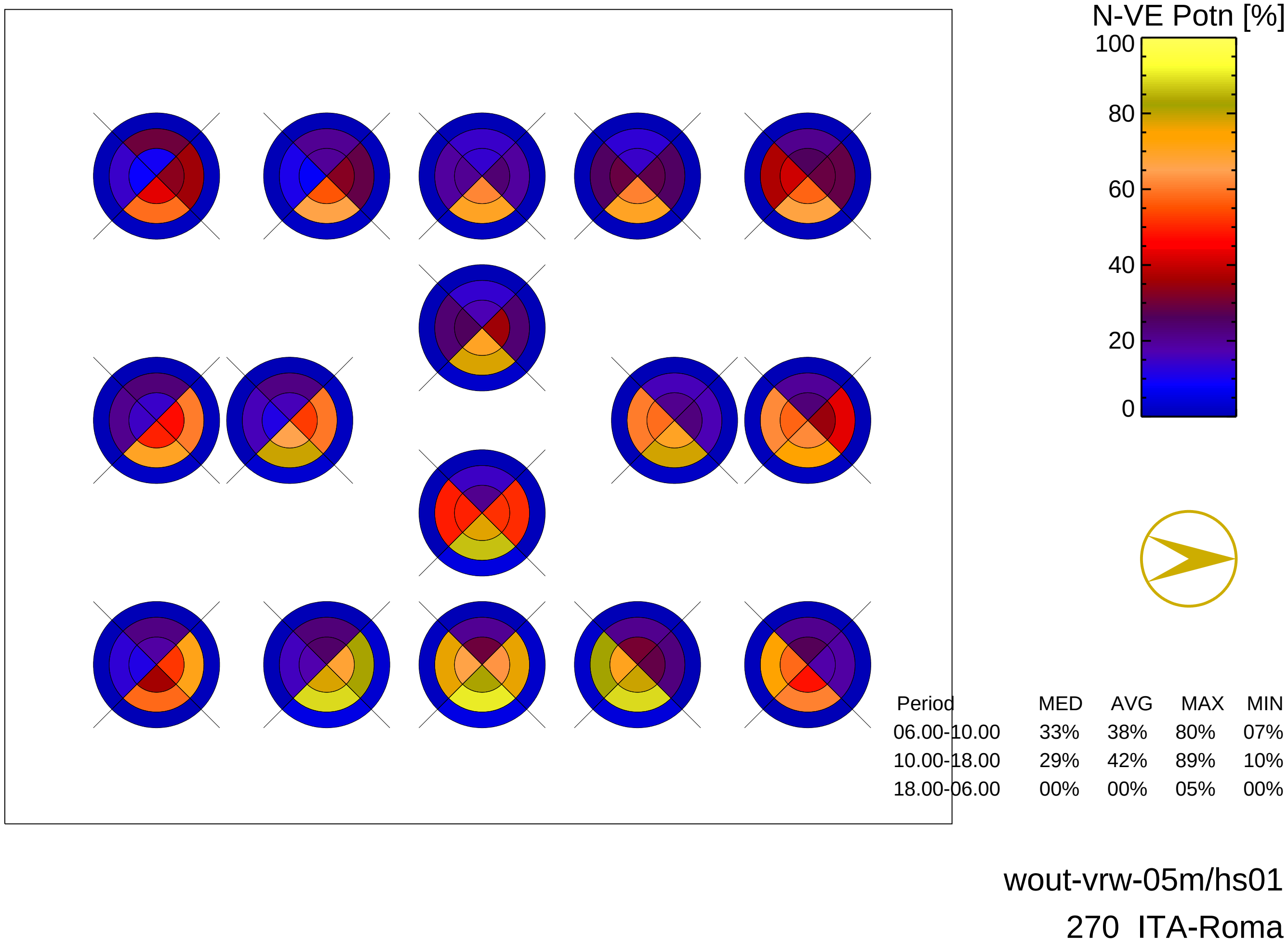

Figure 54: Predicted cumulative N-VE for case without and with skylights (Rome/270).

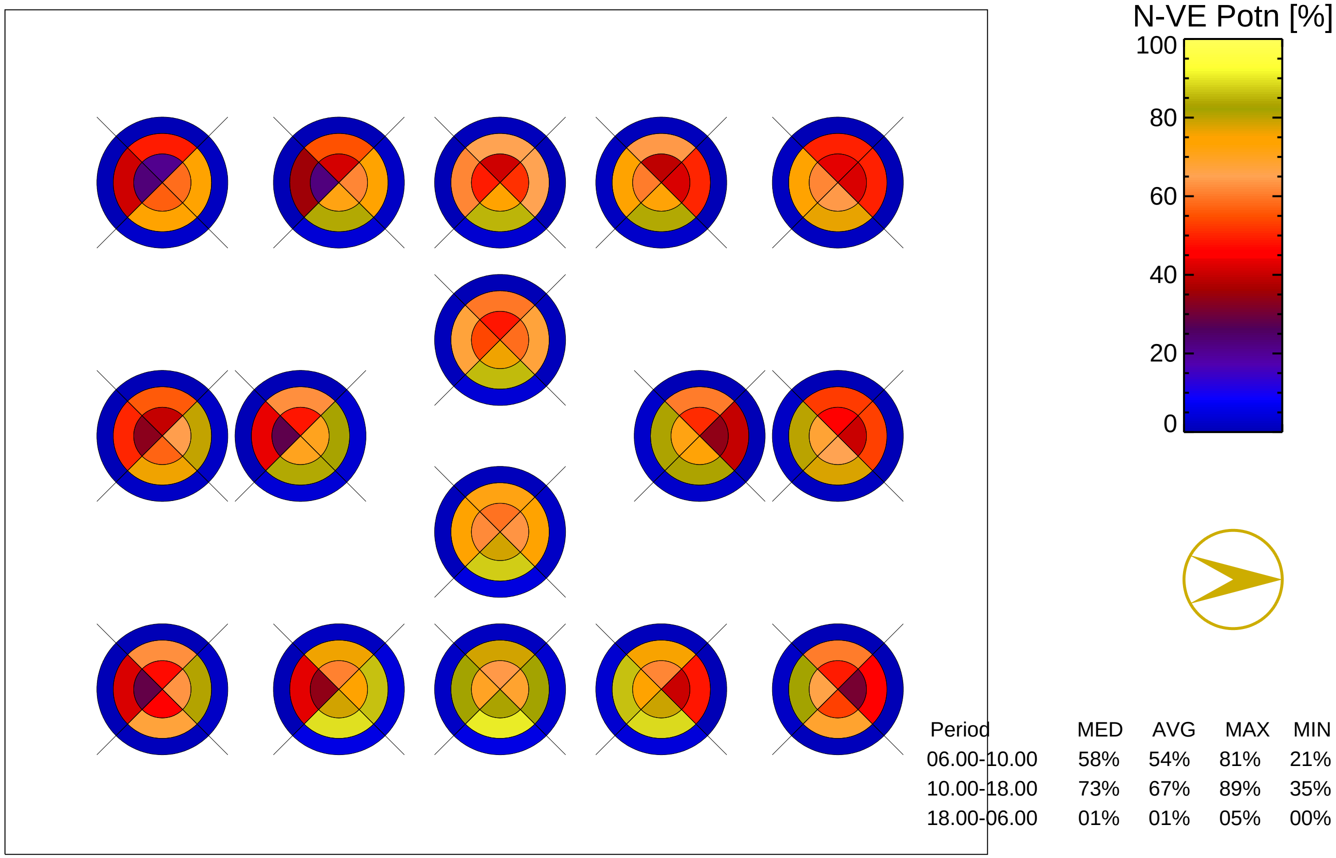

Period	MED	AVG	MAX	MIN
06.00-10.00	58%	54%	81%	21%
10.00-18.00	73%	67%	89%	35%
18.00-06.00	01%	01%	05%	00%

with-vrw-05m/hs01
270 ITA-Roma

Figure 55: Predicted cumulative N-VE for case without and with skylights (Rome/270).

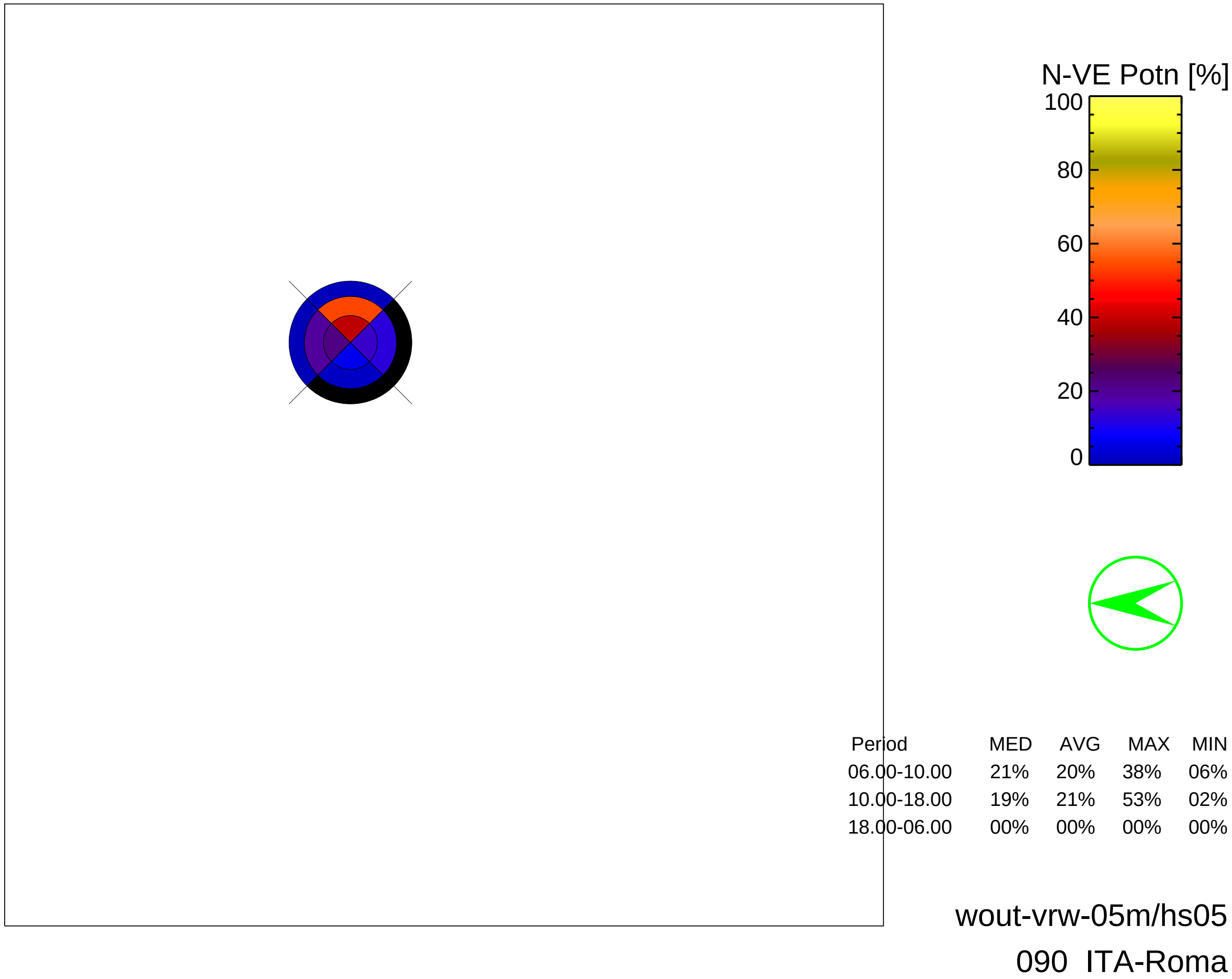

Figure 56: Predicted cumulative N-VE for case without skylights (Rome/090).

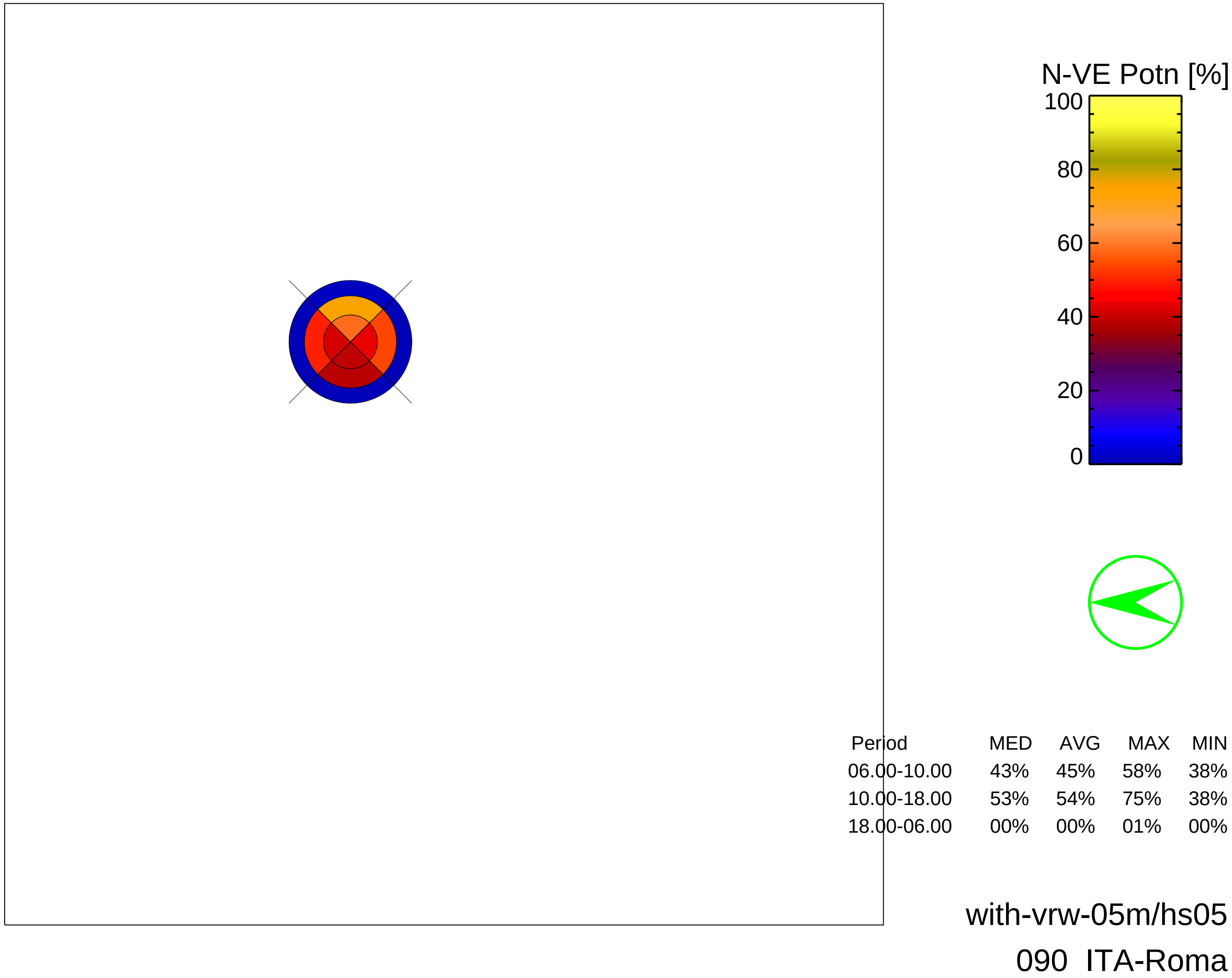

Period	MED	AVG	MAX	MIN
06.00-10.00	43%	45%	58%	38%
10.00-18.00	53%	54%	75%	38%
18.00-06.00	00%	00%	01%	00%

Figure 57: Predicted cumulative N-VE for case with skylights (Rome/090).

8.3 Tabular data for UDI metrics

Numerical data from the plots given in Figures 19 to 24. Note that the entries denote the percentage of the “occupied” year between the hours of 08h00 and 20h00.

Climate / building orientation	UDI-s: 100 - 300 lux		
	without	with	change
DEU-Hamburg ↑	17	8	-9
DEU-Hamburg ←	21	8	-12
DEU-Hamburg ↓	24	9	-15
DEU-Hamburg →	20	8	-11
ESP-Madrid ↑	13	5	-7
ESP-Madrid ←	19	6	-13
ESP-Madrid ↓	24	7	-17
ESP-Madrid →	14	5	-9
FRA-Paris ↑	18	7	-11
FRA-Paris ←	22	8	-13
FRA-Paris ↓	24	8	-16
FRA-Paris →	20	8	-12
GBR-London ↑	18	7	-10
GBR-London ←	22	8	-14
GBR-London ↓	25	8	-17
GBR-London →	21	8	-13
ITA-Roma ↑	16	4	-11
ITA-Roma ←	20	5	-14
ITA-Roma ↓	25	5	-19
ITA-Roma →	17	4	-12
POL-Warsaw ↑	16	7	-8
POL-Warsaw ←	19	7	-11
POL-Warsaw ↓	22	8	-14
POL-Warsaw →	19	8	-11
RUS-Moscow ↑	17	7	-9
RUS-Moscow ←	21	8	-13
RUS-Moscow ↓	24	9	-15
RUS-Moscow →	20	8	-12
SWE-Ostersund ↑	15	7	-7
SWE-Ostersund ←	18	9	-9
SWE-Ostersund ↓	23	9	-13
SWE-Ostersund →	18	9	-9

Table 4: Summary of UDI metric UDI-s: 100 - 300 lux for living Room (wg01)

Climate / building orientation	UDI-a: 300 - 3,000 lux		
	without	with	change
DEU-Hamburg ↑	46	52	6
DEU-Hamburg ←	44	55	11
DEU-Hamburg ↓	43	62	19
DEU-Hamburg →	45	58	12
ESP-Madrid ↑	62	54	-7
ESP-Madrid ←	56	58	2
ESP-Madrid ↓	55	71	16
ESP-Madrid →	63	62	-1
FRA-Paris ↑	49	54	5
FRA-Paris ←	47	57	10
FRA-Paris ↓	46	64	17
FRA-Paris →	49	59	10
GBR-London ↑	47	53	6
GBR-London ←	44	56	12
GBR-London ↓	43	63	20
GBR-London →	46	59	13
ITA-Roma ↑	58	57	-1
ITA-Roma ←	55	59	4
ITA-Roma ↓	52	69	16
ITA-Roma →	59	63	4
POL-Warsaw ↑	46	50	4
POL-Warsaw ←	45	54	8
POL-Warsaw ↓	44	61	17
POL-Warsaw →	45	56	10
RUS-Moscow ↑	47	53	6
RUS-Moscow ←	44	56	12
RUS-Moscow ↓	43	62	19
RUS-Moscow →	45	57	11
SWE-Ostersund ↑	45	47	2
SWE-Ostersund ←	40	49	9
SWE-Ostersund ↓	38	58	19
SWE-Ostersund →	42	53	11

Table 5: Summary of UDI metric UDI-a: 300 - 3,000 lux for living Room (wg01)

Climate / building orientation	UDI: 100 - 3,000 lux		
	without	with	change
DEU-Hamburg ↑	64	61	-3
DEU-Hamburg ←	65	64	0
DEU-Hamburg ↓	67	72	4
DEU-Hamburg →	66	67	0
ESP-Madrid ↑	75	60	-15
ESP-Madrid ←	76	65	-10
ESP-Madrid ↓	80	78	-1
ESP-Madrid →	78	67	-10
FRA-Paris ↑	68	62	-5
FRA-Paris ←	69	66	-3
FRA-Paris ↓	71	73	1
FRA-Paris →	70	67	-2
GBR-London ↑	66	61	-4
GBR-London ←	66	64	-2
GBR-London ↓	69	72	3
GBR-London →	68	68	0
ITA-Roma ↑	74	61	-12
ITA-Roma ←	75	65	-10
ITA-Roma ↓	78	75	-2
ITA-Roma →	76	68	-8
POL-Warsaw ↑	63	58	-4
POL-Warsaw ←	64	61	-2
POL-Warsaw ↓	66	69	2
POL-Warsaw →	65	64	0
RUS-Moscow ↑	65	61	-3
RUS-Moscow ←	66	65	0
RUS-Moscow ↓	68	72	4
RUS-Moscow →	66	66	0
SWE-Ostersund ↑	60	55	-5
SWE-Ostersund ←	59	58	0
SWE-Ostersund ↓	62	68	5
SWE-Ostersund →	61	63	1

Table 6: Summary of UDI metric UDI: 100 - 3,000 lux for living Room (wg01)

Climate / building orientation	UDI-f: < 100 lux		
	without	with	change
DEU-Hamburg ↑	30	20	-10
DEU-Hamburg ←	31	20	-10
DEU-Hamburg ↓	31	20	-11
DEU-Hamburg →	31	20	-10
ESP-Madrid ↑	16	11	-5
ESP-Madrid ←	16	11	-5
ESP-Madrid ↓	18	11	-6
ESP-Madrid →	16	11	-5
FRA-Paris ↑	26	16	-9
FRA-Paris ←	26	16	-9
FRA-Paris ↓	27	16	-10
FRA-Paris →	26	16	-9
GBR-London ↑	30	20	-9
GBR-London ←	30	20	-9
GBR-London ↓	31	20	-10
GBR-London →	30	20	-10
ITA-Roma ↑	21	17	-4
ITA-Roma ←	21	17	-4
ITA-Roma ↓	23	17	-5
ITA-Roma →	22	17	-4
POL-Warsaw ↑	33	23	-9
POL-Warsaw ←	33	23	-9
POL-Warsaw ↓	34	23	-10
POL-Warsaw →	34	23	-10
RUS-Moscow ↑	29	19	-9
RUS-Moscow ←	30	19	-10
RUS-Moscow ↓	30	20	-10
RUS-Moscow →	30	20	-10
SWE-Ostersund ↑	34	27	-7
SWE-Ostersund ←	36	27	-8
SWE-Ostersund ↓	37	27	-9
SWE-Ostersund →	36	27	-9

Table 7: Summary of UDI metric UDI-f: < 100 lux for living Room (wg01)

Climate / building orientation	UDI-e: > 3,000 lux		
	without	with	change
DEU-Hamburg ↑	4	18	13
DEU-Hamburg ←	3	15	11
DEU-Hamburg ↓	0	7	6
DEU-Hamburg →	2	12	9
ESP-Madrid ↑	6	27	21
ESP-Madrid ←	5	21	16
ESP-Madrid ↓	0	8	8
ESP-Madrid →	4	19	15
FRA-Paris ↑	4	20	15
FRA-Paris ←	3	16	12
FRA-Paris ↓	0	9	8
FRA-Paris →	2	14	12
GBR-London ↑	4	18	13
GBR-London ←	3	15	11
GBR-London ↓	0	7	6
GBR-London →	2	12	10
ITA-Roma ↑	5	22	16
ITA-Roma ←	4	19	14
ITA-Roma ↓	0	8	8
ITA-Roma →	3	15	12
POL-Warsaw ↑	4	19	14
POL-Warsaw ←	3	15	11
POL-Warsaw ↓	0	7	7
POL-Warsaw →	2	12	10
RUS-Moscow ↑	4	18	13
RUS-Moscow ←	3	14	10
RUS-Moscow ↓	0	7	6
RUS-Moscow →	2	12	10
SWE-Ostersund ↑	5	17	12
SWE-Ostersund ←	4	13	9
SWE-Ostersund ↓	0	4	3
SWE-Ostersund →	1	9	7

Table 8: Summary of UDI metric UDI-e: > 3,000 lux for living Room (wg01)

Climate / building orientation	UDI-s: 100 - 300 lux		
	without	with	change
DEU-Hamburg ↑	33	11	-21
DEU-Hamburg ←	29	10	-18
DEU-Hamburg ↓	27	10	-16
DEU-Hamburg →	30	10	-19
ESP-Madrid ↑	41	9	-31
ESP-Madrid ←	34	6	-27
ESP-Madrid ↓	31	7	-23
ESP-Madrid →	39	8	-30
FRA-Paris ↑	34	10	-23
FRA-Paris ←	30	9	-20
FRA-Paris ↓	28	9	-18
FRA-Paris →	31	9	-22
GBR-London ↑	35	10	-24
GBR-London ←	31	10	-21
GBR-London ↓	28	9	-19
GBR-London →	32	10	-22
ITA-Roma ↑	39	7	-31
ITA-Roma ←	34	5	-28
ITA-Roma ↓	31	6	-25
ITA-Roma →	36	6	-30
POL-Warsaw ↑	32	10	-21
POL-Warsaw ←	28	10	-18
POL-Warsaw ↓	25	9	-16
POL-Warsaw →	29	9	-19
RUS-Moscow ↑	33	11	-22
RUS-Moscow ←	28	10	-18
RUS-Moscow ↓	27	9	-17
RUS-Moscow →	30	10	-19
SWE-Ostersund ↑	33	11	-21
SWE-Ostersund ←	27	11	-16
SWE-Ostersund ↓	25	9	-15
SWE-Ostersund →	28	11	-16

Table 9: Summary of UDI metric UDI-s: 100 - 300 lux for kitchen (wg02)

Climate / building orientation	UDI-a: 300 - 3,000 lux		
	without	with	change
DEU-Hamburg ↑	24	65	41
DEU-Hamburg ←	29	65	36
DEU-Hamburg ↓	30	61	30
DEU-Hamburg →	27	62	34
ESP-Madrid ↑	31	75	44
ESP-Madrid ←	42	75	32
ESP-Madrid ↓	41	68	27
ESP-Madrid →	36	67	30
FRA-Paris ↑	27	69	42
FRA-Paris ←	32	68	36
FRA-Paris ↓	32	64	31
FRA-Paris →	30	64	34
GBR-London ↑	23	67	43
GBR-London ←	28	66	38
GBR-London ↓	30	63	32
GBR-London →	26	63	36
ITA-Roma ↑	30	73	43
ITA-Roma ←	39	73	33
ITA-Roma ↓	38	68	30
ITA-Roma →	36	67	31
POL-Warsaw ↑	25	65	39
POL-Warsaw ←	30	64	33
POL-Warsaw ↓	31	59	28
POL-Warsaw →	28	60	32
RUS-Moscow ↑	25	66	41
RUS-Moscow ←	29	65	36
RUS-Moscow ↓	31	62	30
RUS-Moscow →	28	63	34
SWE-Ostersund ↑	22	58	36
SWE-Ostersund ←	26	59	32
SWE-Ostersund ↓	30	56	26
SWE-Ostersund →	25	55	30

Table 10: Summary of UDI metric UDI-a: 300 - 3,000 lux for kitchen (wg02)

Climate / building orientation	UDI: 100 - 3,000 lux		
	without	with	change
DEU-Hamburg ↑	58	77	19
DEU-Hamburg ←	58	76	17
DEU-Hamburg ↓	57	71	14
DEU-Hamburg →	58	73	15
ESP-Madrid ↑	72	85	12
ESP-Madrid ←	76	81	5
ESP-Madrid ↓	72	76	3
ESP-Madrid →	75	75	0
FRA-Paris ↑	61	79	18
FRA-Paris ←	62	78	15
FRA-Paris ↓	60	73	12
FRA-Paris →	62	74	12
GBR-London ↑	59	78	18
GBR-London ←	59	76	17
GBR-London ↓	59	72	13
GBR-London →	59	73	14
ITA-Roma ↑	70	81	11
ITA-Roma ←	73	79	5
ITA-Roma ↓	70	75	5
ITA-Roma →	73	74	1
POL-Warsaw ↑	57	75	17
POL-Warsaw ←	58	74	15
POL-Warsaw ↓	57	69	12
POL-Warsaw →	57	70	12
RUS-Moscow ↑	58	77	18
RUS-Moscow ←	58	76	17
RUS-Moscow ↓	58	71	13
RUS-Moscow →	58	73	15
SWE-Ostersund ↑	55	70	15
SWE-Ostersund ←	54	70	15
SWE-Ostersund ↓	55	65	10
SWE-Ostersund →	53	67	13

Table 11: Summary of UDI metric UDI: 100 - 3,000 lux for kitchen (wg02)

Climate / building orientation	UDI-f: < 100 lux		
	without	with	change
DEU-Hamburg ↑	41	21	-20
DEU-Hamburg ←	40	21	-19
DEU-Hamburg ↓	41	21	-19
DEU-Hamburg →	41	21	-19
ESP-Madrid ↑	26	12	-14
ESP-Madrid ←	20	11	-9
ESP-Madrid ↓	24	11	-12
ESP-Madrid →	21	11	-9
FRA-Paris ↑	37	17	-20
FRA-Paris ←	36	17	-18
FRA-Paris ↓	37	17	-19
FRA-Paris →	36	17	-18
GBR-London ↑	41	21	-20
GBR-London ←	40	21	-19
GBR-London ↓	40	21	-19
GBR-London →	40	21	-19
ITA-Roma ↑	31	18	-13
ITA-Roma ←	27	18	-9
ITA-Roma ↓	30	18	-12
ITA-Roma →	27	17	-9
POL-Warsaw ↑	43	24	-18
POL-Warsaw ←	42	24	-17
POL-Warsaw ↓	43	24	-18
POL-Warsaw →	42	24	-17
RUS-Moscow ↑	40	20	-19
RUS-Moscow ←	40	20	-19
RUS-Moscow ↓	39	20	-18
RUS-Moscow →	40	20	-19
SWE-Ostersund ↑	44	28	-15
SWE-Ostersund ←	44	28	-15
SWE-Ostersund ↓	42	28	-14
SWE-Ostersund →	44	28	-16

Table 12: Summary of UDI metric UDI-f: < 100 lux for kitchen (wg02)

Climate / building orientation	UDI-e: > 3,000 lux		
	without	with	change
DEU-Hamburg N	0	0	0
DEU-Hamburg W	0	2	1
DEU-Hamburg S	1	6	5
DEU-Hamburg E	1	5	4
ESP-Madrid N	0	1	1
ESP-Madrid W	1	5	3
ESP-Madrid S	1	10	9
ESP-Madrid E	1	11	9
FRA-Paris N	0	1	1
FRA-Paris W	0	3	3
FRA-Paris S	1	7	6
FRA-Paris E	0	7	6
GBR-London N	0	1	1
GBR-London W	0	2	2
GBR-London S	1	6	5
GBR-London E	1	6	5
ITA-Roma N	0	2	2
ITA-Roma W	0	4	3
ITA-Roma S	1	8	7
ITA-Roma E	1	9	8
POL-Warsaw N	0	1	1
POL-Warsaw W	0	2	2
POL-Warsaw S	1	7	6
POL-Warsaw E	1	6	5
RUS-Moscow N	0	0	0
RUS-Moscow W	0	2	1
RUS-Moscow S	1	7	5
RUS-Moscow E	0	5	4
SWE-Ostersund N	0	0	0
SWE-Ostersund W	0	0	0
SWE-Ostersund S	1	6	4
SWE-Ostersund E	1	3	2

Table 13: Summary of UDI metric UDI-e: > 3,000 lux for kitchen (wg02)

Climate / building orientation	UDI-s: 100 - 300 lux		
	without	with	change
DEU-Hamburg ↑	27	22	-4
DEU-Hamburg ←	24	21	-3
DEU-Hamburg ↓	21	19	-1
DEU-Hamburg →	25	21	-3
ESP-Madrid ↑	30	21	-9
ESP-Madrid ←	18	13	-5
ESP-Madrid ↓	19	16	-3
ESP-Madrid →	26	18	-8
FRA-Paris ↑	28	23	-5
FRA-Paris ←	23	20	-3
FRA-Paris ↓	22	20	-2
FRA-Paris →	26	22	-4
GBR-London ↑	29	23	-5
GBR-London ←	25	22	-3
GBR-London ↓	21	20	-1
GBR-London →	27	23	-3
ITA-Roma ↑	30	22	-7
ITA-Roma ←	23	17	-5
ITA-Roma ↓	21	18	-3
ITA-Roma →	26	19	-6
POL-Warsaw ↑	25	20	-4
POL-Warsaw ←	22	19	-2
POL-Warsaw ↓	19	18	-1
POL-Warsaw →	23	19	-3
RUS-Moscow ↑	27	22	-4
RUS-Moscow ←	23	21	-2
RUS-Moscow ↓	21	19	-1
RUS-Moscow →	25	22	-3
SWE-Ostersund ↑	26	20	-6
SWE-Ostersund ←	21	18	-3
SWE-Ostersund ↓	19	16	-2
SWE-Ostersund →	22	18	-3

Table 14: Summary of UDI metric UDI-s: 100 - 300 lux for hall space (wg03)

Climate / building orientation	UDI-a: 300 - 3,000 lux		
	without	with	change
DEU-Hamburg ↑	38	46	7
DEU-Hamburg ←	42	47	5
DEU-Hamburg ↓	43	47	4
DEU-Hamburg →	39	45	6
ESP-Madrid ↑	47	58	11
ESP-Madrid ←	60	67	6
ESP-Madrid ↓	57	61	4
ESP-Madrid →	50	60	9
FRA-Paris ↑	41	49	8
FRA-Paris ←	46	52	5
FRA-Paris ↓	45	50	4
FRA-Paris →	42	49	6
GBR-London ↑	38	46	8
GBR-London ←	41	48	6
GBR-London ↓	44	48	4
GBR-London →	39	46	6
ITA-Roma ↑	46	55	9
ITA-Roma ←	54	61	6
ITA-Roma ↓	53	58	4
ITA-Roma →	49	57	7
POL-Warsaw ↑	39	47	7
POL-Warsaw ←	42	47	5
POL-Warsaw ↓	43	47	4
POL-Warsaw →	40	46	6
RUS-Moscow ↑	38	46	7
RUS-Moscow ←	42	47	5
RUS-Moscow ↓	43	48	4
RUS-Moscow →	39	45	6
SWE-Ostersund ↑	34	42	8
SWE-Ostersund ←	38	44	5
SWE-Ostersund ↓	41	45	3
SWE-Ostersund →	35	41	6

Table 15: Summary of UDI metric UDI-a: 300 - 3,000 lux for hall space (wg03)

Climate / building orientation	UDI: 100 - 3,000 lux		
	without	with	change
DEU-Hamburg ↑	66	69	3
DEU-Hamburg ←	66	68	2
DEU-Hamburg ↓	64	67	2
DEU-Hamburg →	64	67	2
ESP-Madrid ↑	78	80	2
ESP-Madrid ←	79	80	0
ESP-Madrid ↓	76	77	1
ESP-Madrid →	77	78	1
FRA-Paris ↑	69	73	3
FRA-Paris ←	70	72	2
FRA-Paris ↓	68	71	2
FRA-Paris →	68	71	2
GBR-London ↑	67	70	3
GBR-London ←	67	70	2
GBR-London ↓	66	68	2
GBR-London →	66	69	2
ITA-Roma ↑	76	78	2
ITA-Roma ←	77	79	1
ITA-Roma ↓	74	76	1
ITA-Roma →	75	77	1
POL-Warsaw ↑	65	68	2
POL-Warsaw ←	65	67	2
POL-Warsaw ↓	63	65	2
POL-Warsaw →	63	66	2
RUS-Moscow ↑	66	69	3
RUS-Moscow ←	66	69	2
RUS-Moscow ↓	65	68	2
RUS-Moscow →	65	68	3
SWE-Ostersund ↑	61	63	2
SWE-Ostersund ←	60	62	1
SWE-Ostersund ↓	60	62	1
SWE-Ostersund →	58	60	2

Table 16: Summary of UDI metric UDI: 100 - 3,000 lux for hall space (wg03)

Climate / building orientation	UDI-f: < 100 lux		
	without	with	change
DEU-Hamburg ↑	33	30	-3
DEU-Hamburg ←	32	30	-2
DEU-Hamburg ↓	33	30	-2
DEU-Hamburg →	33	30	-3
ESP-Madrid ↑	20	18	-2
ESP-Madrid ←	16	15	-1
ESP-Madrid ↓	19	17	-1
ESP-Madrid →	17	16	-1
FRA-Paris ↑	29	25	-3
FRA-Paris ←	28	25	-2
FRA-Paris ↓	28	25	-3
FRA-Paris →	28	25	-3
GBR-London ↑	32	29	-3
GBR-London ←	32	29	-3
GBR-London ↓	32	29	-2
GBR-London →	32	29	-3
ITA-Roma ↑	25	22	-2
ITA-Roma ←	22	20	-1
ITA-Roma ↓	23	22	-1
ITA-Roma →	22	21	-1
POL-Warsaw ↑	35	33	-2
POL-Warsaw ←	35	32	-2
POL-Warsaw ↓	35	32	-2
POL-Warsaw →	35	32	-2
RUS-Moscow ↑	32	29	-3
RUS-Moscow ←	32	29	-3
RUS-Moscow ↓	31	28	-2
RUS-Moscow →	32	29	-3
SWE-Ostersund ↑	38	36	-2
SWE-Ostersund ←	38	36	-2
SWE-Ostersund ↓	36	34	-1
SWE-Ostersund →	38	36	-2

Table 17: Summary of UDI metric UDI-f: < 100 lux for hall space (wg03)

Climate / building orientation	UDI-e: > 3,000 lux		
	without	with	change
DEU-Hamburg ↑	0	0	0
DEU-Hamburg ←	1	1	0
DEU-Hamburg ↓	2	2	0
DEU-Hamburg →	2	2	0
ESP-Madrid ↑	0	0	0
ESP-Madrid ←	2	2	0
ESP-Madrid ↓	3	3	0
ESP-Madrid →	3	3	0
FRA-Paris ↑	0	0	0
FRA-Paris ←	1	1	0
FRA-Paris ↓	2	2	0
FRA-Paris →	2	2	0
GBR-London ↑	0	0	0
GBR-London ←	0	1	0
GBR-London ↓	2	2	0
GBR-London →	2	2	0
ITA-Roma ↑	0	0	0
ITA-Roma ←	1	1	0
ITA-Roma ↓	3	3	0
ITA-Roma →	3	3	0
POL-Warsaw ↑	0	0	0
POL-Warsaw ←	0	1	0
POL-Warsaw ↓	2	2	0
POL-Warsaw →	2	2	0
RUS-Moscow ↑	0	0	0
RUS-Moscow ←	1	1	0
RUS-Moscow ↓	2	2	0
RUS-Moscow →	2	2	0
SWE-Ostersund ↑	0	0	0
SWE-Ostersund ←	0	1	0
SWE-Ostersund ↓	2	3	0
SWE-Ostersund →	2	2	0

Table 18: Summary of UDI metric UDI-e: > 3,000 lux for hall space (wg03)

Climate / building orientation	UDI-s: 100 - 300 lux		
	without	with	change
DEU-Hamburg N	0	35	35
DEU-Hamburg W	0	32	32
DEU-Hamburg S	0	28	28
DEU-Hamburg E	0	30	30
ESP-Madrid N	0	38	38
ESP-Madrid W	0	32	32
ESP-Madrid S	0	24	24
ESP-Madrid E	0	29	29
FRA-Paris N	0	35	35
FRA-Paris W	0	32	32
FRA-Paris S	0	28	28
FRA-Paris E	0	31	31
GBR-London N	0	36	36
GBR-London W	0	34	34
GBR-London S	0	29	29
GBR-London E	0	32	32
ITA-Roma N	0	38	38
ITA-Roma W	0	34	34
ITA-Roma S	0	28	28
ITA-Roma E	0	32	32
POL-Warsaw N	0	34	34
POL-Warsaw W	0	31	31
POL-Warsaw S	0	26	26
POL-Warsaw E	0	29	29
RUS-Moscow N	0	34	34
RUS-Moscow W	0	31	31
RUS-Moscow S	0	28	28
RUS-Moscow E	0	30	30
SWE-Ostersund N	0	34	34
SWE-Ostersund W	0	29	29
SWE-Ostersund S	0	25	25
SWE-Ostersund E	0	25	25

Table 19: Summary of UDI metric UDI-s: 100 - 300 lux for small bathroom (wg04)

Climate / building orientation	UDI-a: 300 - 3,000 lux		
	without	with	change
DEU-Hamburg ↑	0	27	27
DEU-Hamburg ←	0	32	32
DEU-Hamburg ↓	0	38	38
DEU-Hamburg →	0	34	34
ESP-Madrid ↑	0	31	31
ESP-Madrid ←	0	43	43
ESP-Madrid ↓	0	51	51
ESP-Madrid →	0	41	41
FRA-Paris ↑	0	32	32
FRA-Paris ←	0	37	37
FRA-Paris ↓	0	42	42
FRA-Paris →	0	37	37
GBR-London ↑	0	27	27
GBR-London ←	0	32	32
GBR-London ↓	0	39	39
GBR-London →	0	34	34
ITA-Roma ↑	0	31	31
ITA-Roma ←	0	38	38
ITA-Roma ↓	0	46	46
ITA-Roma →	0	40	40
POL-Warsaw ↑	0	28	28
POL-Warsaw ←	0	33	33
POL-Warsaw ↓	0	39	39
POL-Warsaw →	0	35	35
RUS-Moscow ↑	0	28	28
RUS-Moscow ←	0	34	34
RUS-Moscow ↓	0	39	39
RUS-Moscow →	0	34	34
SWE-Ostersund ↑	0	18	18
SWE-Ostersund ←	0	26	26
SWE-Ostersund ↓	0	34	34
SWE-Ostersund →	0	29	29

Table 20: Summary of UDI metric UDI-a: 300 - 3,000 lux for small bathroom (wg04)

Climate / building orientation	UDI: 100 - 3,000 lux		
	without	with	change
DEU-Hamburg ↑	0	62	62
DEU-Hamburg ←	0	65	65
DEU-Hamburg ↓	0	66	66
DEU-Hamburg →	0	64	64
ESP-Madrid ↑	0	70	70
ESP-Madrid ←	0	75	75
ESP-Madrid ↓	0	76	76
ESP-Madrid →	0	70	70
FRA-Paris ↑	0	67	67
FRA-Paris ←	0	70	70
FRA-Paris ↓	0	71	71
FRA-Paris →	0	69	69
GBR-London ↑	0	64	64
GBR-London ←	0	66	66
GBR-London ↓	0	68	68
GBR-London →	0	66	66
ITA-Roma ↑	0	70	70
ITA-Roma ←	0	73	73
ITA-Roma ↓	0	74	74
ITA-Roma →	0	72	72
POL-Warsaw ↑	0	62	62
POL-Warsaw ←	0	64	64
POL-Warsaw ↓	0	66	66
POL-Warsaw →	0	64	64
RUS-Moscow ↑	0	62	62
RUS-Moscow ←	0	65	65
RUS-Moscow ↓	0	67	67
RUS-Moscow →	0	64	64
SWE-Ostersund ↑	0	52	52
SWE-Ostersund ←	0	56	56
SWE-Ostersund ↓	0	59	59
SWE-Ostersund →	0	55	55

Table 21: Summary of UDI metric UDI: 100 - 3,000 lux for small bathroom (wg04)

Climate / building orientation	UDI-f: < 100 lux without	with	change
DEU-Hamburg ↑	100	37	-62
DEU-Hamburg ←	100	34	-65
DEU-Hamburg ↓	100	33	-66
DEU-Hamburg →	100	35	-64
ESP-Madrid ↑	98	28	-70
ESP-Madrid ←	98	23	-75
ESP-Madrid ↓	98	22	-76
ESP-Madrid →	98	27	-70
FRA-Paris ↑	99	31	-67
FRA-Paris ←	99	28	-70
FRA-Paris ↓	99	28	-71
FRA-Paris →	99	30	-69
GBR-London ↑	100	36	-64
GBR-London ←	100	34	-66
GBR-London ↓	100	32	-68
GBR-London →	100	34	-66
ITA-Roma ↑	100	31	-70
ITA-Roma ←	100	28	-73
ITA-Roma ↓	100	27	-74
ITA-Roma →	100	29	-72
POL-Warsaw ↑	100	38	-62
POL-Warsaw ←	100	37	-64
POL-Warsaw ↓	100	35	-66
POL-Warsaw →	100	36	-64
RUS-Moscow ↑	99	36	-62
RUS-Moscow ←	99	34	-65
RUS-Moscow ↓	99	31	-67
RUS-Moscow →	99	34	-64
SWE-Ostersund ↑	99	47	-52
SWE-Ostersund ←	99	43	-56
SWE-Ostersund ↓	99	40	-59
SWE-Ostersund →	99	44	-55

Table 22: Summary of UDI metric UDI-f: < 100 lux for small bathroom (wg04)

Climate / building orientation	UDI-e: > 3,000 lux		
	without	with	change
DEU-Hamburg ↑	0	0	0
DEU-Hamburg ←	0	0	0
DEU-Hamburg ↓	0	0	0
DEU-Hamburg →	0	0	0
ESP-Madrid ↑	0	0	0
ESP-Madrid ←	0	0	0
ESP-Madrid ↓	0	0	0
ESP-Madrid →	0	0	0
FRA-Paris ↑	0	0	0
FRA-Paris ←	0	0	0
FRA-Paris ↓	0	0	0
FRA-Paris →	0	0	0
GBR-London ↑	0	0	0
GBR-London ←	0	0	0
GBR-London ↓	0	0	0
GBR-London →	0	0	0
ITA-Roma ↑	0	0	0
ITA-Roma ←	0	0	0
ITA-Roma ↓	0	0	0
ITA-Roma →	0	0	0
POL-Warsaw ↑	0	0	0
POL-Warsaw ←	0	0	0
POL-Warsaw ↓	0	0	0
POL-Warsaw →	0	0	0
RUS-Moscow ↑	0	0	0
RUS-Moscow ←	0	0	0
RUS-Moscow ↓	0	0	0
RUS-Moscow →	0	0	0
SWE-Ostersund ↑	0	0	0
SWE-Ostersund ←	0	0	0
SWE-Ostersund ↓	0	0	0
SWE-Ostersund →	0	0	0

Table 23: Summary of UDI metric UDI-e: > 3,000 lux for small bathroom (wg04)

Climate / building orientation	UDI-s: 100 - 300 lux		
	without	with	change
DEU-Hamburg ↑	41	21	-19
DEU-Hamburg ←	36	17	-18
DEU-Hamburg ↓	27	15	-11
DEU-Hamburg →	32	18	-13
ESP-Madrid ↑	53	21	-31
ESP-Madrid ←	42	12	-29
ESP-Madrid ↓	30	12	-17
ESP-Madrid →	37	17	-19
FRA-Paris ↑	43	20	-22
FRA-Paris ←	37	15	-21
FRA-Paris ↓	29	14	-14
FRA-Paris →	34	17	-16
GBR-London ↑	42	22	-20
GBR-London ←	37	17	-20
GBR-London ↓	28	14	-13
GBR-London →	33	18	-15
ITA-Roma ↑	52	19	-33
ITA-Roma ←	43	13	-29
ITA-Roma ↓	31	12	-19
ITA-Roma →	37	14	-22
POL-Warsaw ↑	41	19	-22
POL-Warsaw ←	35	16	-18
POL-Warsaw ↓	26	14	-11
POL-Warsaw →	32	16	-15
RUS-Moscow ↑	41	21	-19
RUS-Moscow ←	34	17	-17
RUS-Moscow ↓	27	14	-12
RUS-Moscow →	33	19	-13
SWE-Ostersund ↑	39	20	-18
SWE-Ostersund ←	34	16	-17
SWE-Ostersund ↓	25	12	-12
SWE-Ostersund →	28	16	-11

Table 24: Summary of UDI metric UDI-s: 100 - 300 lux for large bathroom (wg05)

Climate / building orientation	UDI-a: 300 - 3,000 lux		
	without	with	change
DEU-Hamburg ↑	9	54	44
DEU-Hamburg ←	18	57	39
DEU-Hamburg ↓	29	59	29
DEU-Hamburg →	22	56	34
ESP-Madrid ↑	6	61	55
ESP-Madrid ←	28	70	41
ESP-Madrid ↓	41	69	28
ESP-Madrid →	26	63	36
FRA-Paris ↑	12	58	46
FRA-Paris ←	22	63	40
FRA-Paris ↓	31	62	31
FRA-Paris →	23	60	37
GBR-London ↑	8	54	45
GBR-London ←	18	59	41
GBR-London ↓	30	61	31
GBR-London →	22	57	35
ITA-Roma ↑	7	62	54
ITA-Roma ←	24	67	43
ITA-Roma ↓	36	67	30
ITA-Roma →	28	66	38
POL-Warsaw ↑	9	54	44
POL-Warsaw ←	19	57	38
POL-Warsaw ↓	30	59	28
POL-Warsaw →	22	57	34
RUS-Moscow ↑	9	54	44
RUS-Moscow ←	20	58	37
RUS-Moscow ↓	30	60	29
RUS-Moscow →	20	56	35
SWE-Ostersund ↑	4	45	41
SWE-Ostersund ←	14	50	35
SWE-Ostersund ↓	29	54	25
SWE-Ostersund →	20	49	29

Table 25: Summary of UDI metric UDI-a: 300 - 3,000 lux for large bathroom (wg05)

Climate / building orientation	UDI: 100 - 3,000 lux		
	without	with	change
DEU-Hamburg ↑	51	75	24
DEU-Hamburg ←	54	75	20
DEU-Hamburg ↓	57	74	17
DEU-Hamburg →	54	75	21
ESP-Madrid ↑	60	83	23
ESP-Madrid ←	71	83	12
ESP-Madrid ↓	71	82	10
ESP-Madrid →	64	80	16
FRA-Paris ↑	55	79	23
FRA-Paris ←	59	78	19
FRA-Paris ↓	60	77	17
FRA-Paris →	57	78	20
GBR-London ↑	51	76	24
GBR-London ←	55	76	20
GBR-London ↓	58	75	17
GBR-London →	55	76	20
ITA-Roma ↑	60	81	21
ITA-Roma ←	67	81	13
ITA-Roma ↓	68	80	11
ITA-Roma →	65	80	15
POL-Warsaw ↑	51	74	22
POL-Warsaw ←	54	74	19
POL-Warsaw ↓	56	73	16
POL-Warsaw →	55	74	18
RUS-Moscow ↑	50	75	24
RUS-Moscow ←	54	75	20
RUS-Moscow ↓	58	75	16
RUS-Moscow →	54	75	21
SWE-Ostersund ↑	43	66	22
SWE-Ostersund ←	49	66	17
SWE-Ostersund ↓	55	67	12
SWE-Ostersund →	48	66	17

Table 26: Summary of UDI metric UDI: 100 - 3,000 lux for large bathroom (wg05)

Climate / building orientation	UDI-f: < 100 lux		
	without	with	change
DEU-Hamburg ↑	49	24	-24
DEU-Hamburg ←	45	24	-21
DEU-Hamburg ↓	42	23	-18
DEU-Hamburg →	45	24	-21
ESP-Madrid ↑	38	15	-23
ESP-Madrid ←	26	13	-13
ESP-Madrid ↓	26	14	-12
ESP-Madrid →	33	15	-18
FRA-Paris ↑	44	20	-23
FRA-Paris ←	39	19	-19
FRA-Paris ↓	38	19	-18
FRA-Paris →	41	20	-21
GBR-London ↑	49	24	-24
GBR-London ←	45	23	-21
GBR-London ↓	41	23	-17
GBR-London →	45	23	-21
ITA-Roma ↑	41	20	-21
ITA-Roma ←	34	19	-14
ITA-Roma ↓	32	19	-13
ITA-Roma →	35	19	-16
POL-Warsaw ↑	49	27	-22
POL-Warsaw ←	47	27	-19
POL-Warsaw ↓	44	26	-17
POL-Warsaw →	45	27	-18
RUS-Moscow ↑	48	24	-24
RUS-Moscow ←	44	23	-20
RUS-Moscow ↓	41	23	-17
RUS-Moscow →	45	23	-21
SWE-Ostersund ↑	55	33	-22
SWE-Ostersund ←	50	32	-17
SWE-Ostersund ↓	43	30	-13
SWE-Ostersund →	50	32	-17

Table 27: Summary of UDI metric UDI-f: < 100 lux for large bathroom (wg05)

Climate / building orientation	UDI-e: > 3,000 lux		
	without	with	change
DEU-Hamburg ↑	0	0	0
DEU-Hamburg ←	0	0	0
DEU-Hamburg ↓	0	1	0
DEU-Hamburg →	0	0	0
ESP-Madrid ↑	0	0	0
ESP-Madrid ←	0	1	0
ESP-Madrid ↓	0	2	1
ESP-Madrid →	0	2	1
FRA-Paris ↑	0	0	0
FRA-Paris ←	0	0	0
FRA-Paris ↓	0	1	0
FRA-Paris →	0	0	0
GBR-London ↑	0	0	0
GBR-London ←	0	0	0
GBR-London ↓	0	1	0
GBR-London →	0	0	0
ITA-Roma ↑	0	0	0
ITA-Roma ←	0	1	0
ITA-Roma ↓	0	2	1
ITA-Roma →	0	1	0
POL-Warsaw ↑	0	0	0
POL-Warsaw ←	0	0	0
POL-Warsaw ↓	0	1	0
POL-Warsaw →	0	0	0
RUS-Moscow ↑	0	0	0
RUS-Moscow ←	0	0	0
RUS-Moscow ↓	0	1	0
RUS-Moscow →	0	0	0
SWE-Ostersund ↑	0	0	0
SWE-Ostersund ←	0	0	0
SWE-Ostersund ↓	0	1	0
SWE-Ostersund →	0	0	0

Table 28: Summary of UDI metric UDI-e: > 3,000 lux for large bathroom (wg05)

Climate / building orientation	UDI-s: 100 - 300 lux		
	without	with	change
DEU-Hamburg ↑	13	34	21
DEU-Hamburg ←	15	31	16
DEU-Hamburg ↓	16	29	12
DEU-Hamburg →	14	31	17
ESP-Madrid ↑	16	38	22
ESP-Madrid ←	20	31	11
ESP-Madrid ↓	22	28	5
ESP-Madrid →	19	32	13
FRA-Paris ↑	14	35	20
FRA-Paris ←	16	31	15
FRA-Paris ↓	17	30	12
FRA-Paris →	15	32	17
GBR-London ↑	13	35	22
GBR-London ←	15	32	16
GBR-London ↓	17	30	13
GBR-London →	15	32	17
ITA-Roma ↑	15	38	22
ITA-Roma ←	19	32	13
ITA-Roma ↓	20	31	10
ITA-Roma →	18	34	16
POL-Warsaw ↑	13	34	20
POL-Warsaw ←	15	30	14
POL-Warsaw ↓	16	28	11
POL-Warsaw →	14	31	16
RUS-Moscow ↑	13	34	21
RUS-Moscow ←	15	31	15
RUS-Moscow ↓	16	29	13
RUS-Moscow →	14	32	17
SWE-Ostersund ↑	11	32	20
SWE-Ostersund ←	14	29	14
SWE-Ostersund ↓	16	26	10
SWE-Ostersund →	13	28	15

Table 29: Summary of UDI metric UDI-s: 100 - 300 lux for stairs (wg06)

Climate / building orientation	UDI-a: 300 - 3,000 lux		
	without	with	change
DEU-Hamburg ↑	5	24	19
DEU-Hamburg ←	9	30	20
DEU-Hamburg ↓	11	33	22
DEU-Hamburg →	6	29	22
ESP-Madrid ↑	5	27	22
ESP-Madrid ←	14	40	26
ESP-Madrid ↓	15	45	30
ESP-Madrid →	8	35	26
FRA-Paris ↑	6	28	22
FRA-Paris ←	10	34	24
FRA-Paris ↓	11	37	26
FRA-Paris →	7	32	25
GBR-London ↑	5	24	19
GBR-London ←	9	30	21
GBR-London ↓	10	34	23
GBR-London →	6	29	22
ITA-Roma ↑	5	28	22
ITA-Roma ←	12	37	25
ITA-Roma ↓	13	40	27
ITA-Roma →	8	33	25
POL-Warsaw ↑	5	24	19
POL-Warsaw ←	9	30	21
POL-Warsaw ↓	11	34	23
POL-Warsaw →	7	29	22
RUS-Moscow ↑	5	24	19
RUS-Moscow ←	9	31	21
RUS-Moscow ↓	11	34	23
RUS-Moscow →	6	28	22
SWE-Ostersund ↑	4	17	13
SWE-Ostersund ←	9	24	15
SWE-Ostersund ↓	11	30	18
SWE-Ostersund →	5	24	18

Table 30: Summary of UDI metric UDI-a: 300 - 3,000 lux for stairs (wg06)

Climate / building orientation	UDI: 100 - 3,000 lux		
	without	with	change
DEU-Hamburg ↑	18	59	40
DEU-Hamburg ←	24	62	37
DEU-Hamburg ↓	27	63	35
DEU-Hamburg →	21	61	39
ESP-Madrid ↑	22	66	44
ESP-Madrid ←	35	72	37
ESP-Madrid ↓	37	73	35
ESP-Madrid →	27	68	40
FRA-Paris ↑	20	64	43
FRA-Paris ←	27	66	39
FRA-Paris ↓	29	67	38
FRA-Paris →	23	65	42
GBR-London ↑	18	60	41
GBR-London ←	25	63	37
GBR-London ↓	28	65	37
GBR-London →	21	62	40
ITA-Roma ↑	21	66	44
ITA-Roma ←	31	70	38
ITA-Roma ↓	33	71	38
ITA-Roma →	26	68	41
POL-Warsaw ↑	18	59	40
POL-Warsaw ←	25	61	35
POL-Warsaw ↓	28	62	34
POL-Warsaw →	21	60	39
RUS-Moscow ↑	18	59	40
RUS-Moscow ←	25	62	36
RUS-Moscow ↓	27	64	36
RUS-Moscow →	21	61	39
SWE-Ostersund ↑	15	50	34
SWE-Ostersund ←	23	54	30
SWE-Ostersund ↓	27	56	29
SWE-Ostersund →	19	53	33

Table 31: Summary of UDI metric UDI: 100 - 3,000 lux for stairs (wg06)

Climate / building orientation	UDI-f: < 100 lux		
	without	with	change
DEU-Hamburg ↑	81	40	-40
DEU-Hamburg ←	74	37	-37
DEU-Hamburg ↓	72	36	-35
DEU-Hamburg →	78	38	-39
ESP-Madrid ↑	76	32	-44
ESP-Madrid ←	62	25	-37
ESP-Madrid ↓	60	24	-36
ESP-Madrid →	71	30	-40
FRA-Paris ↑	78	35	-43
FRA-Paris ←	72	32	-39
FRA-Paris ↓	69	31	-38
FRA-Paris →	76	34	-42
GBR-London ↑	82	40	-41
GBR-London ←	75	37	-37
GBR-London ↓	72	35	-37
GBR-London →	79	38	-40
ITA-Roma ↑	80	35	-44
ITA-Roma ←	70	31	-38
ITA-Roma ↓	68	29	-38
ITA-Roma →	75	33	-42
POL-Warsaw ↑	82	42	-40
POL-Warsaw ←	76	40	-35
POL-Warsaw ↓	73	38	-34
POL-Warsaw →	79	40	-39
RUS-Moscow ↑	80	39	-40
RUS-Moscow ←	73	36	-36
RUS-Moscow ↓	71	35	-36
RUS-Moscow →	78	38	-39
SWE-Ostersund ↑	83	49	-34
SWE-Ostersund ←	75	45	-30
SWE-Ostersund ↓	71	42	-29
SWE-Ostersund →	80	46	-33

Table 32: Summary of UDI metric UDI-f: < 100 lux for stairs (wg06)

Climate / building orientation	UDI-e: > 3,000 lux		
	without	with	change
DEU-Hamburg ↑	0	0	0
DEU-Hamburg ←	0	0	0
DEU-Hamburg ↓	0	0	0
DEU-Hamburg →	0	0	0
ESP-Madrid ↑	0	0	0
ESP-Madrid ←	0	0	0
ESP-Madrid ↓	0	0	0
ESP-Madrid →	0	0	0
FRA-Paris ↑	0	0	0
FRA-Paris ←	0	0	0
FRA-Paris ↓	0	0	0
FRA-Paris →	0	0	0
GBR-London ↑	0	0	0
GBR-London ←	0	0	0
GBR-London ↓	0	0	0
GBR-London →	0	0	0
ITA-Roma ↑	0	0	0
ITA-Roma ←	0	0	0
ITA-Roma ↓	0	0	0
ITA-Roma →	0	0	0
POL-Warsaw ↑	0	0	0
POL-Warsaw ←	0	0	0
POL-Warsaw ↓	0	0	0
POL-Warsaw →	0	0	0
RUS-Moscow ↑	0	0	0
RUS-Moscow ←	0	0	0
RUS-Moscow ↓	0	0	0
RUS-Moscow →	0	0	0
SWE-Ostersund ↑	0	0	0
SWE-Ostersund ←	0	0	0
SWE-Ostersund ↓	0	0	0
SWE-Ostersund →	0	0	0

Table 33: Summary of UDI metric UDI-e: > 3,000 lux for stairs (wg06)

8.4 Tabular data for cumulative non-visual effects

Numerical data from the plots given in Figures 34 to 36. Note that the entries refer to the cumulative annual effect as a percentage for each respective period.

Climate / building orientation	Circadian period : 06h00-10h00 without	with	change
DEU-Hamburg ↑	18.6	31.2	12.5
DEU-Hamburg ←	12.9	25.5	12.6
DEU-Hamburg ↓	12.7	26.0	13.3
DEU-Hamburg →	24.1	34.9	10.8
ESP-Madrid ↑	17.9	29.1	11.2
ESP-Madrid ←	11.1	20.2	9.1
ESP-Madrid ↓	11.3	22.6	11.4
ESP-Madrid →	34.6	41.2	6.6
FRA-Paris ↑	14.8	25.7	10.9
FRA-Paris ←	10.6	21.2	10.6
FRA-Paris ↓	10.8	22.1	11.3
FRA-Paris →	21.8	30.7	8.9
GBR-London ↑	23.8	38.5	14.7
GBR-London ←	15.7	31.0	15.3
GBR-London ↓	15.4	31.4	16.0
GBR-London →	28.6	41.8	13.2
ITA-Roma ↑	26.8	44.3	17.5
ITA-Roma ←	16.5	32.8	16.3
ITA-Roma ↓	17.1	34.9	17.8
ITA-Roma →	38.7	54.8	16.1
POL-Warsaw ↑	29.6	45.4	15.7
POL-Warsaw ←	19.7	37.1	17.4
POL-Warsaw ↓	19.3	37.5	18.2
POL-Warsaw →	34.3	48.4	14.1
RUS-Moscow ↑	18.9	31.1	12.2
RUS-Moscow ←	13.2	25.4	12.1
RUS-Moscow ↓	13.2	26.1	13.0
RUS-Moscow →	26.1	35.7	9.7
SWE-Ostersund ↑	24.3	37.0	12.7
SWE-Ostersund ←	14.7	27.9	13.1
SWE-Ostersund ↓	14.2	28.0	13.8
SWE-Ostersund →	29.7	40.7	11.0

Table 34: Summary of cumulative non-visual effects - Circadian period : 06h00-10h00 for living Room (wg01)

Climate / building orientation	Alertness period : 10h00-18h00		
	without	with	change
DEU-Hamburg ↑	45.0	62.6	17.6
DEU-Hamburg ←	41.5	60.6	19.1
DEU-Hamburg ↓	32.1	55.2	23.1
DEU-Hamburg →	33.8	56.6	22.7
ESP-Madrid ↑	65.9	85.6	19.6
ESP-Madrid ←	57.6	81.0	23.4
ESP-Madrid ↓	43.1	72.3	29.2
ESP-Madrid →	50.3	77.0	26.7
FRA-Paris ↑	49.1	68.7	19.6
FRA-Paris ←	44.7	66.4	21.7
FRA-Paris ↓	36.1	61.7	25.6
FRA-Paris →	38.8	63.7	24.8
GBR-London ↑	43.9	61.9	18.0
GBR-London ←	41.1	60.4	19.3
GBR-London ↓	31.3	54.6	23.3
GBR-London →	32.6	55.6	23.0
ITA-Roma ↑	56.7	75.7	18.9
ITA-Roma ←	55.9	75.5	19.6
ITA-Roma ↓	40.6	66.4	25.8
ITA-Roma →	42.9	68.0	25.1
POL-Warsaw ↑	42.3	58.7	16.5
POL-Warsaw ←	41.6	58.8	17.2
POL-Warsaw ↓	31.4	53.0	21.6
POL-Warsaw →	31.9	53.4	21.5
RUS-Moscow ↑	46.3	63.8	17.5
RUS-Moscow ←	41.0	60.7	19.7
RUS-Moscow ↓	32.1	55.4	23.3
RUS-Moscow →	34.2	57.1	22.9
SWE-Ostersund ↑	44.1	57.8	13.6
SWE-Ostersund ←	39.4	54.5	15.0
SWE-Ostersund ↓	27.7	46.9	19.2
SWE-Ostersund →	29.1	48.5	19.4

Table 35: Summary of cumulative non-visual effects - Alertness period : 10h00-18h00 for living Room (wg01)

Climate / building orientation	Night-time : 18h00-06h00 without	with	change
DEU-Hamburg ↑	1.0	2.1	1.1
DEU-Hamburg ←	2.3	3.2	0.8
DEU-Hamburg ↓	1.4	2.5	1.1
DEU-Hamburg →	1.2	2.2	1.1
ESP-Madrid ↑	3.4	5.4	2.0
ESP-Madrid ←	7.3	7.9	0.6
ESP-Madrid ↓	4.5	6.3	1.8
ESP-Madrid →	4.0	5.7	1.8
FRA-Paris ↑	1.6	3.1	1.5
FRA-Paris ←	3.2	4.3	1.1
FRA-Paris ↓	1.9	3.5	1.5
FRA-Paris →	1.7	3.2	1.5
GBR-London ↑	0.8	1.5	0.7
GBR-London ←	1.8	2.4	0.6
GBR-London ↓	1.2	2.0	0.8
GBR-London →	1.0	1.8	0.8
ITA-Roma ↑	0.6	1.2	0.6
ITA-Roma ←	2.3	2.9	0.6
ITA-Roma ↓	1.1	1.9	0.7
ITA-Roma →	0.9	1.6	0.6
POL-Warsaw ↑	0.5	1.1	0.6
POL-Warsaw ←	1.1	1.7	0.6
POL-Warsaw ↓	0.8	1.5	0.7
POL-Warsaw →	0.9	1.6	0.7
RUS-Moscow ↑	1.2	2.6	1.3
RUS-Moscow ←	2.7	3.7	1.0
RUS-Moscow ↓	1.6	3.0	1.4
RUS-Moscow →	1.4	2.7	1.3
SWE-Ostersund ↑	1.4	2.8	1.4
SWE-Ostersund ←	3.1	4.3	1.2
SWE-Ostersund ↓	2.2	3.7	1.5
SWE-Ostersund →	2.0	3.5	1.5

Table 36: Summary of cumulative non-visual effects - Night-time : 18h00-06h00 for living Room (wg01)

Climate / building orientation	Circadian period : 06h00-10h00		
	without	with	change
DEU-Hamburg ↑	4.5	16.6	12.0
DEU-Hamburg ←	10.3	25.0	14.7
DEU-Hamburg ↓	5.9	19.6	13.7
DEU-Hamburg →	7.0	19.0	12.0
ESP-Madrid ↑	3.5	12.9	9.4
ESP-Madrid ←	16.0	31.7	15.6
ESP-Madrid ↓	5.0	16.2	11.2
ESP-Madrid →	9.8	18.6	8.8
FRA-Paris ↑	3.4	13.4	10.0
FRA-Paris ←	9.3	21.7	12.4
FRA-Paris ↓	4.3	15.3	11.1
FRA-Paris →	6.1	15.9	9.8
GBR-London ↑	5.9	21.2	15.3
GBR-London ←	12.1	30.6	18.5
GBR-London ↓	7.9	25.4	17.5
GBR-London →	8.0	23.3	15.2
ITA-Roma ↑	5.9	22.4	16.5
ITA-Roma ←	16.1	39.4	23.3
ITA-Roma ↓	8.1	27.7	19.6
ITA-Roma →	9.2	26.8	17.6
POL-Warsaw ↑	8.3	26.7	18.5
POL-Warsaw ←	15.3	37.0	21.7
POL-Warsaw ↓	11.0	32.0	21.0
POL-Warsaw →	10.8	29.1	18.3
RUS-Moscow ↑	4.8	16.8	12.0
RUS-Moscow ←	11.6	26.3	14.7
RUS-Moscow ↓	6.0	19.7	13.7
RUS-Moscow →	8.1	19.9	11.8
SWE-Ostersund ↑	5.7	18.7	13.0
SWE-Ostersund ←	13.2	30.4	17.2
SWE-Ostersund ↓	8.4	24.3	15.9
SWE-Ostersund →	8.9	21.9	13.0

Table 37: Summary of cumulative non-visual effects - Circadian period : 06h00-10h00 for kitchen (wg02)

Climate / building orientation	Alertness period : 10h00-18h00		
	without	with	change
DEU-Hamburg ↑	17.4	46.3	29.0
DEU-Hamburg ←	17.5	47.0	29.5
DEU-Hamburg ↓	21.4	52.1	30.7
DEU-Hamburg →	19.1	49.3	30.2
ESP-Madrid ↑	25.2	65.2	40.0
ESP-Madrid ←	27.3	69.0	41.7
ESP-Madrid ↓	32.1	75.8	43.7
ESP-Madrid →	28.8	70.9	42.0
FRA-Paris ↑	19.5	52.3	32.8
FRA-Paris ←	19.8	53.4	33.6
FRA-Paris ↓	23.5	58.0	34.6
FRA-Paris →	21.0	54.9	33.9
GBR-London ↑	16.5	45.5	29.0
GBR-London ←	16.9	46.2	29.4
GBR-London ↓	20.3	51.3	31.0
GBR-London →	18.6	48.8	30.2
ITA-Roma ↑	22.8	57.8	35.0
ITA-Roma ←	24.8	60.3	35.5
ITA-Roma ↓	27.4	64.9	37.4
ITA-Roma →	27.4	64.3	37.0
POL-Warsaw ↑	17.0	44.2	27.2
POL-Warsaw ←	17.9	45.3	27.4
POL-Warsaw ↓	20.5	48.8	28.3
POL-Warsaw →	19.7	48.2	28.5
RUS-Moscow ↑	18.0	46.7	28.8
RUS-Moscow ←	17.3	46.9	29.7
RUS-Moscow ↓	22.3	52.8	30.5
RUS-Moscow →	18.7	48.7	30.1
SWE-Ostersund ↑	16.7	40.3	23.6
SWE-Ostersund ←	15.9	40.4	24.5
SWE-Ostersund ↓	21.7	47.6	25.9
SWE-Ostersund →	18.1	43.8	25.7

Table 38: Summary of cumulative non-visual effects - Alertness period : 10h00-18h00 for kitchen (wg02)

Climate / building orientation	Night-time : 18h00-06h00		
	without	with	change
DEU-Hamburg	0.3	1.2	0.8
DEU-Hamburg	1.0	1.8	0.7
DEU-Hamburg	0.3	1.0	0.7
DEU-Hamburg	1.1	2.1	1.0
ESP-Madrid	1.6	4.2	2.6
ESP-Madrid	4.9	6.1	1.2
ESP-Madrid	1.4	3.7	2.3
ESP-Madrid	4.9	6.9	2.0
FRA-Paris	0.5	1.9	1.4
FRA-Paris	1.5	2.6	1.1
FRA-Paris	0.5	1.7	1.3
FRA-Paris	1.5	3.0	1.5
GBR-London	0.3	0.8	0.6
GBR-London	0.8	1.3	0.5
GBR-London	0.2	0.7	0.5
GBR-London	0.9	1.6	0.7
ITA-Roma	0.2	0.6	0.4
ITA-Roma	1.0	1.4	0.5
ITA-Roma	0.1	0.5	0.3
ITA-Roma	1.0	1.8	0.8
POL-Warsaw	0.1	0.5	0.3
POL-Warsaw	0.4	0.9	0.5
POL-Warsaw	0.1	0.4	0.3
POL-Warsaw	0.5	1.0	0.5
RUS-Moscow	0.4	1.4	1.1
RUS-Moscow	1.1	2.1	1.0
RUS-Moscow	0.3	1.3	1.0
RUS-Moscow	1.2	2.5	1.3
SWE-Ostersund	0.5	1.5	1.1
SWE-Ostersund	1.4	2.5	1.1
SWE-Ostersund	0.3	1.2	0.9
SWE-Ostersund	1.5	2.8	1.3

Table 39: Summary of cumulative non-visual effects - Night-time : 18h00-06h00 for kitchen (wg02)

Climate / building orientation	Circadian period : 06h00-10h00		
	without	with	change
DEU-Hamburg ↑	3.1	14.4	11.3
DEU-Hamburg ←	14.1	28.0	14.0
DEU-Hamburg ↓	6.5	20.6	14.1
DEU-Hamburg →	3.1	13.0	9.9
ESP-Madrid ↑	2.7	11.4	8.7
ESP-Madrid ←	24.7	37.8	13.1
ESP-Madrid ↓	5.7	17.7	12.0
ESP-Madrid →	2.6	7.6	5.0
FRA-Paris ↑	2.5	12.0	9.5
FRA-Paris ←	12.4	24.4	12.1
FRA-Paris ↓	4.3	15.9	11.6
FRA-Paris →	2.4	10.2	7.8
GBR-London ↑	4.0	18.1	14.1
GBR-London ←	16.9	34.1	17.2
GBR-London ↓	8.9	26.7	17.7
GBR-London →	3.9	16.5	12.6
ITA-Roma ↑	4.3	19.2	15.0
ITA-Roma ←	20.5	45.5	24.9
ITA-Roma ↓	8.4	29.3	20.9
ITA-Roma →	4.0	16.2	12.2
POL-Warsaw ↑	6.0	22.8	16.9
POL-Warsaw ←	21.6	41.1	19.5
POL-Warsaw ↓	13.1	33.6	20.5
POL-Warsaw →	5.8	21.1	15.4
RUS-Moscow ↑	3.5	14.7	11.2
RUS-Moscow ←	16.0	29.6	13.6
RUS-Moscow ↓	6.8	20.7	13.9
RUS-Moscow →	3.4	12.7	9.4
SWE-Ostersund ↑	3.8	15.4	11.7
SWE-Ostersund ←	19.0	34.5	15.5
SWE-Ostersund ↓	10.1	26.1	16.0
SWE-Ostersund →	3.7	14.1	10.4

Table 40: Summary of cumulative non-visual effects - Circadian period : 06h00-10h00 for large bathroom (wg05)

Climate / building orientation	Alertness period : 10h00-18h00		
	without	with	change
DEU-Hamburg ↑	13.1	40.0	27.0
DEU-Hamburg ←	15.4	43.2	27.8
DEU-Hamburg ↓	28.4	54.7	26.2
DEU-Hamburg →	22.8	49.9	27.1
ESP-Madrid ↑	20.8	55.8	35.0
ESP-Madrid ←	29.7	65.1	35.5
ESP-Madrid ↓	45.4	80.4	35.0
ESP-Madrid →	34.8	69.1	34.3
FRA-Paris ↑	15.5	46.6	31.1
FRA-Paris ←	19.3	50.8	31.5
FRA-Paris ↓	30.8	60.5	29.7
FRA-Paris →	24.3	54.8	30.5
GBR-London ↑	12.6	39.5	26.9
GBR-London ←	14.3	41.8	27.5
GBR-London ↓	27.5	53.8	26.2
GBR-London →	22.9	49.6	26.8
ITA-Roma ↑	18.6	51.1	32.5
ITA-Roma ←	21.8	54.1	32.3
ITA-Roma ↓	35.7	68.8	33.1
ITA-Roma →	33.4	65.5	32.1
POL-Warsaw ↑	13.0	38.7	25.7
POL-Warsaw ←	14.1	40.1	26.0
POL-Warsaw ↓	27.2	51.0	23.8
POL-Warsaw →	24.2	49.6	25.4
RUS-Moscow ↑	13.0	39.9	26.9
RUS-Moscow ←	16.0	43.9	27.9
RUS-Moscow ↓	29.9	55.6	25.7
RUS-Moscow →	21.8	49.2	27.4
SWE-Ostersund ↑	10.6	31.1	20.5
SWE-Ostersund ←	12.6	34.8	22.2
SWE-Ostersund ↓	29.9	50.8	20.9
SWE-Ostersund →	22.9	45.2	22.3

Table 41: Summary of cumulative non-visual effects - Alertness period : 10h00-18h00 for large bathroom (wg05)

Climate / building orientation	Night-time : 18h00-06h00		
	without	with	change
DEU-Hamburg ↑	0.3	1.2	0.9
DEU-Hamburg ←	0.2	0.9	0.7
DEU-Hamburg ↓	0.2	0.9	0.7
DEU-Hamburg →	1.6	2.5	0.9
ESP-Madrid ↑	1.8	4.3	2.5
ESP-Madrid ←	1.3	3.0	1.7
ESP-Madrid ↓	1.3	3.4	2.1
ESP-Madrid →	6.6	7.5	0.9
FRA-Paris ↑	0.5	1.9	1.4
FRA-Paris ←	0.4	1.5	1.2
FRA-Paris ↓	0.4	1.6	1.3
FRA-Paris →	2.2	3.5	1.3
GBR-London ↑	0.2	0.9	0.6
GBR-London ←	0.1	0.7	0.5
GBR-London ↓	0.1	0.6	0.5
GBR-London →	1.4	1.9	0.5
ITA-Roma ↑	0.1	0.6	0.5
ITA-Roma ←	0.2	0.5	0.3
ITA-Roma ↓	0.1	0.4	0.3
ITA-Roma →	1.6	2.4	0.8
POL-Warsaw ↑	0.1	0.5	0.4
POL-Warsaw ←	0.1	0.6	0.5
POL-Warsaw ↓	0.0	0.3	0.3
POL-Warsaw →	0.7	1.2	0.4
RUS-Moscow ↑	0.3	1.5	1.2
RUS-Moscow ←	0.2	1.2	0.9
RUS-Moscow ↓	0.2	1.2	1.0
RUS-Moscow →	1.7	2.9	1.2
SWE-Ostersund ↑	0.4	1.6	1.2
SWE-Ostersund ←	0.4	1.4	1.1
SWE-Ostersund ↓	0.2	1.1	0.9
SWE-Ostersund →	2.1	3.2	1.2

Table 42: Summary of cumulative non-visual effects - Night-time : 18h00-06h00 for large bathroom (wg05)

8.5 Tabular data for electric lighting saving

Numerical data from the plots given in Figures 25 to 33. The absolute and the relative amount saved are given in kWh/yr and as a percentage. Individual data are given for all the cases evaluated.

Climate / building orientation	Lighting Energy without [kWh/yr]	Lighting Energy with [kWh/yr]	Saving [kWh/yr]	Percentage saving [%]
DEU-Hamburg ↑	124.6	97.2	27.4	22.0
DEU-Hamburg ←	124.6	97.4	27.2	21.8
DEU-Hamburg ↓	126.3	97.7	28.6	22.7
DEU-Hamburg →	124.0	97.2	26.8	21.6
ESP-Madrid ↑	107.2	89.5	17.6	16.4
ESP-Madrid ←	106.3	89.7	16.6	15.6
ESP-Madrid ↓	110.0	90.2	19.9	18.1
ESP-Madrid →	102.4	88.8	13.6	13.3
FRA-Paris ↑	121.2	94.2	27.0	22.3
FRA-Paris ←	120.7	94.3	26.4	21.9
FRA-Paris ↓	122.4	94.5	27.8	22.7
FRA-Paris →	119.2	94.0	25.2	21.2
GBR-London ↑	120.8	96.3	24.5	20.3
GBR-London ←	121.3	96.6	24.7	20.3
GBR-London ↓	122.9	96.9	26.0	21.1
GBR-London →	120.7	96.4	24.3	20.1
ITA-Roma ↑	106.4	92.1	14.3	13.4
ITA-Roma ←	107.3	92.4	14.9	13.9
ITA-Roma ↓	110.2	92.9	17.2	15.7
ITA-Roma →	103.3	91.7	11.6	11.2
POL-Warsaw ↑	122.0	98.8	23.2	19.0
POL-Warsaw ←	122.5	99.2	23.3	19.0
POL-Warsaw ↓	124.0	99.4	24.6	19.8
POL-Warsaw →	122.3	98.9	23.4	19.1
RUS-Moscow ↑	122.4	95.7	26.6	21.8
RUS-Moscow ←	122.2	96.0	26.3	21.5
RUS-Moscow ↓	124.2	96.2	28.0	22.5
RUS-Moscow →	122.2	95.7	26.5	21.7
SWE-Ostersund ↑	123.4	99.4	24.0	19.5
SWE-Ostersund ←	125.9	99.8	26.1	20.7
SWE-Ostersund ↓	127.3	100.2	27.1	21.3
SWE-Ostersund →	125.5	99.6	26.0	20.7

Table 43: Living room [wg01] - profile A (default) [1.00 0.30 1.00] [0 0 0 0 1 0 0 0 0]. Lighting energy use without and with skylights, energy and percentage saving.

Climate / building orientation	Lighting Energy without [kWh/yr]	Lighting Energy with [kWh/yr]	Saving [kWh/yr]	Percentage saving [%]
DEU-Hamburg ↑	147.1	113.0	34.1	23.2
DEU-Hamburg ←	147.4	113.4	34.0	23.1
DEU-Hamburg ↓	150.7	114.0	36.7	24.3
DEU-Hamburg →	147.3	113.2	34.1	23.2
ESP-Madrid ↑	125.5	100.4	25.0	19.9
ESP-Madrid ←	124.0	101.7	22.3	18.0
ESP-Madrid ↓	131.0	102.4	28.6	21.8
ESP-Madrid →	116.8	99.2	17.6	15.0
FRA-Paris ↑	146.3	109.2	37.1	25.4
FRA-Paris ←	144.9	109.5	35.5	24.5
FRA-Paris ↓	148.9	110.2	38.8	26.0
FRA-Paris →	143.6	109.1	34.6	24.1
GBR-London ↑	142.9	110.2	32.7	22.9
GBR-London ←	144.7	110.7	34.0	23.5
GBR-London ↓	147.9	111.5	36.4	24.6
GBR-London →	144.6	110.6	34.0	23.5
ITA-Roma ↑	127.8	99.7	28.2	22.0
ITA-Roma ←	130.4	101.1	29.3	22.5
ITA-Roma ↓	137.0	102.2	34.8	25.4
ITA-Roma →	123.0	99.3	23.7	19.3
POL-Warsaw ↑	141.4	112.7	28.6	20.3
POL-Warsaw ←	143.1	113.3	29.8	20.8
POL-Warsaw ↓	145.6	113.9	31.7	21.8
POL-Warsaw →	143.3	113.2	30.1	21.0
RUS-Moscow ↑	145.3	111.0	34.3	23.6
RUS-Moscow ←	145.3	111.4	33.9	23.3
RUS-Moscow ↓	148.8	112.2	36.6	24.6
RUS-Moscow →	145.9	111.4	34.4	23.6
SWE-Ostersund ↑	143.7	115.6	28.1	19.6
SWE-Ostersund ←	146.2	117.8	28.3	19.4
SWE-Ostersund ↓	149.4	118.4	31.0	20.7
SWE-Ostersund →	146.6	117.6	29.0	19.8

Table 44: Living room [wg01] - profile B [1.00 0.30 1.00] [1 1 1 1 1 1 1 1 1]. Lighting energy use without and with skylights, energy and percentage saving.

Climate / building orientation	Lighting Energy without [kWh/yr]	Lighting Energy with [kWh/yr]	Saving [kWh/yr]	Percentage saving [%]
DEU-Hamburg ↑	177.9	125.7	52.2	29.4
DEU-Hamburg ←	178.2	126.1	52.0	29.2
DEU-Hamburg ↓	182.2	126.9	55.3	30.3
DEU-Hamburg →	179.6	126.3	53.3	29.7
ESP-Madrid ↑	129.4	99.0	30.5	23.5
ESP-Madrid ←	129.2	99.8	29.4	22.8
ESP-Madrid ↓	137.5	101.2	36.3	26.4
ESP-Madrid →	127.3	98.9	28.4	22.3
FRA-Paris ↑	162.7	114.6	48.1	29.5
FRA-Paris ←	162.2	115.1	47.1	29.1
FRA-Paris ↓	166.2	115.8	50.4	30.3
FRA-Paris →	162.5	114.9	47.6	29.3
GBR-London ↑	172.5	126.4	46.0	26.7
GBR-London ←	173.0	127.0	46.0	26.6
GBR-London ↓	177.3	128.0	49.4	27.8
GBR-London →	175.1	127.3	47.8	27.3
ITA-Roma ↑	141.3	115.3	26.0	18.4
ITA-Roma ←	140.4	115.3	25.1	17.8
ITA-Roma ↓	148.6	117.5	31.1	20.9
ITA-Roma →	141.5	116.0	25.5	18.0
POL-Warsaw ↑	182.1	135.6	46.6	25.6
POL-Warsaw ←	181.9	136.0	45.9	25.2
POL-Warsaw ↓	186.2	136.8	49.3	26.5
POL-Warsaw →	184.5	136.3	48.2	26.1
RUS-Moscow ↑	172.4	122.9	49.5	28.7
RUS-Moscow ←	173.2	123.5	49.7	28.7
RUS-Moscow ↓	178.1	124.3	53.7	30.2
RUS-Moscow →	175.6	123.6	52.0	29.6
SWE-Ostersund ↑	185.1	142.0	43.1	23.3
SWE-Ostersund ←	192.9	142.8	50.2	26.0
SWE-Ostersund ↓	196.5	144.2	52.3	26.6
SWE-Ostersund →	195.3	143.3	52.0	26.6

Table 45: Living room [wg01] - profile C [1.00 1.00 1.00] [0 0 0 0 1 0 0 0 0]. Lighting energy use without and with skylights, energy and percentage saving.

Climate / building orientation	Lighting Energy without [kWh/yr]	Lighting Energy with [kWh/yr]	Saving [kWh/yr]	Percentage saving [%]
DEU-Hamburg ↑	224.4	155.5	68.9	30.7
DEU-Hamburg ←	225.2	156.0	69.2	30.7
DEU-Hamburg ↓	232.8	158.1	74.8	32.1
DEU-Hamburg →	229.8	156.9	72.9	31.7
ESP-Madrid ↑	161.2	118.6	42.6	26.4
ESP-Madrid ←	160.7	120.5	40.2	25.0
ESP-Madrid ↓	176.7	123.9	52.8	29.9
ESP-Madrid →	158.2	119.2	39.0	24.6
FRA-Paris ↑	214.5	141.0	73.5	34.2
FRA-Paris ←	213.1	141.3	71.8	33.7
FRA-Paris ↓	221.0	143.5	77.6	35.1
FRA-Paris →	214.9	141.9	73.0	34.0
GBR-London ↑	221.1	152.5	68.7	31.0
GBR-London ←	222.9	152.8	70.1	31.4
GBR-London ↓	230.6	155.4	75.3	32.6
GBR-London →	228.1	154.2	73.9	32.4
ITA-Roma ↑	180.7	130.8	49.8	27.6
ITA-Roma ←	177.4	131.3	46.0	26.0
ITA-Roma ↓	193.4	135.5	57.9	29.9
ITA-Roma →	179.0	132.1	46.9	26.2
POL-Warsaw ↑	225.8	162.6	63.2	28.0
POL-Warsaw ←	225.0	163.1	61.9	27.5
POL-Warsaw ↓	232.1	165.2	66.9	28.8
POL-Warsaw →	230.7	164.2	66.5	28.8
RUS-Moscow ↑	220.9	150.7	70.2	31.8
RUS-Moscow ←	223.2	151.4	71.7	32.1
RUS-Moscow ↓	230.6	154.0	76.6	33.2
RUS-Moscow →	228.2	152.7	75.5	33.1
SWE-Ostersund ↑	226.4	172.8	53.6	23.7
SWE-Ostersund ←	232.7	178.1	54.6	23.5
SWE-Ostersund ↓	240.6	180.7	59.9	24.9
SWE-Ostersund →	238.3	179.6	58.6	24.6

Table 46: Living room [wg01] - profile D [1.00 1.00 1.00] [1 1 1 1 1 1 1 1 1]. Lighting energy use without and with skylights, energy and percentage saving.

Climate / building orientation	Lighting Energy without [kWh/yr]	Lighting Energy with [kWh/yr]	Saving [kWh/yr]	Percentage saving [%]
DEU-Hamburg ↑	456.5	350.7	105.8	23.2
DEU-Hamburg ←	434.2	346.4	87.7	20.2
DEU-Hamburg ↓	449.7	348.3	101.3	22.5
DEU-Hamburg →	440.5	348.6	91.9	20.9
ESP-Madrid ↑	426.7	323.8	102.9	24.1
ESP-Madrid ←	364.7	310.4	54.3	14.9
ESP-Madrid ↓	419.0	320.4	98.6	23.5
ESP-Madrid →	384.5	318.3	66.2	17.2
FRA-Paris ↑	457.8	345.6	112.2	24.5
FRA-Paris ←	429.8	340.7	89.1	20.7
FRA-Paris ↓	454.1	343.9	110.2	24.3
FRA-Paris →	439.4	343.5	95.8	21.8
GBR-London ↑	449.3	341.6	107.7	24.0
GBR-London ←	425.4	337.1	88.3	20.7
GBR-London ↓	439.4	338.7	100.7	22.9
GBR-London →	436.1	339.6	96.5	22.1
ITA-Roma ↑	444.4	315.9	128.6	28.9
ITA-Roma ←	381.2	302.5	78.7	20.6
ITA-Roma ↓	432.5	311.0	121.5	28.1
ITA-Roma →	421.1	313.6	107.5	25.5
POL-Warsaw ↑	433.0	342.0	91.0	21.0
POL-Warsaw ←	415.0	338.4	76.6	18.5
POL-Warsaw ↓	423.3	339.3	84.0	19.8
POL-Warsaw →	423.9	340.7	83.2	19.6
RUS-Moscow ↑	451.7	346.1	105.5	23.4
RUS-Moscow ←	428.7	342.5	86.2	20.1
RUS-Moscow ↓	445.5	343.7	101.8	22.8
RUS-Moscow →	433.2	343.5	89.7	20.7
SWE-Ostersund ↑	449.9	350.8	99.1	22.0
SWE-Ostersund ←	425.0	346.3	78.7	18.5
SWE-Ostersund ↓	438.1	345.9	92.2	21.0
SWE-Ostersund →	432.7	348.5	84.2	19.5

Table 47: Kitchen [wg02] - default profile [1.00 0.15 1.00] [0 1 0 1 0 1 0]. Lighting energy use without and with skylights, energy and percentage saving.

Climate / building orientation	Lighting Energy without [kWh/yr]	Lighting Energy with [kWh/yr]	Saving [kWh/yr]	Percentage saving [%]
DEU-Hamburg ↑	504.5	483.6	21.0	4.2
DEU-Hamburg ←	492.3	474.0	18.2	3.7
DEU-Hamburg ↓	495.7	477.2	18.5	3.7
DEU-Hamburg →	497.8	478.4	19.4	3.9
ESP-Madrid ↑	453.6	429.0	24.6	5.4
ESP-Madrid ←	395.2	386.8	8.4	2.1
ESP-Madrid ↓	437.6	417.9	19.7	4.5
ESP-Madrid →	416.1	401.3	14.8	3.6
FRA-Paris ↑	493.0	470.4	22.5	4.6
FRA-Paris ←	475.1	456.5	18.5	3.9
FRA-Paris ↓	486.6	465.4	21.2	4.4
FRA-Paris →	482.7	462.9	19.7	4.1
GBR-London ↑	486.9	465.7	21.2	4.4
GBR-London ←	476.0	457.1	18.8	4.0
GBR-London ↓	476.2	458.0	18.2	3.8
GBR-London →	481.4	461.3	20.1	4.2
ITA-Roma ↑	439.5	414.3	25.2	5.7
ITA-Roma ←	392.5	380.1	12.4	3.2
ITA-Roma ↓	418.7	400.3	18.5	4.4
ITA-Roma →	417.6	398.1	19.5	4.7
POL-Warsaw ↑	486.8	468.8	18.1	3.7
POL-Warsaw ←	479.2	462.6	16.6	3.5
POL-Warsaw ↓	477.2	461.6	15.6	3.3
POL-Warsaw →	482.5	465.4	17.1	3.5
RUS-Moscow ↑	498.4	476.9	21.6	4.3
RUS-Moscow ←	487.1	468.1	19.0	3.9
RUS-Moscow ↓	488.6	469.6	18.9	3.9
RUS-Moscow →	491.2	471.3	19.9	4.0
SWE-Ostersund ↑	509.7	492.2	17.5	3.4
SWE-Ostersund ←	503.9	488.7	15.2	3.0
SWE-Ostersund ↓	492.1	478.3	13.8	2.8
SWE-Ostersund →	509.0	492.8	16.2	3.2

Table 48: Entrance hall [wg03] - default profile [1.00 0.30 0.75] [1]. Lighting energy use without and with skylights, energy and percentage saving.

Climate / building orientation	Lighting Energy without [kWh/yr]	Lighting Energy with [kWh/yr]	Saving [kWh/yr]	Percentage saving [%]
DEU-Hamburg ↑	101.8	72.8	29.1	28.5
DEU-Hamburg ←	101.8	66.7	35.1	34.5
DEU-Hamburg ↓	101.8	69.2	32.6	32.0
DEU-Hamburg →	101.8	75.7	26.1	25.6
ESP-Madrid ↑	101.8	81.4	20.4	20.1
ESP-Madrid ←	101.8	66.6	35.2	34.6
ESP-Madrid ↓	101.8	79.9	22.0	21.6
ESP-Madrid →	101.8	85.7	16.1	15.8
FRA-Paris ↑	101.8	76.6	25.3	24.8
FRA-Paris ←	101.8	70.5	31.3	30.7
FRA-Paris ↓	101.8	74.7	27.1	26.6
FRA-Paris →	101.8	79.7	22.1	21.7
GBR-London ↑	101.8	69.2	32.6	32.0
GBR-London ←	101.8	62.6	39.3	38.6
GBR-London ↓	101.8	64.0	37.8	37.1
GBR-London →	101.8	72.3	29.5	29.0
ITA-Roma ↑	101.8	70.1	31.8	31.2
ITA-Roma ←	101.8	55.2	46.6	45.8
ITA-Roma ↓	101.8	63.8	38.1	37.4
ITA-Roma →	101.8	75.6	26.3	25.8
POL-Warsaw ↑	101.8	64.9	36.9	36.3
POL-Warsaw ←	101.8	57.8	44.0	43.2
POL-Warsaw ↓	101.8	58.4	43.4	42.7
POL-Warsaw →	101.8	67.9	33.9	33.3
RUS-Moscow ↑	101.8	72.6	29.3	28.7
RUS-Moscow ←	101.8	66.6	35.3	34.6
RUS-Moscow ↓	101.8	69.5	32.3	31.7
RUS-Moscow →	101.8	77.0	24.9	24.4
SWE-Ostersund ↑	101.8	73.2	28.6	28.1
SWE-Ostersund ←	101.8	65.3	36.5	35.9
SWE-Ostersund ↓	101.8	66.8	35.0	34.4
SWE-Ostersund →	101.8	76.1	25.7	25.3

Table 49: Small bathroom [wg04] - default profile [1.00 0.05 0.20] [1 1]. Lighting energy use without and with skylights, energy and percentage saving.

Climate / building orientation	Lighting Energy without [kWh/yr]	Lighting Energy with [kWh/yr]	Saving [kWh/yr]	Percentage saving [%]
DEU-Hamburg ↑	273.0	177.8	95.2	34.9
DEU-Hamburg ←	223.0	167.1	55.9	25.1
DEU-Hamburg ↓	245.9	170.7	75.2	30.6
DEU-Hamburg →	270.0	178.2	91.8	34.0
ESP-Madrid ↑	276.5	192.1	84.4	30.5
ESP-Madrid ←	191.0	157.4	33.6	17.6
ESP-Madrid ↓	258.0	187.2	70.8	27.4
ESP-Madrid →	267.1	213.8	53.3	20.0
FRA-Paris ↑	276.2	188.3	87.9	31.8
FRA-Paris ←	226.5	176.1	50.4	22.2
FRA-Paris ↓	261.0	183.8	77.2	29.6
FRA-Paris →	273.4	190.8	82.6	30.2
GBR-London ↑	267.6	162.9	104.7	39.1
GBR-London ←	209.7	151.0	58.7	28.0
GBR-London ↓	230.4	152.7	77.7	33.7
GBR-London →	265.0	163.4	101.6	38.3
ITA-Roma ↑	272.7	149.3	123.4	45.2
ITA-Roma ←	168.3	114.6	53.7	31.9
ITA-Roma ↓	233.3	132.8	100.5	43.1
ITA-Roma →	267.6	163.0	104.6	39.1
POL-Warsaw ↑	256.6	150.5	106.1	41.3
POL-Warsaw ←	198.5	141.9	56.6	28.5
POL-Warsaw ↓	207.6	141.8	65.8	31.7
POL-Warsaw →	255.4	150.2	105.3	41.2
RUS-Moscow ↑	271.3	179.1	92.3	34.0
RUS-Moscow ←	218.1	169.9	48.2	22.1
RUS-Moscow ↓	243.9	173.1	70.8	29.0
RUS-Moscow →	269.3	178.7	90.6	33.7
SWE-Ostersund ↑	272.4	180.3	92.1	33.8
SWE-Ostersund ←	212.0	166.6	45.4	21.4
SWE-Ostersund ↓	228.2	166.8	61.4	26.9
SWE-Ostersund →	267.2	180.5	86.7	32.4

Table 50: Large bathroom [wg05] - default profile [1.00 0.05 0.20] [1 1]. Lighting energy use without and with skylights, energy and percentage saving.

Climate / building orientation	Lighting Energy without [kWh/yr]	Lighting Energy with [kWh/yr]	Saving [kWh/yr]	Percentage saving [%]
DEU-Hamburg ⮉	190.5	178.4	12.1	6.4
DEU-Hamburg ⮈	190.5	169.1	21.4	11.2
DEU-Hamburg ⮋	190.4	164.4	26.0	13.7
DEU-Hamburg ⮊	190.5	170.1	20.5	10.7
ESP-Madrid ⮉	190.5	174.2	16.3	8.6
ESP-Madrid ⮈	189.9	160.0	29.9	15.7
ESP-Madrid ⮋	189.9	151.9	38.1	20.0
ESP-Madrid ⮊	190.5	160.7	29.9	15.7
FRA-Paris ⮉	190.5	174.2	16.3	8.6
FRA-Paris ⮈	190.4	166.3	24.1	12.7
FRA-Paris ⮋	190.4	161.7	28.7	15.1
FRA-Paris ⮊	190.5	167.2	23.3	12.2
GBR-London ⮉	190.5	177.2	13.4	7.0
GBR-London ⮈	190.3	166.7	23.7	12.4
GBR-London ⮋	190.3	162.9	27.4	14.4
GBR-London ⮊	190.5	169.1	21.4	11.3
ITA-Roma ⮉	190.5	174.8	15.8	8.3
ITA-Roma ⮈	190.5	165.1	25.5	13.4
ITA-Roma ⮋	190.5	160.0	30.6	16.1
ITA-Roma ⮊	190.5	166.6	24.0	12.6
POL-Warsaw ⮉	190.5	176.8	13.7	7.2
POL-Warsaw ⮈	190.4	163.0	27.4	14.4
POL-Warsaw ⮋	190.4	160.2	30.3	15.9
POL-Warsaw ⮊	190.5	169.1	21.4	11.3
RUS-Moscow ⮉	190.5	179.4	11.2	5.9
RUS-Moscow ⮈	190.3	168.1	22.3	11.7
RUS-Moscow ⮋	190.5	164.5	26.0	13.6
RUS-Moscow ⮊	190.5	171.0	19.6	10.3
SWE-Ostersund ⮉	190.5	185.5	5.0	2.6
SWE-Ostersund ⮈	190.3	172.4	17.9	9.4
SWE-Ostersund ⮋	190.2	166.1	24.2	12.7
SWE-Ostersund ⮊	190.5	174.2	16.3	8.6

Table 51: Stairs [wg06] - default profile [1.00 0.30 0.75] [1 1 1 1 1 1 1 1 1 1]. Lighting energy use without and with skylights, energy and percentage saving.

8.6 CBDM versus the standard daylight factor

Design guidelines recommend daylight provision in terms of the long-established daylight factor (DF). Formulated in the UK over fifty years ago, the daylight factor is simply the ratio of internal illuminance to unobstructed horizontal illuminance under standard CIE overcast sky conditions [48]. It is usually expressed as a percentage, so there is no consideration of absolute values. The luminance of the CIE standard overcast sky is rotationally symmetrical about the vertical axis, i.e. about the zenith. And, of course, there is no sun. Thus for a given building design, the predicted DF is insensitive to either the building orientation (due to the symmetry of the sky) or the intended locale (since it is simply a ratio). In other words, the predicted DF value would be the same if the building had north-facing windows in Stornoway or south-facing windows in Brighton. The same would be true if the locations were Seattle and Miami - or indeed for any city in any country. It now appears to be widely accepted that the daylight factor method does not allow for improvement by incremental means (e.g. the 'clear sky' options in LEED/ASHRAE) and that significant advancement can only be achieved by considering predictions for absolute values of daylight illuminance founded on realistic meteorological data, i.e. climate-based daylight modelling [10]. Climate-based modelling delivers predictions of absolute quantities (e.g. illuminance) that are dependent both on the locale (i.e. geographically-specific climate data is used) and the building orientation (i.e. the illumination effect of the sun and non-overcast sky conditions are included), in addition to the building's composition and configuration. In short, CBDM delivers realistic predictions of absolute daylight quantities (e.g. lux levels) allowing for the prediction of a wide range of performance data that is essentially unachievable using the daylight factor approach.

Acknowledgements

Much of this work was carried out whilst Mardaljevic was at De Montfort University. The head image used in Figure 9 is courtesy of the NIGMS Image Gallery.

References

[1] M Andersen, J Mardaljevic, and SW Lockley. A framework for predicting the non-visual effects of daylight – Part I: photobiology-based model. *Lighting Research and Technology*, 44(1):37–53, 03 2012.

[2] Ann R. Webb. Considerations for lighting in the built environment: Non-visual effects of light. *Energy and Buildings*, 38(7):721–727, 2006.

[3] Belinda L. Collins. Review of the psychological reaction to windows. *Lighting Research and Technology*, 8(2):80–88, 1976.

[4] L. Heschong. Daylighting and human performance. *ASHRAE Journal*, 44(6):65–67, 2002.

[5] Karen Falloon, Bruce Arroll, C Raina Elley, and Antonio Fernando. The assessment and management of insomnia in primary care. *BMJ*, 342, 2011.

[6] J. Mardaljevic and A. Nabil. The useful daylight illuminance paradigm: A replacement for daylight factors. *Lux Europa, Berlin*, pages 169–174, 2005.

[7] RT 2005. Reglementation Thermique, Guide Reglementaire, CSTB France.

[8] J. A. Clarke. *Energy Simulation in Building Design 2nd Edition*. Butterworth-Heinemann, 2001.

[9] D. B. Crawley, L. K. Lawrie, F. C. Winkelmann, W. F. Buhl, Y. J. Huang, C. O. Pedersen, R. K. Strand, R. J. Liesen, Daniel E. Fisher, M. J. Witte, and J. Glazer. EnergyPlus: creating a new-generation building energy simulation program. *Energy and Buildings*, 33(4):319–331, 2001.

[10] J. Mardaljevic. Examples of climate-based daylight modelling. *CIBSE National Conference 2006: Engineering the Future, 21-22 March, Oval Cricket Ground, London, UK*, 2006.

[11] J. Mardaljevic. Simulation of annual daylighting profiles for internal illuminance. *Lighting Research and Technology*, 32(3):111–118, 1 2000.

[12] C. F. Reinhart and S. Herkel. The simulation of annual daylight illuminance distributions – a state-of-the-art comparison of six RADIANCE-based methods. *Energy and Buildings*, 32(2):167–187, 2000.

[13] C. F. Reinhart, J. Mardaljevic, and Z. Rogers. Dynamic daylight performance metrics for sustainable building design. *Leukos*, 3(1):7–31, 2006.

[14] J. Mardaljevic. Quantification of parallax errors in sky simulator domes for clear sky conditions. *Lighting Research and Technology*, 34(4):313–327, 2002.

[15] S W A Cannon-Brookes. Simple scale models for daylighting design: Analysis of sources of error in illuminance predictiont. *Lighting Research and Technology*, 29(3):135–142, 9 1997.

[16] A. Thanachareonkit, J. L. Scartezzini, and M. Andersen. Comparing daylighting performance assessment of buildings in scale models and test modules. *Solar Energy*, 79(2):168–182, 2005.

[17] P. R. Tregenza and I. M. Waters. Daylight coefficients. *Lighting Research and Technology*, 15(2):65–71, 1 1983.

[18] G. Ward Larson and R. Shakespeare. *Rendering with Radiance: The Art and Science of Lighting Visualization*. San Francisco: Morgan Kaufmann, 1998.

[19] J. Mardaljevic. The BRE-IDMP dataset: a new benchmark for the validation of illuminance prediction techniques. *Lighting Research and Technology*, 33(2):117–134, 2001.

[20] J. Mardaljevic. *Daylight Simulation: Validation, Sky Models and Daylight Coefficients*. PhD thesis, De Montfort University, Leicester, UK, 2000.

[21] J. Mardaljevic. Sky model blends for predicting internal illuminances: A comparison against measured sky luminance distributions. *Lux Europa, Berlin*, pages 249–253, 2005.

[22] A Nabil and J. Mardaljevic. Useful daylight illuminance: a new paradigm for assessing daylight in buildings. *Lighting Research and Technology*, 37(1):41–57, 2005.

[23] H. Noguchi, T. Itou, S. Katayama, E. Koyama, T. Morita, and M. Sato. Effects of bright light exposure in the office(proceedings of the 7th international congress of physiological anthropology). *Journal of physiological anthropology and applied human science*, 23(6):368, 2004.

[24] D. R. G. Hunt. The use of artificial lighting in relation to daylight levels and occupancy. *Building and Environment*, 14(1):21–33, 1979.

[25] C. F. Reinhart and K Voss. Monitoring manual control of electric lighting and blinds. *Lighting Research and Technology*, 35(3):243–258, 2003.

[26] D. R. G. Hunt. Predicting artificial lighting use - a method based upon observed patterns of behaviour. *Lighting Research and Technology*, 12(1):7–14, 1980.

[27] S.W. Lockley and D. J. Dijk. Functional genomics of sleep and circadian rhythm. *Journal of Applied Physiology*, 92:852–862, 2002.

[28] T.A. Wehr, D. Aeschbach, and W.C Jr. Duncan. Evidence for a biological dawn and dusk in the human circadian timing system. *The Journal of Physiology*, 535(3):937–951, 2001.

[29] S.W. Lockley. Influence of light on circadian rhythmicity in humans. *L. R. Squire (Ed.) Encyclopaedia of Neuroscience. Oxford, UK*, 2008.

[30] .J.A. Veitch, G. van den Beld, G. Brainard, and J.E. Roberts. Ocular lighting effects on human physiology and behaviour. *CIE Publication, Vienna, Austria*, 158, 2004.

[31] P. R. Boyce, J. W. Beckstead, N. H. Eklund, R. W. Strobel, and M. S. Rea. Lighting the graveyard shift: The influence of a daylight-simulating skylight on the task performance and mood of night-shift workerst. *Lighting Research and Technology*, 29(3):105–134, 9 1997.

[32] Peter Mills, Susannah Tomkins, and Luc Schlangen. The effect of high correlated colour temperature office lighting on employee wellbeing and work performance. *Journal of Circadian Rhythms*, 5(1):2, 2007.

[33] A.U. Viola, L.M. James, L.J. Schlangen, and D.J. Dijk. Blue-enriched white light in the workplace improves self-reported alertness, performance and sleep quality. *Scandinavian Journal of Work Environ Health*, 34(4):297–306, 2008.

[34] L.M. Wilson. Intensive care delirium. *Archives of Internal Medicine*, 130:225–226, 1972.

[35] J.M. Walsh, B.S. Rabin, R. Day, J.N. Williams, K. Choi, and J.D. Kang. The effect of sunlight on postoperative analgesic medication use: A prospective study of patients undergoing spinal surgery. *Psychosomatic Medicine*, 67(1):156–163, 2005.

[36] K.M. Beauchemin and P. Hays. Dying in the dark: Sunshine, gender and outcomes in myocardial infarction. *The Royal Society of Medicine*, 91:352–354, 1998.

[37] R.F. Riemersma-van der Lek, D.F. Swaab, J. Twisk, E.M. Hol, W.J. Hoogendijk, and E.J. Van Someren. Effect of bright light and melatonin on cognitive and noncognitive function in elderly residents of group care facilities: a randomized controlled trial. *JAMA–The Journal of the American Medical Association*, 299(22):2642–55, 2008.

[38] C. S. Pechacek, M. Andersen, and S. W. Lockley. Preliminary method for prospective analysis of the circadian efficacy of (day) light with applications to healthcare architecture. *Leukos*, 5(1):1–26, 2008.

[39] George C. Brainard, John P. Hanifin, Jeffrey M. Greeson, Brenda Byrne, Gena Glickman, Edward Gerner, and Mark D. Rollag. Action spectrum for melatonin regulation in humans: Evidence for a novel circadian photoreceptor. *Journal of Neuroscience*, 21(16):6405–6412, 2001.

[40] C. Cajochen, J.M. Zeitzer, C.A. Czeisler, and D.J. Dijk. Dose-response relationship for light intensity and ocular and electroencephalographic correlates of human alertness. *Behavioral Brain Research*, 115:75–83, 2000.

[41] J. Phipps-Nelson, J.R. Redman, D.J. Dijk, and S.M. Rajaratnam. Daytime exposure to bright light, as compared to dim light, decreases sleepiness and improves psychomotor vigilance performance. *Sleep*, 26(6):695–700, 2003.

[42] P. Badia, B. Myers, M. Boecker, J. Culpepper, and J.R. Harsh. Bright light effects on body temperature, alertness, eeg and behavior. *Physiology & Behavior*, 50:583–8, 1991.

[43] C. Lafrance, M. Dumont, P. Lesperance, and C. Lambert. Daytime vigilance after morning bright light exposure in volunteers subjected to sleep restriction. *Physiology & Behavior*, 63:803–10, 1998.

[44] C. S. Pechacek. Space, Light, and Time: Prospective Analysis of Circadian Illumination for Health-Based Daylighting with Applications to Healthcare Architecture. Master's thesis, M.Sc. thesis in Architectural Studies (SMArchS), Building Technology Program, MIT, 2008.

[45] Colorimetry - Part 2: CIE Standard Illuminants. 2006.

[46] Sat Bir S Khalsa, Megan E Jewett, Christian Cajochen, and Charles A Czeisler. A phase response curve to single bright light pulses in human subjects. *The Journal of Physiology*, 549(3):945–952, 2003.

[47] J. Wienold and J. Christoffersen. Evaluation methods and development of a new glare prediction model for daylight environments with the use of ccd cameras. *Energy and Buildings*, 38(7):743–757, 2006.

[48] R. G. Hopkinson. Architectural Physics - Lighting. *Her Majesty's Stationery Office, London*, 1963.